Identification of novel retinoid receptors and their roles in vertebrate and invertebrate nervous systems

Christopher J. Carter, Hon. B.Sc.

A thesis submitted to the Department of Biological Sciences in partial fulfillment of the requirements for the degree of Doctorate of Philosophy

July 18, 2011

Brock University

St. Catharines, Ontario

Abstract

In vertebrates, signaling by retinoic acid (RA) is known to play an important role in embryonic development, as well as organ homeostasis in the adult. In organisms such as adult axolotls and newts, RA is also important for regeneration of the CNS, limb, tail, and many other organ systems. RA mediates many of its effects in development and regeneration through nuclear receptors, known as retinoic acid receptors (RARs) and retinoid X receptors (RXRs).

This study provides evidence for an important role of the RA receptor, RARβ2, in regeneration of the spinal cord and tail of the adult newt. It has previously been proposed that the ability of the nervous system to regenerate might depend on the presence or absence of this RARβ2 isoform. Here, I show for the very first time, that the regenerating spinal cord of the adult newt expresses this β2 receptor isoform, and inhibition of retinoid signaling through this specific receptor with a selective antagonist inhibits tail and spinal cord regeneration. This provides the first evidence for a role of this receptor in this process.

Another species capable of CNS regeneration in the adult is the invertebrate, *Lymnaea stagnalis*. Although RA has been detected in a small number of invertebrates (including *Lymnaea*), the existence and functional roles of the retinoid receptors in most invertebrate non-chordates, have not been previously studied. It has been widely believed, however, that invertebrate non-chordates only possess the RXR class of retinoid receptors, but not the RARs. In this study, a full-length RXR cDNA has been cloned, which was the first retinoid receptor to be discovered in *Lymnaea*. I then went on to clone

the very first full-length RAR cDNA from any non-chordate, invertebrate species. The functional role of these receptors was examined, and it was shown that normal molluscan development was altered, to varying degrees, by the presence of various RXR and RAR agonists or antagonists. The resulting disruptions in embryogenesis ranged from eye and shell defects, to complete lysis of the early embryo. These studies strongly suggest an important role for both the RXR and RAR in non-chordate development.

The molluscan RXR and RAR were also shown to be expressed in the adult, non-regenerating CNS, as well as in individual motor neurons regenerating in culture. More specifically, their expression displayed a non-nuclear distribution, suggesting a possible non-genomic role for these 'nuclear' receptors. It was shown that immunoreactivity for the RXR was present in almost all regenerating growth cones, and (together with N. Farrar) it was shown that this RXR played a novel, non-genomic role in mediating growth cone turning toward retinoic acid. Immunoreactivity for the novel invertebrate RAR was also found in the regenerating growth cones, but future work will be required to determine its functional role in nerve cell regeneration.

Taken together, these data provide evidence for the importance of these novel retinoid receptors in development and regeneration, particularly in the adult nervous system, and the conservation of their effects in mediating RA signaling from invertebrates to vertebrates.

Acknowledgements

First and foremost, I want to thank my long-time supervisor, Dr. Gaynor Spencer. She has been there for me over my years as an undergraduate and graduate student, and I do not know how I could have completed this journey without her. It has been a great honour to be her student for so many years. In fact, I should be thanking Dr. Alan Bown for introducing me to Dr. Spencer almost 10 years ago when she was new to Brock University. She has taught me so many things, both in research and life in general. I was also fortunate to be co-supervised by Dr. Robert Carlone. Both supervisors provided me with expertise, understanding, and patience, adding considerably to my graduate experience. I appreciate all their contributions of time, ideas, and funding to make my Ph.D. experience productive and stimulating.

For this dissertation I would like to thank my thesis committee members, my predoctoral examining committee, and my Ph.D. thesis examiners: Dr. Joffre Mercier, Dr. Jeff Stuart, Dr. Miriam Richards, Dr. Adonis Skandalis, Dr. David Gabriel and Dr. Martin Petkovich (Queen's University, Kingston, Ont). Thank you for your time, interest, helpful comments and insightful questions. I would also like to thank Beulah Alexander, Caroline Barrow and the Graduate Program Director (Dr. Miriam Richards) for assistance and guidance, particularly with the numerous forms that had to be completed during my time as a graduate student.

I wish to thank Dr. Hiroyuki Kagechika (University of Tokyo, Japan) for the generous gifts of the various RXR and RAR agonists and antagonists used throughout this thesis. I would like to thank Dr. Adonis Skandalis for his initial guidance in teaching me fundamental molecular biology techniques in his lab so many years ago as an

undergraduate student. I also need to thank Nicholas Vesprini for all of his assistance with statistics over the years in the Spencer lab.

For the use of equipment vital to my research, I wish to thank Dr. Charles Després for the use of the Odyssey infrared imager, Dr. Katrina Brudzynski for the use of the UV spectrophotometer, Dr. Sandra Peters for the use of the cryostat sectioning apparatus, the CCOVI department for the use of the UV gel-doc system, and to Dr. Jeff Stuart for use of the Milli-Q water system. I would also like to thank the staff of Science Stores for their endless searches of hard to find materials.

The members of the Spencer and Carlone groups have contributed immensely to my personal and professional time at Brock University. The group has been a source of friendship as well as good advice and collaboration. If I had to name everyone I have worked with over the years, this acknowledgement section would become a chapter in my thesis, not including all of my friends from outside my research group at Brock. I am grateful to you all for making this long journey a pleasant one.

I thank the Natural Sciences and Engineering Research Council of Canada for providing me with a Canada Graduate Scholarship award and for The Premier's Research Excellence Award (to Dr. Spencer) which made my research possible.

Lastly, I would like to thank my family for all of their love and encouragement. It has been a long haul, and maybe now they will stop asking me "Are you done yet?" Most of all, I want to thank my loving, supportive, encouraging, and patient wife Miranda whose faithful support during my Ph.D. (especially during the final stages) is so appreciated. Thank you.

Table of Contents

List of Figures

Appendix I

Appendix II

List of Tables

List of Abbreviations

RA	Retinoic acid
9-*cis* RA	The 9-*cis* isoform of retinoic acid
All-*trans* RA	The all-*trans* isoform of retinoic acid
AF-1 / AF-2	Activation function (domains 1 or 2)
ADH	Alcohol dehydrogenase
ANOVA	Analysis of variance
BMP	Bone morphogenic protein
bp	Base pair
CM	Brain-conditioned medium
CNS	Central nervous system
CRABP	Cellular retinoic acid-binding protein
CRBP	Cellular retinol-binding protein
CST	Corticospinal tract
Cyp26	A P450 enzyme that degrades RA
DAPI	4'-6-Diamidino-2-phenylindole (nuclear counterstain)
DBD	DNA binding domain
DRG	Dorsal root ganglion
DM	Defined medium
DMSO	Dimethyl sulfoxide
EDTA	Ethylenediaminetetraacetic acid
EF1α	Elongation factor 1-alpha
EFAP cells	Early FMRFamide-like immunoreactive Anteriorly Projecting cells
EST	Expressed sequence tag
GAPDH	Glyceraldehyde 3-phosphate dehydrogenase
GTPase	A hydrolase enzymes that can bind and hydrolyze guanosine triphosphate
HPLC	High pressure liquid chromatography
kDa	kiloDalton
LBD	Ligand binding domain
mORF	Major open reading frame
NGS	Normal goat serum
NTD	N-terminal domain
PA	Post-amputation

PBS	Phosphate-buffered saline
PBT	Phosphate-buffered saline with 0.1% Triton X-100
PeA	Pedal A
PPAR	Peroxisome proliferator-activated receptor
RALDH	Retinaldehyde dehydrogenase
RAR	Retinoic acid receptor
RAREs	Retinoic acid response elements
RACE	Rapid amplification of cDNA ends
RBPs	Retinol-binding proteins
RMP	Resting membrane potential
PMSF	Phenylmethanesulfonylfluoride
RT-PCR	Reverse transcription polymerase chain reaction
RXR	Retinoid X receptor
SC	Spinal cord
SDR	Short-chain dehydrogenase/reductase
SDS	Sodium dodecyl sulfate
SHH	Sonic hedgehog
sORF	Small open reading frame
TAE buffer	A solution containing a mixture of Tris base, acetic acid and EDTA
TR	Thyroid receptor
UTR	Untranslated region
VDR	Vitamin D receptor

Chapter 1: Introduction

1.01 General Introduction

Many signaling molecules that were once thought to only be important during the process of development are now known to be just as important in critical processes after embryogenesis. In the adult, these molecules can be important for processes such as regeneration of various tissues and organs, maintenance of cell proliferation, and synaptic plasticity. Due to the preservation of this signaling from embryo to adult, many believe that events such as organ regeneration are similar to the events that occur during development of that same organ. Retinoic acid (RA) is a molecule that has long been known to have an important role in the development of embryonic structures including the nervous system and notochord of chordates. In adults of many species, RA has also been implicated in regeneration of several organ systems including eye, gut, limb and tail (Collins and Mao, 1999; Maden and Hind, 2003). In the adult nervous system, RA is known to influence neurite outgrowth and affect synaptic plasticity in the hippocampus (Bonnet et al., 2008).

Previously, a large portion of research has focused on the role of RA in vertebrate systems, and much less is known regarding the role of RA in development and regeneration of invertebrates. The work that I present in this study investigated the role of RA in both vertebrates and invertebrates. In particular, I have identified novel retinoid receptors in the vertebrate newt, *Notophthalmus viridescens*, and the invertebrate mollusc, *Lymnaea stagnalis*. I have also investigated the roles of these novel receptors in spinal cord and tail regeneration in the newt, and in development and nerve regeneration in the mollusc.

1.02 Retinoic Acid Synthesis

RA is classified as a retinoid, which encompasses any compound, biologically active or inactive, that is an analogue of retinol. Retinol is one of the forms of vitamin A (in animals) which is derived from the metabolism of carotenoids found in many different fruits and vegetables. Alternatively, animals can obtain retinol by eating animal tissues that have already converted carotenoids to retinol. Dietary intake in most animals is the only method for obtaining retinoids, since *de novo* synthesis pathways are not present (Theodosiou et al., 2010). These compounds can be stored in the body as retinyl esters (mainly in the liver) and upon specific signals, can be converted back to retinol for use in other areas of the body. Retinol is transported through the bloodstream to target areas bound to retinol-binding proteins (RBPs) (Maden, 2007). Retinol then uncouples from RBP and enters the cytoplasm of target cells through interaction with a transmembrane protein known in vertebrate systems as STRA6 and is immediately bound to cellular retinol-binding protein (CRBP). Once inside the cell, retinol can be converted to retinal by the action of alcohol dehydrogenase (ADH) or short-chain dehydrogenase/reductase (SDR) enzymes. The last step in RA synthesis is the irreversible conversion of retinal to RA by an oxidation reaction involving retinaldehyde dehydrogenase (RALDH). Once RA is produced, it is bound to cellular RA-binding proteins (CRABPs) which aid in the transport of RA within the cell (autocrine signaling) or for transport out of the cell (paracrine signaling) (Fig. 1). When signaling in an autocrine fashion, RA can uncouple from CRABPs, readily pass through the nuclear membrane where it binds with ligand activated nuclear transcription factors, known as retinoid receptors, which can lead to changes in gene activity.

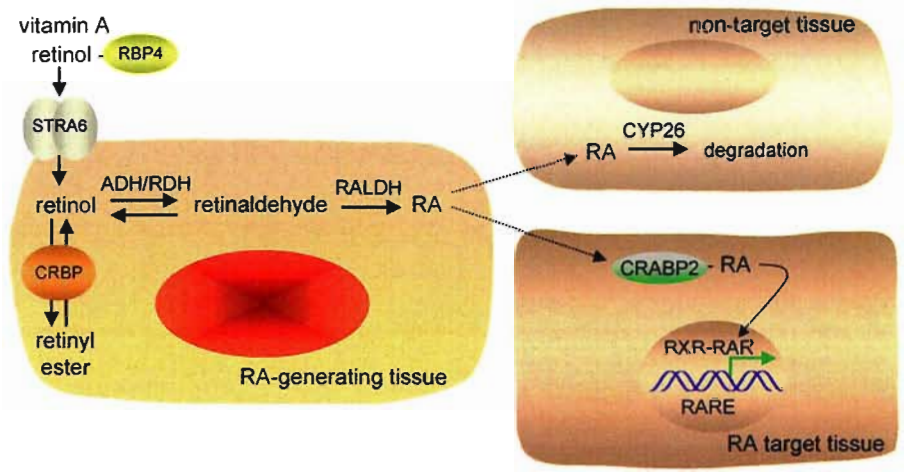

Figure 1. Retinoic acid synthesis and signaling pathway (Duester, 2008).

In the formation of RA within the cytoplasm of the cell, multiple isoforms can result, including the major isoforms all-*trans* RA and 9-*cis* RA (Fig. 2). There still exists some uncertainty regarding whether all-*trans* RA and 9-*cis* RA are formed through separate pathways from 9-*cis* and all-*trans* retinol, or whether there is an isomerization reaction that exists between them after the action of RALDH (Maden and Hind, 2003). For example, there is some evidence in vertebrates for the existence of a 9-*cis* retinol dehydrogenase enzyme that suggests a separate pathway for the synthesis of 9-*cis* RA (Romert et al., 1998; Tryggvason et al., 2001).

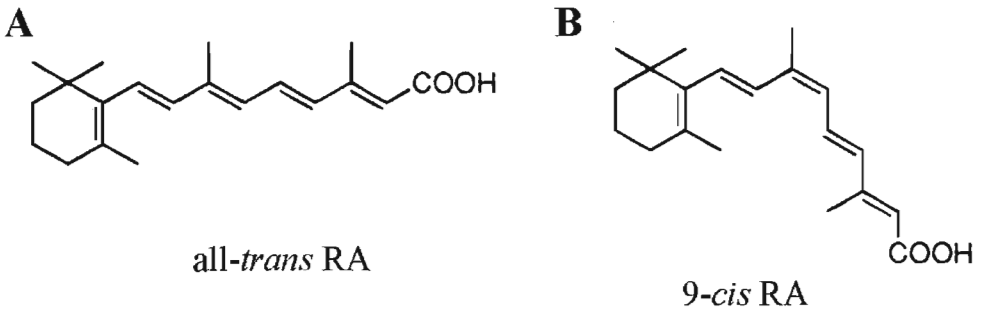

Figure 2. Retinoic acid (RA) isomers (A) all-*trans* RA and (B) 9-*cis* RA.

To control the levels of RA in cells and tissues of the body, there needs to be a balance between synthesis and catabolism. Catabolism of RA is accomplished through the action of enzymes from the CYP26 family. These enzymes oxidize RA to polar water-soluble metabolites such as 4-hydroxy RA and 4-oxo RA, that can subsequently be excreted in bile and urine (Blomhoff and Blomhoff, 2006).

1.03 Retinoid-dependent signaling

The effects of RA are generally mediated through binding to members of the nuclear receptor family called retinoid receptors. These retinoid receptors are grouped into two classes, retinoic acid receptors (RARs) and retinoid X receptors (RXRs). The RARs mediate gene expression by binding as heterodimers with RXRs, to the retinoic acid response elements (RAREs) in target genes, thus eliciting changes in their expression (see Fig. 1). In human, rat, and mouse, there are three RARs (α,β,γ) and three RXRs (α,β,γ) and each of these various subtypes has its own associated isoforms (e.g. RARβ1 to 5). The RARs and RXRs are thought to bind different isoforms of RA in order to be activated. Studies have found that RARs can be activated by both all-*trans* RA and 9-*cis* RA (Allenby et al., 1994), whereas RXRs almost exclusively bind 9-*cis* RA, at least in vertebrates (Heyman et al., 1992). In numerous vertebrate species, both RARs and RXRs have been identified, but to date, only RXRs have been cloned in non-chordate invertebrates.

1.04 Retinoid receptor structure

Similar to other known nuclear receptors, RAR and RXR have a modular structure consisting of 6 regions of homology classified as A to F regions from the N-terminal to the C-terminal region (Fig. 3). The most conserved areas are the C and E regions which encompass the DNA-binding domain (DBD) and the ligand binding domain (LBD). The other regions A/B, D and F are poorly conserved but still have important functions in mediating RA signaling (Rochette-Egly and Germain, 2009).

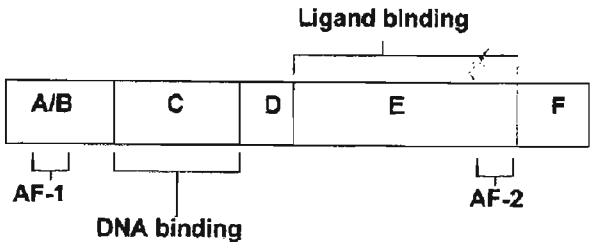

Figure 3. Schematic representation of a nuclear receptor with functional domains A to F

The A/B region is also known as the N-terminal activation function (AF)-1 domain (NTD) and acts autonomously and ligand-independently. One interesting feature of this AF-1 domain is that it contains consensus phosphorylation sites for proline-dependent kinases, which have been proposed to play a role in controlling transcription of RA target genes (Nagpal et al., 1993). The C region (or DBD) confers sequence-specific DNA recognition and is comprised of two zinc-finger domains which contact the RARE sites specific to that receptor. The D region has traditionally been considered as the 'hinge' region, allowing rotational flexibility between the DBD and the LBD and avoiding steric hindrance. The E region (or LBD) contains the ligand-binding pocket and is comprised of mainly hydrophobic residues that form a shape that matches the volume

of the RA ligand. This E region is also known to contain the main dimerization domain and the ligand-dependent activation function-2 (AF-2). The F region contains a helical region called helix 12, but its function is still poorly understood. One study has suggested that the F region (in the absence of ligand) may control the ability of RARs to interact with corepressors (Farboud and Privalsky, 2004). Another study has shown evidence that the F region may be capable of binding to specific mRNAs and controlling their translational capabilities (Poon and Chen, 2008).

1.05 RA signaling and embryonic development

Both experimental and clinical approaches have revealed that retinoids exert a wide variety of effects on the embryonic body plan and formation of various organs, cell proliferation, differentiation, and apoptosis (Mark et al., 2009). Normal development is based on precise levels of RA regulated by synthesis and catabolism pathways of the cell. If these levels are altered from their normal levels (either increased or decreased), abnormal body growth and development occurs (McCaffery et al., 2003). In fact, if embryos are treated with higher than normal levels of exogenous RA, almost every organ can be affected if the RA is given at a specific time during development (Zile, 2001). Furthermore, if vitamin A function is diminished in embryos (often as a result of elimination from diet), they develop gross abnormalities in their central nervous systems, cardiovascular systems and trunk, eventually leading to death. Interestingly, these vitamin A-deficient abnormalities in the developing embryo can be rescued by administering the natural ligand for RAR, all-*trans* RA.

In contrast to altering retinoid levels, many studies have used transgenic mice that contain mutations introduced at loci encoding RAR and RXRs. Many of the abnormalities in these mutant mice resemble those observed in the vitamin A-deficient embryos (Mark et al., 2009). However, the major advantage of these mutation experiments is that the importance of specific RAR and/or RXR subtypes can be elucidated. For example, it has been well established that RXRα is the main RXR subtype involved in embryogenesis (Mark et al., 2009). RXRα-null mutants display multiple heart abnormalities and eye defects, whereas RXRβ- and RXRγ-null mutants do not display any obvious morphological defects (Krezel et al., 1996). Through compound mutants involving RXR and RAR, it has been determined that retinoic acid signals are transduced by specific RXRα/RAR heterodimers during the course of development. In other words, RXRα/RARα, RXRα/RARβ and RXRα/RARγ heterodimers have been shown to be the functional units for RA signaling during vertebrate embryogenesis.

RA is also an important signaling molecule involved in the normal development of the central nervous system. All-*trans* RA is essential for cellular growth and differentiation in developing animals. It has been found that all-*trans* RA is present in the embryonic spinal cord and also detected at relatively high levels after development in both the brain and spinal cord of adult vertebrates (Maden et al., 1998; Werner and Deluca, 2002). Depletion of vitamin A in quail embryos revealed the need for vitamin A in proper segmentation of the posterior hindbrain, neurite outgrowth and neural crest survival (Gale et al., 1999). Retinoid receptor knock-out experiments revealed a similar

importance for RA signaling in proper hindbrain and neural crest formation in mice (Zile, 2001).

1.06 RA signaling and regeneration

Although many studies have focused on the role of vitamin A and RA in embryonic development, it has recently become evident that RA is also required for many regenerative processes in the adult. In particular, in the adult CNS, RA signaling is important in the olfactory bulb and the subventricular zone, areas known to retain synaptic plasticity into adulthood (Thompson et al., 2002). RA has also been implicated in postnatal differentiation of pyramidal neurons in various cortical areas of the brain, the mature basal ganglia and in the hippocampus (Wagner et al., 2002). Interestingly, the basal ganglia area (in the forebrain) has been shown to express multiple RA receptors, CRBPs and is supplied with RA, from the action of RALDH within surrounding dopaminergic nerve terminals (McCaffery and Drager, 1994). Disruption of RA synthesis in this area can lead to Parkinson's-type symptoms (e.g. catatonia) and even basal ganglia lesions (McCaffery and Drager, 1994)

In the developing nervous system, RA-deficiency in quail embryos can prevent neurite outgrowth from the spinal cord into the periphery (Maden et al., 1996). Since this indicated a role for RA in permitting neurite outgrowth from the CNS, it was postulated that perhaps RA would also promote outgrowth from damaged axons of neurons in the adult CNS. Corcoran et al. (2002) performed a study in which they showed that although all-*trans* RA could induce neurite outgrowth from mouse embryonic neurons and embryonic spinal cord, the adult spinal cord did not respond to all-*trans* RA in the same

manner. The authors suggested that during the transition from embryo to adult, some of the RA machinery responsible for the induction of neurite outgrowth may have become inactive. In fact, in vertebrates that retain the ability to regenerate CNS tissue in adulthood, all-*trans* RA is still able promote neurite outgrowth (Dmetrichuk et al., 2005). This may suggest that these regeneration-capable species (such as the newt) retain the expression of necessary RA machinery.

One of the most fascinating events in the field of adult regeneration is the ability to regenerate full limbs and tails after amputation. This occurs in newts, axolotls and many species of salamanders. Early experiments with axolotl limbs showed that treatment with exogenous all-*trans* RA induced a concentration-dependent increase in the amount of regenerated tissue in the proximo-distal axis. For example, high levels of all-*trans* RA applied after amputation of the axolotl limb at the mid-radius and ulna caused an extra elbow joint to appear along with all of the other distal limb structures (Fig. 4B).

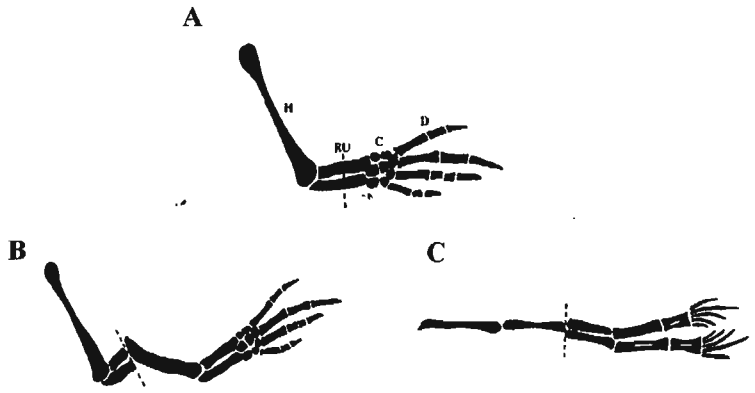

Figure 4. Defective regeneration after limb amputation and vitamin A treatment. (A) Control limb regenerate showing the normal complement of cartilages. H = humerus, RU = radius and ulna, c = carpals, d = digits 1 to 4. (B) Increasing vitamin A treatment proximalized the limb regenerate. (C) At very high doses, duplication can take place. (modified from Maden et al., 1998)

In some species such as *Rana temporaria*, high levels of RA can induce regeneration of multiple limb structures (Maden, 1983) (Fig 4C). The opposite effect was seen in amputated axolotl limbs treated with disulfiram, which inhibits the action of the RA synthesizing enzyme, RALDH (Maden, 1998). Disulfiram treatment produced almost complete inhibition of limb regeneration.

1.07 Vertebrate model species, *Notophthalmus viridescens* (Eastern newt)

Amphibians have long been used in the study of regeneration processes, as they have an amazing ability to regenerate numerous structures including limbs, tails, jaws and the lens of the eye. The ability to regenerate these complex structures is considered by many authors to be ancestral and to have been lost in other vertebrate species, including humans (Sanchez, 2000). In some cases, regeneration shows many parallels with development. For example, gene expression analyses in *Xenopus* tadpoles have shown that subsequent limb and tail regeneration involves the re-activation of various developmental signaling pathways involving proteins such as fibroblast growth factors and Homeobox genes (Beck et al., 2006). However, there are also some different processes involved that are unique to regeneration. For example, regeneration-competent wound healing is generally rapid and involves covering the wound surface with a specialized epidermis that lacks an underlying dermis and basement membrane (Neufeld et al., 1996). Following wound healing, the differentiated cells of the stump must dedifferentiate and re-enter the cell cycle, or else reserve stem cell populations must be mobilized and recruited to the wound site.

It has been clearly demonstrated that the presence of nerves is essential for normal limb and tail regeneration *in vivo* (Singer, 1952). Regeneration of the spinal cord also occurs in close conjunction with tail regeneration and has been shown to play an essential role in its maintenance. In the newt, *Notophthalmus viridescens* (Fig. 5), it has previously been shown that all-*trans* RA can increase both the number and length of axons extending from spinal cord explants (Prince and Carlone, 2003). It was also shown that the tail blastema (a mass of dedifferentiated cells from which a new tail will form), co-cultured with spinal cord explants had the same effect on the number and length of regenerating axons as seen with the all-*trans* RA treatment (Prince and Carlone, 2003) suggesting that the tail blastema is a source of all-*trans* RA. However, this study did not identify a specific retinoid receptor that may be involved in the regenerative response to all-*trans* RA.

Figure 5. The amphibian, *Notophthalmus viridescens* (red-spotted newt).

In the regenerating limb tissue of the newt, four full-length RAR isoforms have been detected to date, two α and two δ types (equivalent to the mammalian RARγ), but the RARβ isoform has been reported to be absent (Maden and Hind, 2003). RARβ (specifically the RARβ2 subtype), found in other vertebrates, appears to specifically mediate the effects of RA on neurite outgrowth in the peripheral nervous system, which

has the ability to regenerate. For example, Corcoran et al. (2000) showed that all-*trans* RA could stimulate neurite extension in cultured embryonic dorsal root ganglion (DRG) neurons and that this response involved the upregulation of RARβ2. More importantly, it was shown in adult DRG neurons (that do not respond to all-*trans* RA) that transduction with an RARβ2-expression vector alone was enough to stimulate neurite extension (Corcoran et al., 2002). Our lab has recently shown in *N. viridescens*, that RA-stimulated neurite outgrowth from newt spinal cord explants was abolished in the presence of antagonists selective for RARβ (Dmetrichuk et al., 2005) (Fig. 6). This was a curious finding since, as mentioned previously, it was reported that newts do not contain RARβ isoforms (Maden and Hind, 2003). Interestingly, the same RARβ-selective antagonist (LE135) also inhibited limb regeneration in the closely related species of the axolotl, *Ambystoma mexicanum* (del Rincon and Scadding, 2002). Given these findings that RARβ-selective antagonists decrease regeneration, it is possible that a newt RARβ does

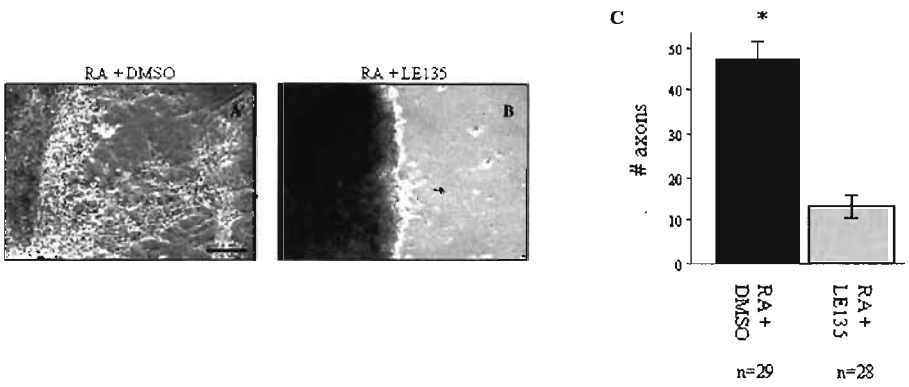

Figure 6. An RARβ-selective antagonist significantly decreased RA-induced axonal outgrowth from newt spinal cord. (A) Spinal cord explants cultured in RA (containing the vehicle control, DMSO) or (B) RA and LE135. Scale bar: 50μm (C) Graph depicting significant reduction in RA-induced axonal outgrowth in the presence of RARβ antagonist. *RA treatment elicited significantly more axons than in the presence of the antagonist solution ($p < 0.05$). (modified from Dmetrichuk et al., 2005)

exist and that this receptor plays an important role in tail and CNS regeneration in newts, as it does in other vertebrate cells.

1.08 Axon guidance

Axon guidance is an important aspect of nervous system development and regeneration. As growing axons extend towards their targets, they are guided by a variety of extracellular cues that are either diffusible or surface-bound. At the growing end of the axon, a structure known as the growth cone (Fig. 7A) can steer axons toward (attraction), or away from (repulsion) the source of the signal. Since these signals can change the direction of the developing growth cone, internal changes within the growth cone itself must first occur. Many of these changes involve synthesis of proteins that affect the internal actin cytoskeleton and are responsible for the overall shape of the growth cone (Dos Remedios et al., 2003). Actin filaments within the growth cone are dynamic in nature, and movement is generated by extending or retracting finger-like projections called filopodia and membranous sheets called lamellipodia (Brown et al., 2000) (Fig. 7B).

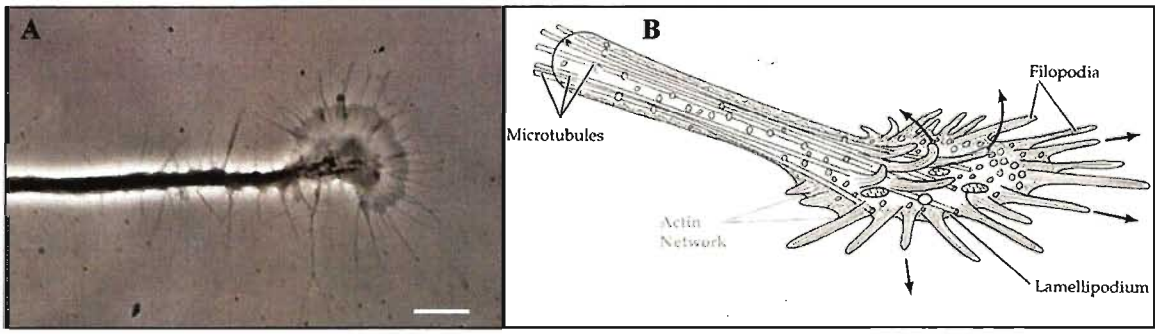

Figure 7. Structure of a regenerating growth cone (A) Phase contrast picture of a *Lymnaea* growth cone from a cultured PeA neuron. Scale bar: 25μm (B) A schematic view of the growth cone at the end of the axon highlighting the lamellipodium and filopodia. The arrows indicate the direction of the extending filopodia (from Smith, 1988).

Numerous molecules have been implicated as chemoattractants in axon guidance. These include ephrins, netrins, slits, and semaphorins (Huber et al., 2003). Several morphogens (substances that define different cell fates) have also been shown to play a role in growth cone guidance including bone morphogenic protein (BMP), Wnt family members, and sonic hedgehog (SHH) (for review, see Farrar and Spencer, 2008). Many of these signals that the growth cone can encounter ultimately activate pathways that involve intracellular regulators of the Rho GTPase family. The most widely studied Rho GTPases are Rho, Rac and Cdc42, which play important roles in regulating cytoskeletal dynamics for processes such as growth cone guidance. It is the interplay between these various Rho GTPases and their spatial distribution that dictates whether a growth cone will be attracted to or repelled from a particular extracellular guidance cue.

1.09 RA as a chemotropic molecule

The first evidence implicating RA as a guidance molecule used dissociated cultures of embryonic chick neural tissue. Using a custom designed Dunn chamber, a gradient of all-*trans* RA was produced, and the regenerating neurons responded by growing up the gradient towards the source of RA (Maden et al., 1998). Later Dmetrichuk et al. (2005) showed directional outgrowth towards RA from cultured newt adult spinal cord explants. Beads soaked in all-*trans* RA were co-cultured with the newt spinal cord explants, and it was shown that the newly regenerating axons grew preferentially towards the beads (Dmetrichuk et al., 2005). Dmetrichuk et al. (2006) then went on to show for the first time in any species that RA could induce turning of a single growth cone. More importantly, using cells from the CNS of *Lymnaea stagnalis* (Fig 8A),

it was shown that both the all-*trans* and 9-*cis* isomers of RA displayed similar chemotropic effects, although the signaling machinery involved was not previously identified (Dmetrichuk et al., 2006; Dmetrichuk et al., 2008).

1.10 *Lymnaea stagnalis* as a model for studying RA

The CNS of *Lymnaea stagnalis* has previously proven a useful model system for the study of regeneration and neurite outgrowth (Fig. 8B). In fact, a previous study has shown that identified *L. stagnalis* neurons can functionally regenerate primary neurites after nerve crush *in vivo* (Wildering et al., 2001). As previously mentioned, our lab has also shown that RA can induce neurite outgrowth in *Lymnaea* neurons and act as a chemoattractive factor, inducing growth cone turning toward a source of RA (Dmetrichuk et al., 2006; Dmetrichuk et al., 2008). Additionally, it was found that both all-*trans* and 9-*cis* RA exerted neurotrophic effects on *Lymnaea* neurons and maintained their electrical excitability and resting membrane potential (RMP) for up to 6 day in culture. Through the use of HPLC and mass spectrophotometry, Dmetrichuk et al. (2008) also showed the presence of both RA isomers in the CNS and hemolymph of *L. stagnalis*. Other work in our lab showed that RA enhanced neurite branching in intact *Lymnaea* CNSs after nerve crush injury (Vesprini and Spencer, 2010). Despite all of RA's effects on outgrowth and regeneration, there is no previous evidence for receptors or RA signaling pathways in *Lymnaea.*

Recently, the first cloned molluscan RXR cDNA was reported in the freshwater snail *Biomphalaria glabrata* (*Bg*RXR), which is very closely related to *Lymnaea*

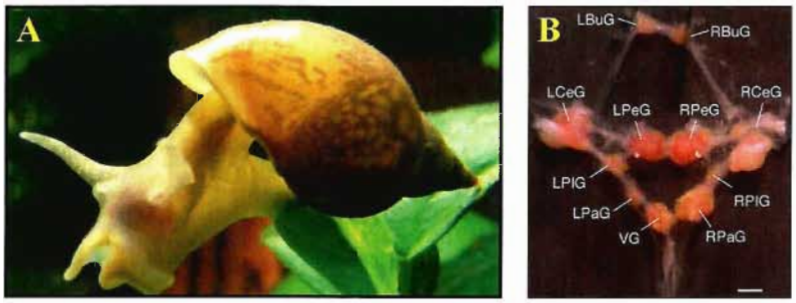

Figure 8. The invertebrate model system of study. (A) The mollusc, ***Lymnaea stagnalis***. (B) The dissected central ring ganglia of ***Lymnaea stagnalis***. LBuG and RBuG: left and right buccal ganglia; LCeG and RCeG: left and right cerebral ganglia; LPeG and RPeG: left and right pedal ganglia; LPlG and RPlG: left and right pleural ganglia; LPaG and RPaG: left and right parietal ganglia; VG: visceral ganglion. Scale bar: 1 mm (Feng et al., 2009).

stagnalis. It was also shown that this molluscan RXR show greater sequence identity with the mouse RXRα than with other known arthropod homologues and can bind with vertebrate RXR ligands. The *Bg*RXR was shown to bind 9-*cis* RA (the natural ligand of vertebrate RXRs) and this binding induced transcriptional activation (Bouton et al., 2005). Thus, there is evidence for the existence of molluscan retinoid receptors (RXRs) suggesting that a *Lymnaea* RXR may also be present and possibly mediating tropic and trophic effects of RA, specifically the 9-*cis* isomer. However, RXRs in vertebrates do not have appreciable affinity for the all-*trans* RA isomer. Given the evidence for all-*trans* RA in the *Lymnaea* CNS and its role in exerting trophic and tropic effects *in vitro* and enhancing regeneration *in situ*, it is conceivable that a separate signaling pathway may exist for this isomer. The all-*trans* RA isoform is the natural ligand for the RAR, and in vertebrates, both RXR and RAR are known to exist and exert the effects of 9-*cis* and all-*trans* RA accordingly. To date, no RARs have been cloned from any invertebrate non-chordate species, although there are recent reports of orthologs that have been predicted from genomic databases (Albalat and Canestro, 2009; Campo-Paysaa et al., 2008). Given

all of the evidence provided here, it may thus be possible that signaling pathways involving RAR are present in *Lymnaea*.

1.11 Objectives

From studies using RARβ-selective antagonists (del Rincon and Scadding, 2002; Dmetrichuk et al., 2005), there is compelling functional evidence for the existence of a RARβ in the newt, *Notophthalmus viridescens*. My first aim for this study was to clone a full-length RARβ receptor cDNA from the CNS of the newt and if successful, to study its specific role in tail and spinal cord regeneration.

Our lab has also provided evidence for trophic and tropic effects of RA on molluscan neurons from the CNS of *Lymnaea stagnalis*, but despite evidence for RA in the CNS, no components of the retinoid signaling pathway have yet been identified in this species. My aim was to identify various components of the RA signaling pathway. In particular, I first aimed to clone the RXR cDNA, as there was previous evidence for the existence of molluscan RXRs. I then aimed to characterize its expression and investigate its functional role in non-chordate development and regeneration.

A full-length, non-chordate RAR had never been cloned, but there was evidence from genome screening for the presence of an RAR ortholog in another non-chordate, molluscan species. My next aim was to clone the first full-length, non-chordate RAR cDNA and to then also characterize its expression and to attempt to investigate its functionality.

Chapter 2:

Cloning and expression of a retinoic acid receptor β2 subtype from the adult newt: Evidence for a role in tail and caudal spinal cord regeneration.

2.01 Abstract

Adult urodele amphibians such as the newt, *Notophthalmus viridescens*, have a unique ability to regenerate limbs, tail, spinal cord, eye structures and many vital organs. It has previously been shown that a retinoic acid receptor antagonist, selective for the RARβ sub-type, was able to inhibit RA-induced neurite outgrowth from cultured adult newt spinal cord (Dmetrichuk et al., 2005), as well as epimorphic regeneration of the limb (del Rincon and Scadding, 2002). However, the existence of a newt homologue of the RARβ subtype has been controversial. In the present study, I have cloned the first full-length RARβ cDNA from adult newt CNS tissue. This receptor shares a high degree of homology with the RARβ2 isoform, which has recently been implicated as the key transducer of the retinoic acid signal during regeneration. For example, RARβ2 expression has been implicated in the ability of CNS tissue to regenerate in response to retinoic acid (Corcoran et al., 2002).

The newly cloned *N. viridescens* RARβ2 cDNA (termed *Nv*RARβ2) was found to be expressed in various adult organs that are capable of regeneration, such as the spinal cord, gut and liver. *Nv*RARβ2 transcripts are expressed in the regenerating tail of adult newts, predominantly in the regenerating spinal cord, in addition to the blastema mesenchyme located just below the wound epidermis. Interestingly, following amputation of the tail, both the RARβ2 mRNA and protein are upregulated over 21 days post-amputation. Pharmacological inhibition of RARβ, immediately following amputation, caused a significant decrease in the length of tail regenerate, when measured after 21 days. Although somewhat unexpected, a synthetic RARβ2-selective agonist also significantly reduced tail regenerate length after 21 days of treatment.

Together, these data provide the first evidence for a newt RARβ2 isoform, and support an important role for this *Nv*RARβ2 in caudal spinal cord and newt tail regeneration.

2.02 Introduction

Unlike the adult mammalian CNS, the spinal cord and brain of adult urodele amphibians are capable of extensive functional regeneration after injury (Chernoff, 1996; Endo et al., 2007). One of the conditions in which the spinal cord of the urodeles undergoes regeneration is when the tail (which contains spinal cord) is amputated and a new tail regenerates.

Tail regeneration in newts occurs in two major steps: first the dedifferentiation of adult cells into a stem cell state similar to embryonic cells, and second, the development of these cells into new tissue. The regeneration process begins immediately after amputation and results in the epidermis migrating to cover the stump (in less than 12 hours), to form a structure called the wound epithelium. Over the next several days there are changes in the underlying stump tissues that eventually result in the formation of a structure called the blastema about 9-10 days later; (Iten and Bryant, 1976). The blastema consists of a mass of dedifferentiated, proliferating mesenchymal cells which will eventually differentiate into a variety of cell types, including osteoblasts (bone cells), chondrocytes (cartilage cells) and adipocytes (fat cells) (Zipori, 2004).

This process of tail regeneration is also closely accompanied by ependymal outgrowth from the severed spinal cord. Ependymal cells are classified as glial cells that form an epithelial lining in the central canal of the mature spinal cord. It has previously been shown that these ependymal cells act in a neurotrophic manner and are essential for successful tail regeneration. After tail amputation, the cells lining the ependymal canal proliferate and give rise to an ependymal tube (which terminates in a structure called the ependymal bulb) in which neurogenesis occurs (Benraiss et al., 1999). The ependymal

tube extends into the blastema, and will ultimately lay the foundation for the formation of new spinal cord. The ependymal cells provide a favourable substratum as well as guidance cues for the actively regenerating spinal cord axons (Nordlander and Singer, 1978). The ependymal cells have also been implicated in possibly providing a source of neuronal precursors (Benraiss et al., 1999) for the new spinal cord.

It has been well established that RA is an important molecule in the development, patterning and regeneration of CNS tissue (Maden and Hind, 2003). For example, in urodele amphibians (eg. newts and axolotls) where regeneration of CNS, limb and tail tissues occurs naturally, RA can have significant effects on neurite outgrowth (Dmetrichuk et al., 2005), the establishment of proximal-distal, anterior-posterior and dorsal-ventral positional information (Pecorino et al., 1996), as well as cellular proliferation and differentiation in the limb blastema mesenchyme and wound epithelium (Maden, 1998; Viviano and Brockes, 1996).

Normally, RA exerts its effects on these processes by entering the nucleus and binding to two classes of ligand-activated nuclear transcription factors: the retinoic acid receptors (RARs) and the retinoid X receptors (RXRs) (Maden and Hind, 2003). In the regenerating newt limb, five RAR isoforms have been detected, two α and three δ types, with the newt δ type being the equivalent to the mammalian γ type (Maden, 1996). No RXRs have yet been isolated from urodele amphibians (however, see Appendix 1), but at least three are suspected to be expressed and bind as heterodimers with the five RAR isoforms (Maden, 1997; Maden and Hind, 2003). Each specific combination of heterodimer could potentially be responsible for the varying effects of RA on development and regeneration in these species (Maden, 1997). For example, *in vivo*

activation of a single RARδ2 isoform in blastema mesenchyme (by biolistic transfection of a chimeric thyroid-hormone/RAR δ2 receptor), mediates proximal-distal specification of positional information (Pecorino et al., 1996).

In mammals, another isoform, RARβ2, appears to specifically mediate the effects of RA on neurite outgrowth in peripheral nervous tissue capable of regenerating neurites (namely embryonic and adult dorsal root ganglia (DRG) neurons). Importantly, expression of this specific β2 isoform is consistent with the ability of mouse embryonic spinal cord neurons to regenerate (Corcoran et al., 2002). However, spinal cord explants from adult mice can not regenerate and RARβ2 expression is absent; exogenous RA does not produce neurite extension from these explants (Corcoran et al., 2002). Interestingly, transduction of adult mouse and rat spinal cord *in vitro* with a minimal equine infectious anemia virus constitutively expressing RARβ2 led to prolific neurite outgrowth in these tissues (Corcoran et al., 2002). Similar effects on neurite outgrowth and functional recovery *in vivo* have been obtained with over-expression of RARβ2 by lentiviral vectors in adult DRG or corticospinal tract (CST) neurons in models of CNS injury (Wong et al., 2006; Yip et al., 2006).

We have previously demonstrated that spinal cord explants from adult newts show extensive neurite outgrowth in response to exogenous RA (Dmetrichuk et al., 2005; Prince and Carlone, 2003). Similar results in response to exogenous RA were obtained with spinal cord explants from larval salamanders (Hunter et al., 1991). Interestingly, the RA-stimulated outgrowth from newt spinal cord neurons was abolished in the presence of a selective antagonist of RARβ, LE135 (Dmetrichuk et al., 2005). These data strongly suggest that a RARβ subtype might be mediating the neurite-stimulating effects of RA in

the newt, as is known to occur in mammalian embryos. Curiously, it has been previously reported that newts do not contain any RARβ isoforms (Maden and Hind, 2003), despite an earlier report of a partial RARβ-like receptor from adult newt limb tissue (Giguere et al., 1989).

In this study, I have cloned a full-length newt homolog of RARβ from the adult newt, *Notophthalmus viridescens* that displays highest similarity to other vertebrate RARβs, specifically the RARβ2 isoform. I next determined the expression pattern of this newt RARβ (termed *Nv*RARβ2) in various organs and tissues, including the caudal spinal cord and tail during various stages of tail regeneration. With the use of an RARβ-selective agonist and antagonist, I then investigated a potential functional role for this newt RARβ in adult newt tail regeneration.

2.03 Material and Methods

Animal care and surgery

All procedures were approved by the Brock University Animal Care and Use Committee. Adult Eastern red-spotted newts, *Notophthalmus viridescens* were used for all experiments and were acquired from Boreal Northwest (St. Catharines, Ontario). Adults were housed in plastic containers for the duration of experiments and fed a diet of liver and brine shrimp three times per week, with dechlorinated water being changed following feeding.

For all surgical procedures, newts were anesthetized by full immersion in 0.1% solution of *m*-aminobenzoic acid ethyl ester methane sulfonate (pH 7.0, MS-222, Sigma). For all regeneration experiments, the tail was amputated approximately 1cm caudal to the cloaca. Following surgery, newts were allowed to recover on ice for approximately 20 minutes, at which time they were placed onto a damp paper towel to recover fully.

Cloning of *N. viridescens* RARβ2

Total RNA was isolated from a mixture of newt brain and spinal cord tissue according to procedures outlined in the GenElute™ Mammalian Total RNA Purification Kit (Sigma-Aldrich). cDNA was generated from the total RNA using random hexamer and oligo-dT primers according to instructions in the ThermoScript™ RT kit (Invitrogen). Touchup-PCR was performed using the GoTaq® Hot Start Polymerase kit (Promega) using the following degenerate primers: 5´-cactacggcgtctccgcntgygarggnt-3´ and 5´-ggtgatcttcatcaggatctttggraacatrtg-3´. Amplification was performed according to

the following cycling program: 94°C for 2 min, 94°C for 30 sec , 42 °C for 30 sec and 72 °C for 50 sec, followed by 29 cycles at increasing annealing temperatures in increments of +0.4°C per cycle. This was followed by 15 cycles at 94°C for 30 sec, 58°C for 30 sec and 72°C for 50 sec, followed by a final extension at 72°C for 5 min. Using this initial PCR product as a template, a second round of PCR was performed using the same program with nested degenerate primers: 5´-ccggaacgaccggaayaaraaraa-3´ and 5´-ggccgaagccggcrttrtgcat-3´, to produce a product of 437 bp. All sequencing was performed by York University (Toronto, Ontario) using a 3730 DNA sequencer from Applied Biosystems. Full-length cDNA was obtained through multiple rounds of 5´ and 3´ RACE with cDNA prepared from the same newt brain and spinal cord preparations using the SMART RACE cDNA amplification kit (Clonetech).

Reverse Transcriptase-PCR

Reverse transcription was performed for each tissue sample in a final volume of 20 µL with 1 µg total RNA according to the protocol for the iScript™ cDNA Synthesis Kit (BioRad). PCR was performed with 1 µL of RT product with iTaq™ DNA Polymerase (BioRad). The specific primers used were 5′-ggcccgtcctcatgcatgcttca-3′ (Forward) and 5′-cttctcggtgaggtcgtccagctcg-3′ (Reverse) to produce a 486bp product according to the following program: 95°C for 3 min, followed by 35 cycles of 95°C for 30 sec , 65°C for 30 sec and 72 °C for 45 sec. The nucleotide sequences of the control elongation factor 1α (EF1α) primers were 5′-ccatgtgtgtggagagcttctca-3′ (Forward) and 5′-ggctcttgtgatggaccctaatg-3′ (Reverse) yielding an amplification product of 290bp.

Analysis of the products was carried out on 1% agarose gels in TAE buffer stained with ethidium bromide.

Antibody preparation

Antibodies were designed against a synthetic peptide from the predicted 'hinge' region of the *Nv*RARβ2 covering the amino acid residues 175-188, between the DNA binding domain (DBD) and ligand binding domain (LBD). This region was chosen based on solvent accessibility of the predicted 3D structure using the NACCESS program (Hubbard and Thorton, 1993) and on the degree of antigenicity along the polypeptide chain using a bioinformatic tool called JaMBW (Toldo, 1997) with the ANTIGENIC PLOT function (predicted by the algorithm of Hopp and Woods, 1981). This custom made *Nv*RARβ2 antibody was produced in New Zealand white rabbits and affinity purified from the antisera by Pacific Immunology Corp. A commercial antibody against human glyceraldehyde phosphate dehydrogenase (GAPDH) (Abcam Inc.) was also used in Western blotting procedures as a normalizing control. This human GAPDH antibody successfully recognizes the same GAPDH protein in the newt.

Western Blot Analysis

Immediately following tissue collection, the various organs and tail blastemas were frozen in liquid nitrogen and stored at -80°C until required for protein isolation. Each tissue sample was placed in lysis buffer and homogenized for 20 seconds using a PowerGen hand held tissue homogenizer (Fisher Scientific). In order to determine the protein concentration in each supernatant, the BCA protein assay (Pierce) was used, as

per the manufacturer's instructions. 10μg of total protein from each sample was made up to 20ul with lysis buffer and combined with an equal volume of protein loading buffer. The prepared samples were loaded onto a 4% stacking, 12% resolving polyacrylamide gel and run at 100V for 2-3 hours. Gels were then blotted at 100V for 60 minutes onto nitrocellulose membrane (BioRad). Blots were blocked in blocking solution (3% non-fat skim milk powder/0.1% Tween-20 in PBS) for 1 hour, followed by incubation overnight at 4°C with either one of two primary antibodies (1:1000 custom-made *Nv*RARβ2 antibody in blocking solution; 1:10,000 GAPDH antibody in blocking solution). Membranes were next washed 4 times, for 5 minutes each, in PBS/0.1%Tween-20 and incubated in the dark for 45 minutes in Alexa Fluor 680 goat anti-rabbit secondary antibody (1:15,000 in blocking solution; Invitrogen). Membranes were then washed again with PBS/0.1%Tween20, with a final rinse of PBS. Membranes were stored in PBS in the dark at 4°C until visualization at 700nm using an Odyssey Infrared Imaging System (LI-COR Biosciences). The Western blot experiments were performed three times.

Immunofluorescence of *Nv*RARβ2

For immunostaining experiments, the adult newt tail blastemas, at various stages of regeneration, were fixed in 4% paraformaldehyde in PBS at 4°C overnight, and washed in 10% sucrose/PBS for 2 hours, 20% sucrose/PBS for 2 hours, and then overnight at 4°C in 30% sucrose/PBS. After embedding the fixed tail blastemas in Optimal Cutting Temperature (O.C.T.) Compound (Tissue-Tek), serial 20μm sections were cut using a cryostat (Leica microsystems) and placed on Superfrost Plus slides

(Fisher Scientific). The samples were washed in PBS and then permeablized in 0.3% Triton X-100 in PBS (PBT) for 30 min and blocked in 5% normal goat serum (NGS) in PBT for 1 hour at room temperature. The samples were then incubated at 4°C overnight with the primary *Nv*RARβ2-specific antibody diluted 1:100 in blocking solution. As a control, some preparations were incubated only in blocking solution, without the primary antibody, at 4°C overnight. All samples were then washed in PBT 3 x 5 minutes and incubated in 1:500 dilution of Alexa Fluor 488 goat anti-rabbit secondary antibody (Invitrogen) in blocking buffer at RT for 2 hours. The samples were then washed in PBT 3 x 5 min, and then the nuclei were counterstained with DAPI for 2 min, followed by a final wash in PBS. An anti-fade Fluorosave mounting media (Calbiochem) was then applied to the slides and cover slips added. The samples were visualized on a laser confocal microscope (Nikon Canada Inc) and images were captured with NIS-Elements software (Nikon Canada Inc).

Agonist and antagonist treatments of whole animals undergoing tail regeneration

Adult newts were anaesthetized in MS-222 (as mentioned previously), and had the distal third of the tail amputated with a razor blade. Subsequently, the newts were maintained in dechlorinated tap water containing 10^{-6}M LE135 (an RARβ-selective antagonist; a kind gift from H. Kagechika, Tokyo) or in a bath containing 0.01% DMSO (vehicle control) for 21 days. Although DMSO is known to have cytotoxic effects at higher concentrations (above 2% v/v), concentrations less than 0.5% have been shown to be noncytotoxic (Sumida et al., 2011). In fact, treatment of newts with 0.01% DMSO did not appear to have any negative effects on health, or tail regeneration compared to

dechlorinated tap water treatment alone (data not shown). A separate series of experiments was later performed with 10^{-6}M AC261066 (a highly isoform selective agonist for RARβ2; ACADIA Pharmaceuticals Inc.) with a separate group of 0.01% DMSO controls, for 21 days. The newts were fed beef liver three times per week, and the solutions were changed twice weekly. If the solutions appeared cloudy (due to uneaten food particles and waste) before the assigned solution changes, then a quick filtering was performed with a Whatman® filter for coarse particle removal.

After 21 days, all of the newts were removed from their solutions and were photographed under a dissecting microscope using a Nikon DS-U2 camera equipped with NIS Elements software. The length of tail regenerates was determined and a Student's t-test was performed to test for significant differences between the drug and DMSO treatments. Following measurements, the LE135- and DMSO-treated tails were removed for Western blotting, to compare *Nv*RARβ2 protein levels in the tail regenerates. Following the AC261066 (and corresponding DMSO) treatments, the newts were placed back into dechlorinated tap water, and pictures of the tails were taken once again, 5 weeks later.

2.04 Results

The newt RARβ shares a high degree of homology with other vertebrate RARβ2s

Using degenerate primers designed from other known vertebrate RARβ sequences, I was able to generate an initial cDNA fragment from a mixture of newt brain and spinal cord tissue using a modified touchup RT-PCR protocol. Multiple rounds of 5´ and 3´ RACE from the initial cDNA fragment were needed to elucidate the full-length newt RARβ. The final full-length cDNA I obtained was 2,251 bp with a 1347 bp open reading frame that encodes a putative 448 amino acid protein (termed *Nv*RARβ2; accession no. AY847515; as found to be most similar to other vertebrate RARβ2s). Using the Basic Local Alignment Search Tool (BLAST) I determined that this *Nv*RARβ2 has an overall amino acid identity of ~90% with RARβ2 sequences from other vertebrates including *Rattus norvegicus* (rat), *Coturnix coturnix* (common quail), and *Homo sapiens* (human) (Fig. 9). I was confident that this is an RARβ isoform since the closest overall amino acid identity with RARα is 79% (*Xenopus* RARα; accession no. AAI69954) and with RARγ is 73% (*Xenopus* RARγ; AAB47116). As is commonly seen with other nuclear receptors, the most conserved regions in the *Nv*RARβ2 protein sequence are the predicted DNA-binding domain (DBD; Region C), which shares ~99% amino acid identity with the rat RARβ2 DBD (accession no. XP_001059523) and the predicted ligand-binding domain (LBD; Region E) which shares 96% amino acid identity with the rat RARβ LBD (Fig. 9).

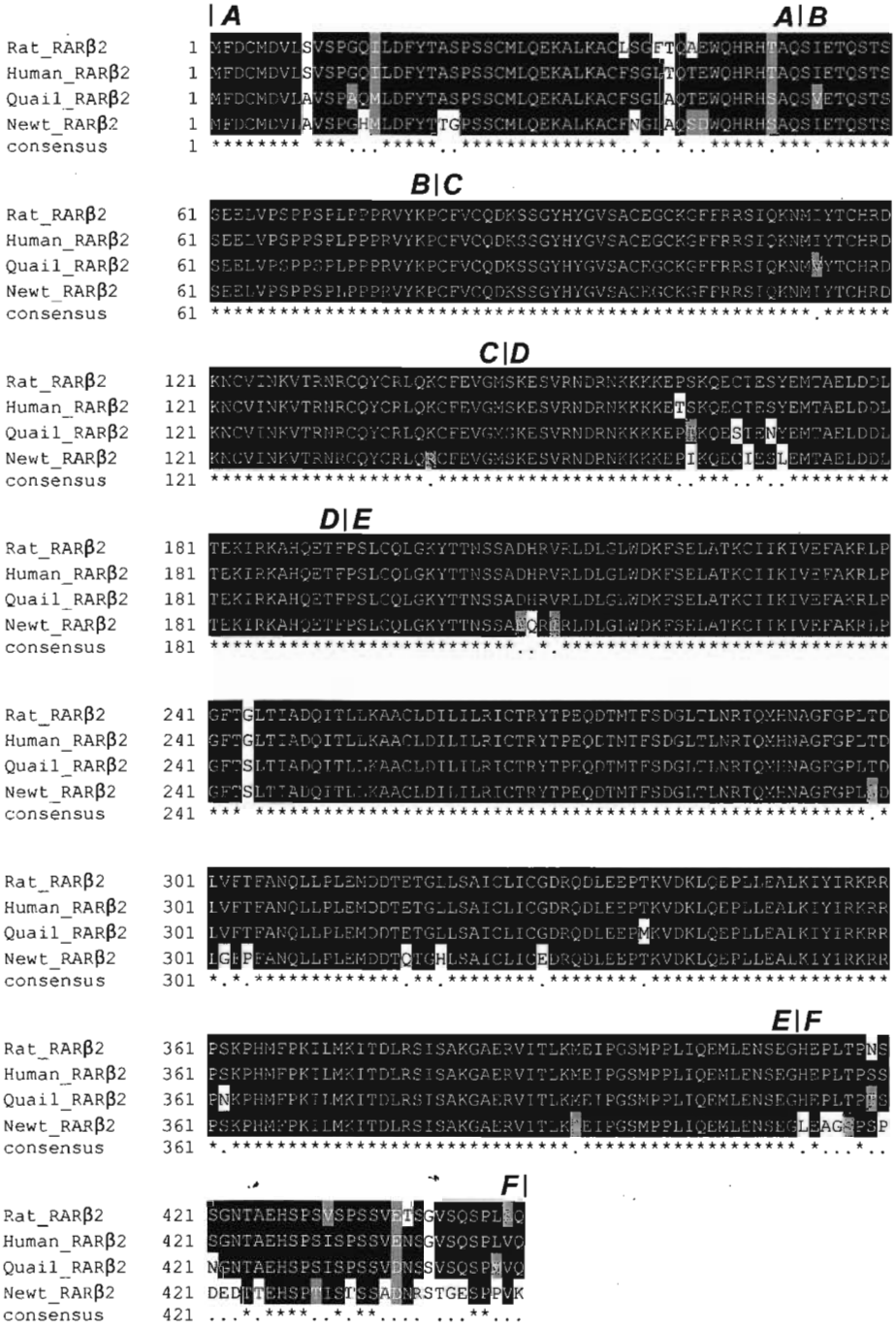

Figure 9. The newt RARβ2 sequence. Multiple alignment of the *Notophthalmus viridescences* RARβ2 (Newt RARβ2; accession no. AY847515), Rat RARβ2 (accession no. EDL94092), Human RARβ2 (accession no. NP_000956), and Quail RARβ2 (accession# AAD23398) proteins. Note the overall high degree of amino acid conservation, especially in the C region which contains the DNA-binding domain (DBD) and in the large E region which contains the ligand-binding domain (LBD; where retinoic acid binds).

Of the RARβ isoforms that are currently known (RARβ1→5), the differences in their amino acid sequence are primarily in the A domain at the N-terminus (except for RARβ5 protein which is missing the A, B, and part of the C domain) (Nagpal et al., 1992; Peng et al., 2004; Zelent et al., 1991). The remaining domains of the RARβ isoforms (up to the terminal F domain) are identical in sequence homology within a given species. The differences in the A region of the different β isoforms not only pertain to the amino acid sequence, but also to the length of the A region. From Figure 9, the alignment of my newly found newt RARβ sequence with other vertebrate RARβ2 protein sequences illustrates that the A region not only displays high amino acid similarity, but also shares an identical length with other RARβ2 receptors.

_Nv_RARβ2 mRNA contains an unusually large 5'UTR region

Previous work has shown that the mouse RARβ2 mRNA contains a long 5′ untranslated region (5′UTR) of 461bp that shares high homology with the human RARβ2 5′UTR region (Zelent et al., 1991). This region in the mouse is known to form very stable secondary structures and contains five upstream small open reading frames (sORFs) preceding the major open reading frame (mORF). Through mutation of these sORFs in mice embryos, it was determined that these sORFs play an important role in control of tissue specific expression and developmentally regulated gene expression of RARβ2 (Zimmer et al., 1994). In Figure 10, the 5′ UTR of *Nv*RARβ2 is depicted along with a portion of the A region of the mORF. This newt 5′ UTR is exactly 795bp and is thus larger than either the mouse or the human 5′ UTR. This makes it closer to the more elaborate 5′ UTR (690bp) of the amphibian RARδ1 sequence obtained from

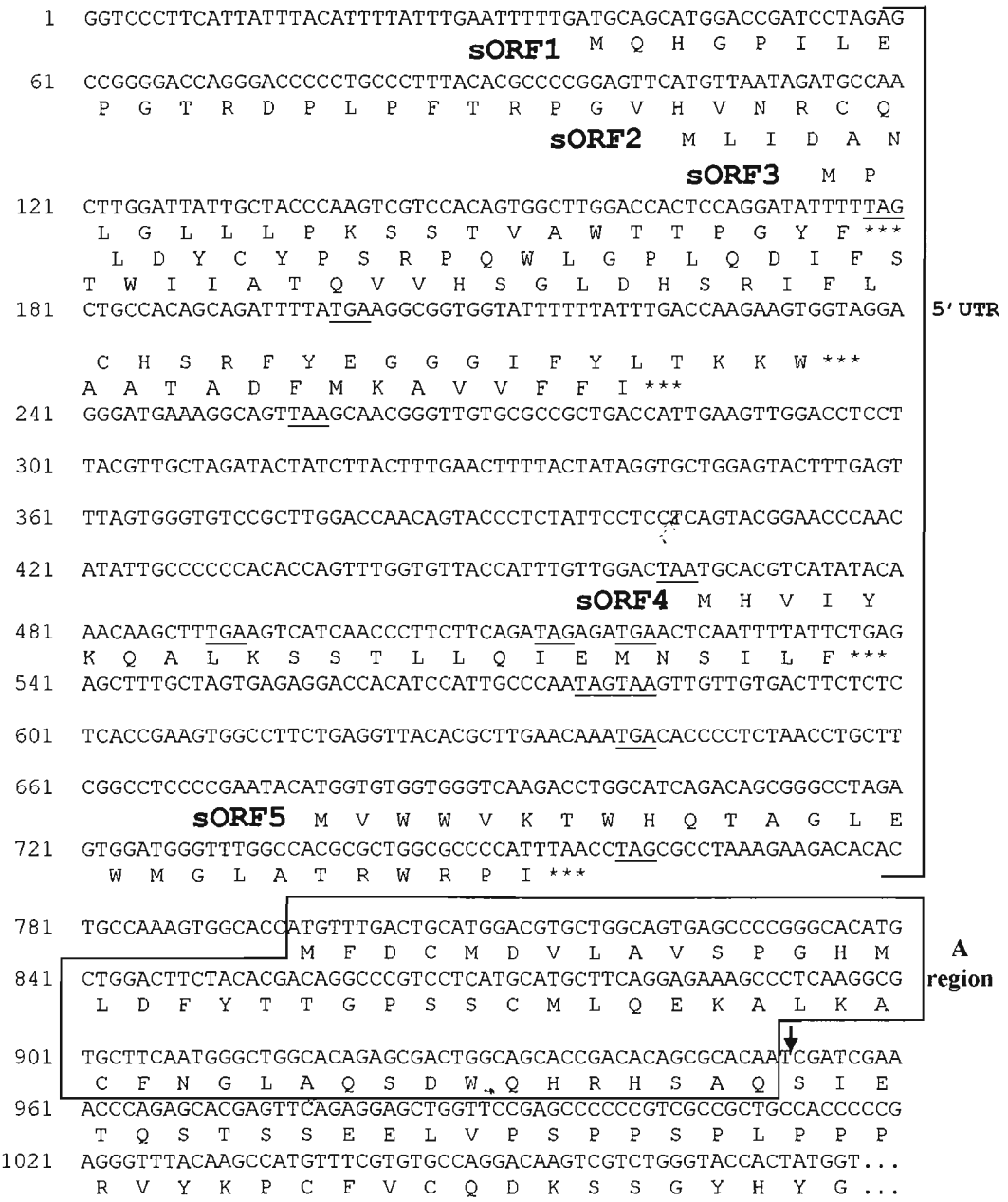

Figure 10. The newly cloned *Nv*RARβ2 cDNA contains an exceptionally long 5′-UTR region. The 5′-UTR (square bracket) and part of the ORF 'A' region (boxed) of the newly sequenced *Nv*RARβ2 cDNA are shown above. All in frame termination codons which lie upstream to the major ORF are underlined. Below the *Nv*RARβ2 5′-UTR sequence, the deduced amino acid sequences of all possible upstream sORFs are indicated. Three successive asterisks indicate a stop codon at the end of the sORFs. The black arrow indicates the site where, in mice and humans, RARβ2 differs in the 5′ end from other known RARβ isoforms.

Notophthalmus viridescens (Ragsdale, Jr. et al., 1993). Interestingly, the *Nv*RARβ2 5′ UTR contains five sORFs (Fig. 10) which is the same number of sORFs in the mouse and human RARβ2s, though there is not a high degree of sequence homology between them. Whether these *Nv*RARβ2 sORFS in the 5′ UTR region play a role in tissue-specific or developmental gene regulation of *Nv*RARβ2 remains to be determined. The *Nv*RARβ2 5′ UTR may also possess strong secondary structures such as predicted from the mouse RARβ2, as sequencing of the newt RARβ2 5′ UTR region was difficult and often needed reagents such as betaine to relax GC rich areas.

_Nv_RARβ2 mRNA expression in regeneration-competent tissues

Although it has been previously shown that RA can induce regeneration in mammalian embryonic CNS tissue, it was reported that adult mammalian CNS cannot respond because RARβ2 is transcriptionally inactivated (Maden and Hind, 2003). I have shown that RARβ2 mRNA is present in the newt CNS, through its initial discovery using degenerate primers and subsequent sequencing of the entire mRNA. However, from this initial work, it was not evident whether the expression was restricted to either the spinal cord or the brain, or whether it was present in both. In the newt, both the brain and spinal cord are capable of extensive regeneration, as are other various organs such as the liver (Williams, 1959). My next aim was thus to determine, using RT-PCR, whether mRNA expression could be detected in tissues of the adult newt that are capable of regeneration. The results of the RT-PCR showed that *Nv*RARβ2 mRNA was not only present in the brain and spinal cord, but was also present in the gut and to a lesser degree in the liver (Fig 11). The transcript was, however, undetectable in the kidney (Fig. 11) though,

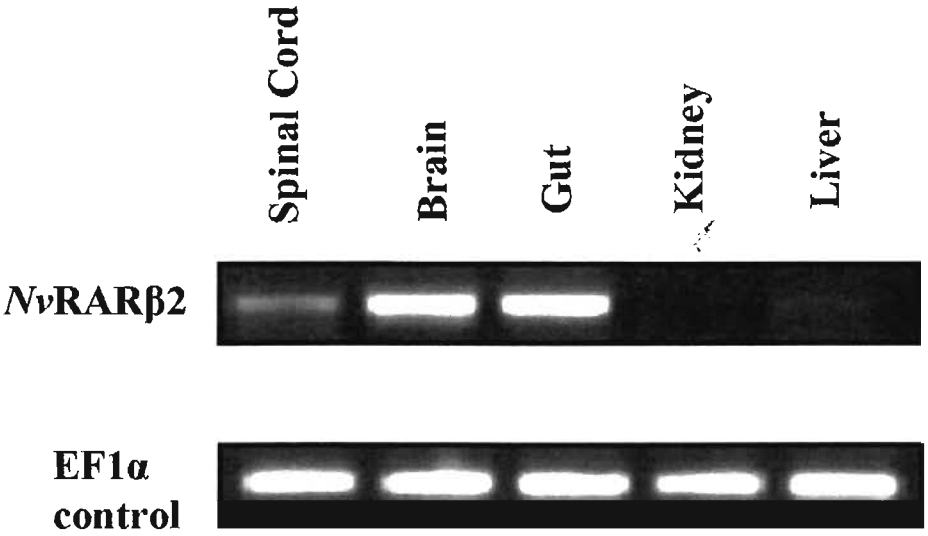

Figure 11. *Nv*RARβ2 mRNA expression in regeneration-competent tissues. RT-PCR analysis revealed the presence of *Nv*RARβ2 mRNA in the acutely isolated newt spinal cord, brain, gut, and low levels in the liver. There were no detectable levels of *Nv*RARβ2 mRNA in the kidney. The newt EF1α was used as a control.

interestingly, there are no previous reports of kidney regeneration in the newt. Primers designed against the newt EF1α were used as a control for RT-PCR. EF1α, a translation elongation factor, is a well-known housekeeping gene commonly used as a control in RT-PCR experiments (Sturzenbaum and Kille, 2001).

Previously, it has been shown that the limb blastema of newts, specifically the wound epithelium, synthesize and release RA (Viviano and Brockes, 1996). In order to transduce the RA signal, the RA must first bind to retinoid receptors. RARδ and RARα sequences have been identified in newt limb blastemas, but no full-length RARβ sequence has ever been cloned from a regenerating blastema. I next performed RT-PCR on amputated limb and tail tissue, in addition to their regenerate blastema tissue after 8 days, in an attempt to identify an RARβ transcript. In Figure 12, it is evident that there is a small, but detectable level of *Nv*RARβ2 mRNA in both the limb and tail at the time of amputation. By day 8 post-amputation (PA), the results indicate that there is a higher level of *Nv*RARβ2 mRNA in both the limb and tail blastemas compared to day 0 (experiment repeated three times). These results indicate that at least at the level of transcription, *Nv*RARβ2 expression is upregulated in the regenerating tail region as a result of amputation.

_Nv_RARβ2 protein is present in some regeneration-competent tissues

Given that the *Nv*RARβ2 transcript is present in tissues of the newt that are known to regenerate, my next aim was to determine if the translation product is also present. Using a custom-made antibody against a synthetic peptide from the 'hinge'

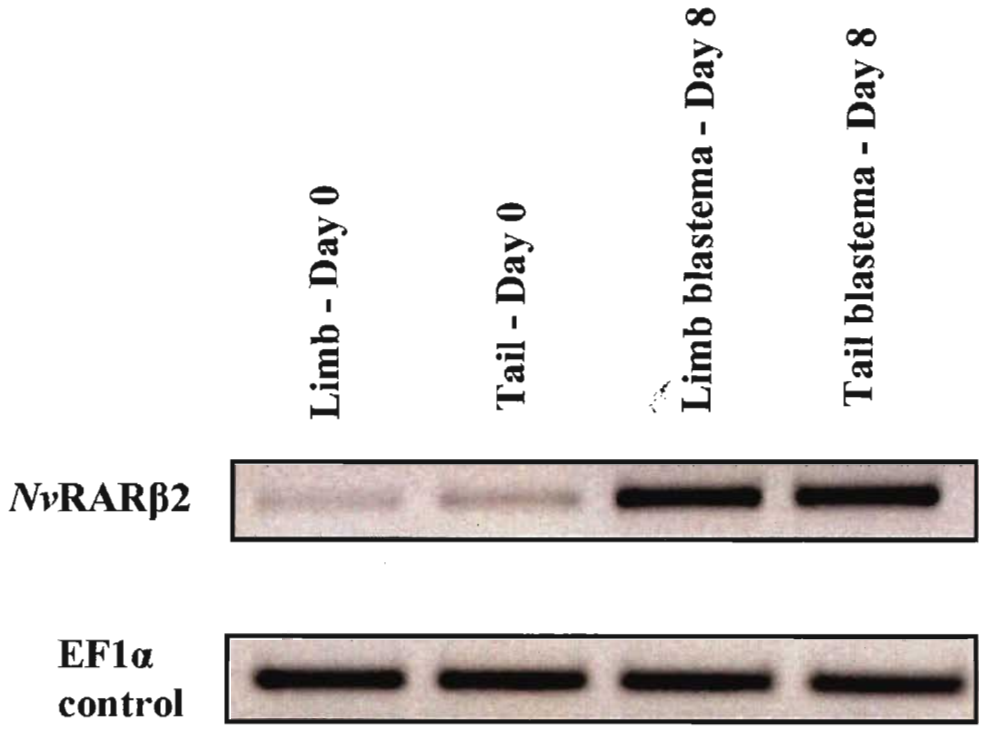

Figure 12. *Nv*RARβ2 mRNA expression increases in limb and tail blastemas after amputation. Low levels of *Nv*RARβ2 mRNA were detected in the acutely amputated newt limb and tail tissues. There was an increase in mRNA levels in the regenerating blastema tissues 8 days after amputation. The newt EF1α was used as a control. Inverting the picture of the gel (white background, black bands) gave better contrast to view the faint 'day 0' bands.

region between the DBD and the LBD of *Nv*RARβ2, Western blot analysis was performed in order to determine the presence of *Nv*RARβ2 protein in regenerating and non-regenerating tissues. Tissues that displayed positive reactivity (spinal cord, brain and gut) revealed a band approximately 50 kDa in size, which is very close to the predicted molecular weight of 50.5 kDa. Although the RT-PCR experiments had previously indicated low levels of mRNA in the liver, the *Nv*RARβ2 protein was actually not detectable in the liver using Western blotting. *Nv*RARβ2 protein was, however, present in the spinal cord and brain, with levels appearing higher in the brain. This finding correlates well with the previous RT-PCR analysis showing higher levels of *Nv*RARβ2 mRNA in the brain compared to the spinal cord. Although I previously did not test for *Nv*RARβ2 mRNA in the gut, it is clear from the Western blot that the gut displayed the highest level of *Nv*RARβ2 protein expression (Fig. 13). This result is intriguing, since the gut is also known to retain regenerative capabilities in the adult newt (O'Steen and Walker, 1962). Consistent with the RT-PCR results, there were no detectable *Nv*RARβ2 protein levels in the kidney. The housekeeping gene, glyceraldehyde 3-phosphate dehydrogenase (GAPDH; an enzyme in the glycolysis pathway) was used as a control for these Western blotting experiments. EF1α would have been an ideal choice to maintain consistency with the RT-PCR experiments, but an antibody capable of detecting newt EF1α was not available.

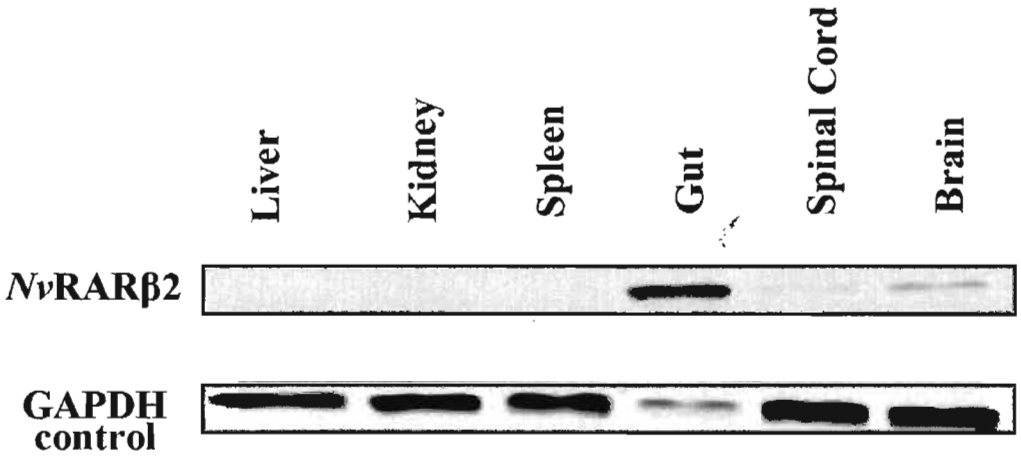

Figure 13. *Nv*RARβ2 protein is detectable in some regeneration-competent tissues. Western blot analysis of various tissues revealed the presence of *Nv*RARβ2 protein in the acutely isolated gut, brain and to a lesser extent in the spinal cord, but undetectable levels in levels in the liver, kidney and spleen. The newt GAPDH was used as a control.

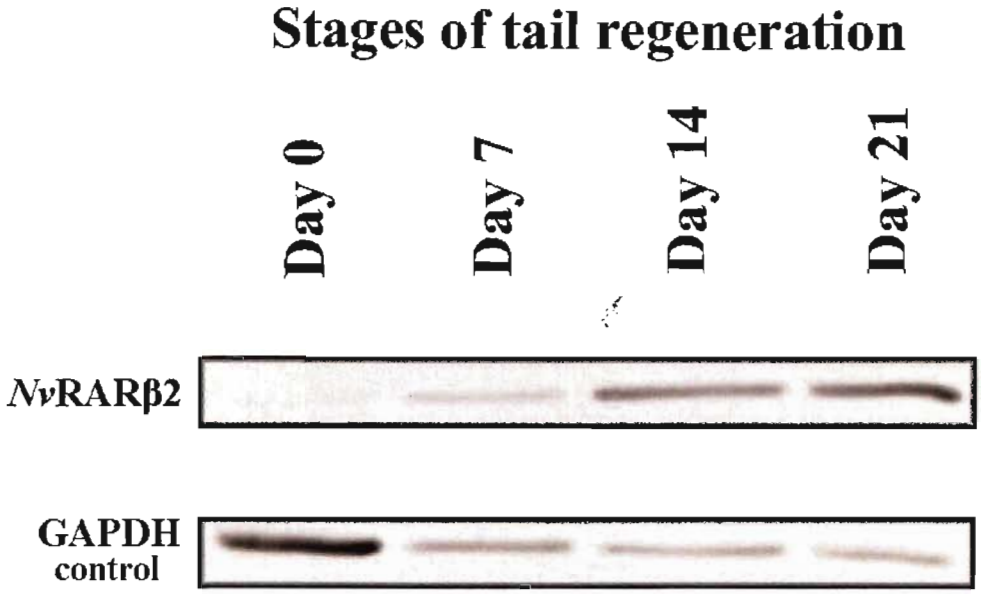

Figure 14. *Nv*RARβ2 protein levels rise in progressing stages of tail regeneration. Western blot analysis at 4 different stages of newt tail regeneration revealed a stepwise increase in the levels of *Nv*RARβ2 protein from day 0 through day 21. The newt GAPDH was used as a control.

*Nv*RARβ2 protein is upregulated in the regenerating newt tail

My next aim was to determine whether *Nv*RARβ2 protein was present in the regenerating tail blastema (containing the caudal tip of the spinal cord) and whether these levels are altered during the first 21 days after amputation. Western blotting indicated that at day 0, there was a very low expression level of *Nv*RARβ2, suggesting that there may be a basal level of *Nv*RARβ2 protein present in the unamputated tail, though this signal may likely originate from the caudal spinal cord (as described below). At day 7, the level of *Nv*RARβ2 protein increased, and it continued to increase by day 14, showing the highest expression on day 21 (Fig. 14). RARβ protein has shown similar elevated levels in transected sciatic nerves of rats (Zhelyaznik and Mey, 2006). However, I could not discern whether the newt RARβ levels in this study were from the regenerating central nerves of the spinal cord, or from the other regenerating structures of the tail blastema.

*Nv*RARβ2 is present in the spinal cord of the regenerating tail

Our lab has previously shown that RA significantly enhances the outgrowth of neurites from cultured spinal cord explants of *Notophthalmus viridescens*, and that this outgrowth was inhibited by the RARβ-selective antagonist, LE135 (Dmetrichuk et al., 2005). Since RARβ2 was previously suggested to be the key transducer of the regenerative RA signal in embryonic mouse DRG neurons (Corcoran et al., 2000) and upregulation of RARβ2 alone stimulated regeneration of neurites in the adult mouse spinal cord *in vitro* (Corcoran et al., 2002), I next aimed to determine whether the newly identified *Nv*RARβ2 is expressed in the spinal cord of the regenerating tail, and if so, to determine its localization. Using the *Nv*RARβ2-specific custom-made antibody, I

performed immunohistochemistry on various stages of tail regeneration. When the tail was acutely isolated (day 0) and cross-sectioned, *Nv*RARβ2 immunoreactivity was detected in the region known to contain ependymal cells surrounding the central canal of the spinal cord (Fig. 15Ai; red arrow). There was also strong staining around the periphery of the spinal cord (Fig. 15Ai; yellow arrow), consistent with the layer of meninges that surround and protect the CNS. Interestingly, the cells of the meninges are also known to secrete all-*trans* RA (Siegenthaler et al., 2009) and have been implicated in guiding axons during newt spinal cord regeneration (Zukor et al., 2011). The presence of *Nv*RARβ2 in the spinal cord at day 0 is consistent with the detectable levels present in total protein from acutely isolated tails by the Western blot (day 0; Fig. 14). By day 7 PA, a cross-section of the tail blastema also revealed immunoreactivity in the ependymal cells surrounding the central canal (Fig. 15Bi, red arrow) and in the region known to contain the meninges (Fig. 15Bi; yellow arrow; which is similar in distribution to Figure 15Ai). On day 14 of tail regeneration, sagittal sections of the blastema were prepared and examined to determine the rostral-caudal distribution of *Nv*RARβ2 protein in the ependymal tube extending into the blastema. Immunoreactivity is evident in this ependymal tube, which will eventually become the new spinal cord (Fig 15Ci; purple arrow). There is also reactivity in the ependymal bulb at the caudal tip of the ependymal tube (Fig. 15Ci; pink arrow).

_Nv_RARβ2 signals in the spinal cord and epidermis of day 21 blastemas

From the Western blot results in Figure 14, it was shown that the highest expression of *Nv*RARβ2 protein in the newt tail regenerates occurred on day 21 PA. I

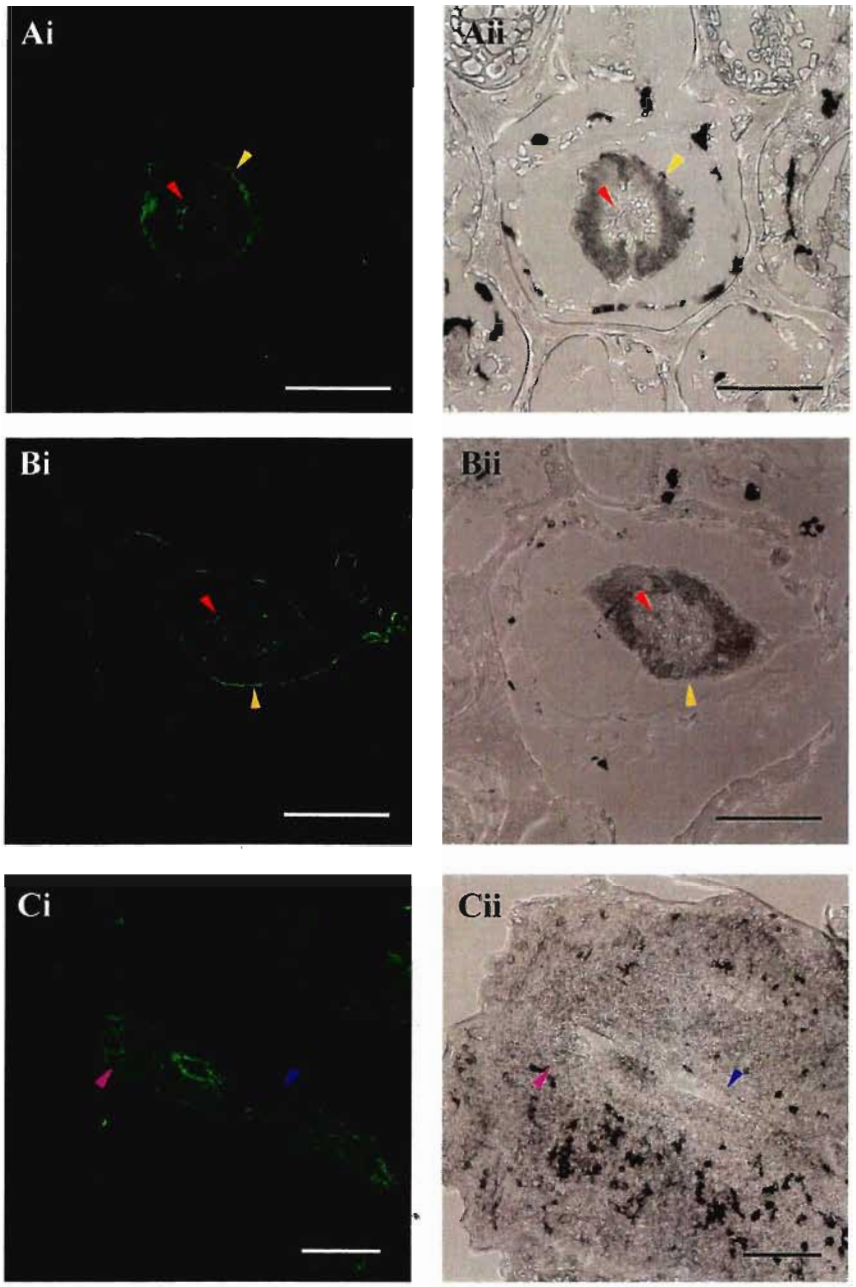

Figure 15. *Nv*RARβ2 is present in the spinal cord region of the regenerating tail. (Ai,ii) Immediately after amputation of the newt tail (day 0), immunostaining of a cross-section with the *Nv*RARβ2 antibody revealed a signal in the ependymal cells surround the central canal of the spinal cord (red arrows), and also the outer perimeter of the spinal cord (yellow arrows), which may contain some of the dura matter. (Bi,ii) Immunostaining of a similar cross-section at day 7 of tail regeneration with the *Nv*RARβ2 antibody also displayed signal in the ependymal cell region (red arrows) and periphery of the spinal cord (yellow arrows). (Ci,ii) Immunostaining of a sagittal section at day 14 of tail regeneration with the *Nv*RARβ2 antibody revealed a signal throughout the blastema but a strong signal is seen along the ependymal tube (purple arrow) and into the ependymal bulb (pink arrow), which will eventually become new spinal cord in the fully regenerated tail. All scale bars: 250 μm.

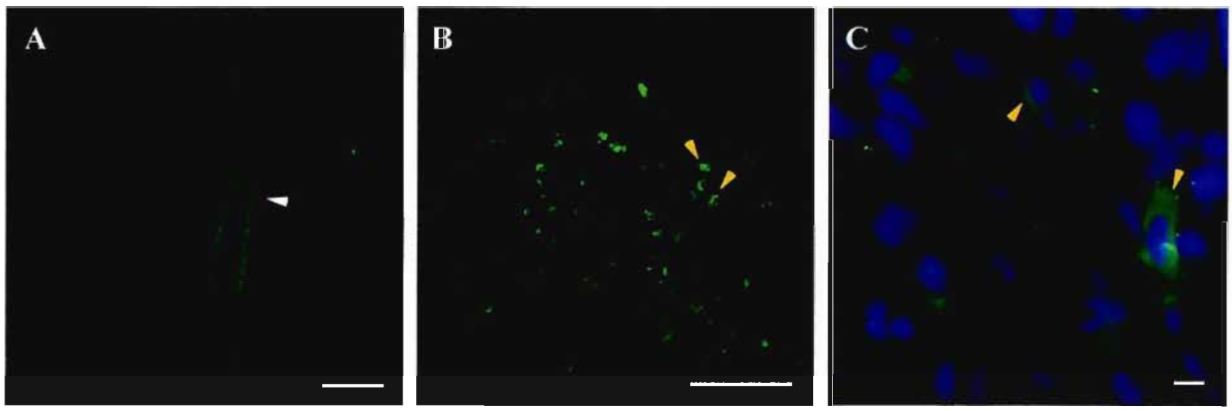

Figure 16. *Nv*RARβ2 is present in the spinal cord and mesenchyme region of the regenerating tail at day 21. (A) Strong immunoreactivity is still observed in the regenerating spinal cord at day 21 (white arrow). Scale bar: 150 μm. (B) In the mesenchyme region towards the tip of the regenerating tail blastema, there are numerous cells that display strong immunostaining for *Nv*RARβ2 (yellow arrows). Scale bar: 150 μm. (C) Upon higher magnification of the mesenchymal region, the *Nv*RARβ2 immunostaining in these cells appears to be localized to the cytoplasm. Note the lack of *Nv*RARβ2 staining in the nuclei stained blue with DAPI. Scale bar: 20 μm.

next aimed to determine the localization of *Nv*RARβ2 protein in sagittal sections of day 21 tail regenerates. In Figure 16A (white arrow), day 21 tail blastemas showed expression of *Nv*RARβ2 in the regenerating spinal cord within the blastema. In addition, a closer inspection of the mesenchyme region towards the tip of the tail blastema revealed strong immunoreactivity in a number of loose mesenchyme cells (Fig. 16B). It is known that the wound epidermis and mesenchyme are sources of RA synthesis during regeneration of the axolotl limb (Maden, 1998). If this is true during newt tail regeneration, and RA can upregulate RARβ2 as previously shown (Corcoran et al., 2002), then this may explain the strong immunoreactivity for RARβ2 in this mesenchyme area. Interestingly, higher magnification of this mesenchyme domain revealed that these *Nv*RARβ2-positive cells display a cytoplasmic localization of RARβ2 as there is little overlap with the nuclear DAPI stain (Fig. 16C).

An RARβ-selective antagonist (LE135) inhibits tail regeneration

It has previously been shown that the RARβ-selective antagonist LE135 can inhibit normal patterning during limb regeneration in the axolotl, *Ambystoma mexicanum* (del Rincon and Scadding, 2002) and can also inhibit neurite outgrowth from spinal cord cultures of *N. viridescens* (Dmetrichuk et al., 2005). However, an RARβ cDNA had never been fully cloned from either the axolotl or the newt. Since I had found that *Nv*RARβ2 is upregulated in newt tail regeneration (Fig. 14), I next aimed to use LE135 in order to elucidate a functional role for the RARβ2 receptor in this process. Adult newts undergoing caudal tail regeneration were bath-treated with the RARβ-selective antagonist

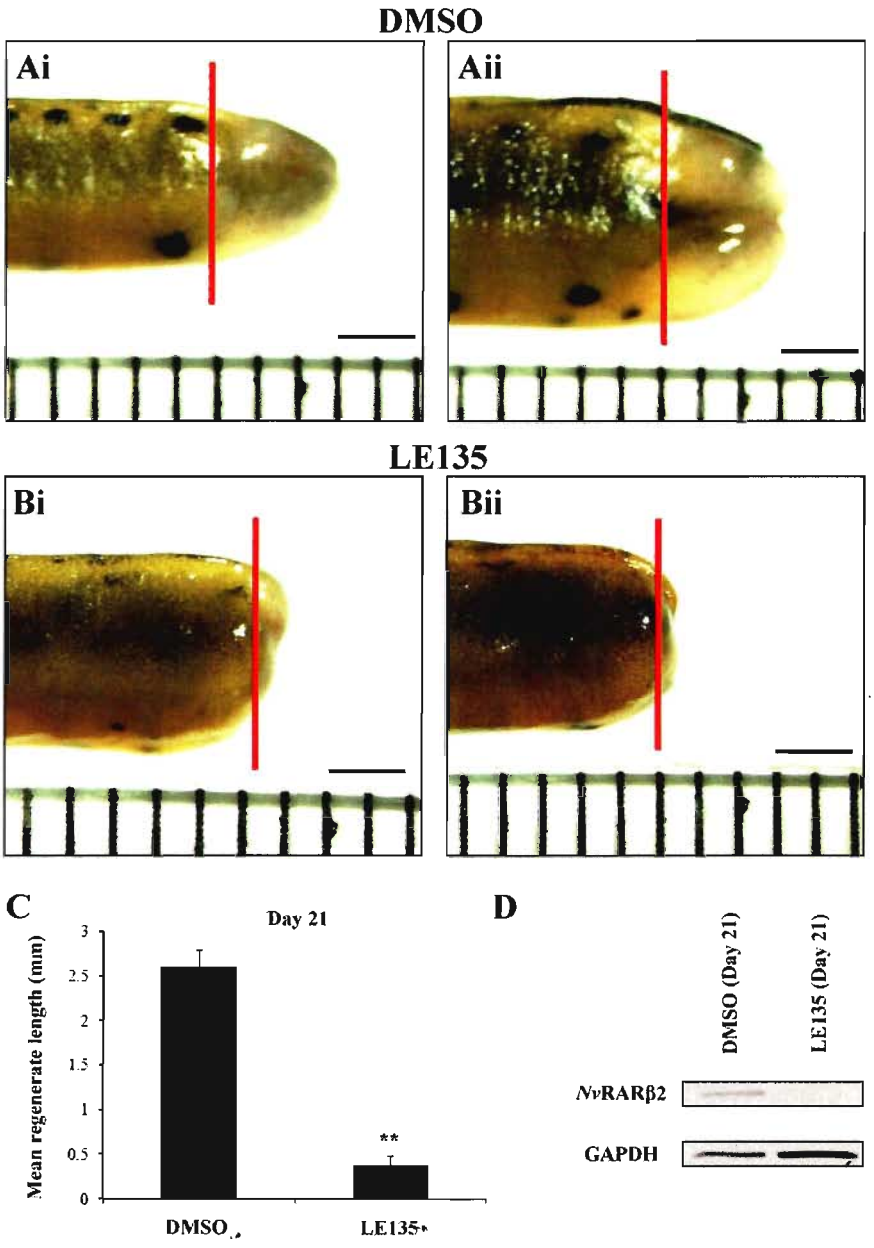

Figure 17. The RARβ-selective inhibitor, LE135, significantly reduces the length of tail regenerates. (Ai,ii) Two representative examples of newt tail regenerates after 21 days of immersion in the vehicle control DMSO (0.01% in dechlorinated water). The mean length of all regenerates was 2.60±0.19mm (n=8). (Bi,ii) Two representative examples of newt tail regenerates after 21 days of immersion in 10^{-6}M LE135. The mean length of these LE135-treated regenerates was 0.38±0.09 mm (n=8) which was significantly less than the vehicle control group (C; student t-test, **p<0.01). All scale bars: 2 mm. (D) For both test and control conditions, the tail regenerates were removed following measurements at day 21 and total protein was extracted for Western blot analysis. Using the *Nv*RARβ2 antibody, signal was detected in the DMSO-treated group, whereas no signal was apparent in the LE135-treated group.

LE135 (10^{-6}M), beginning at the time of amputation. The length of the tail regenerates was measured after 21 days of treatment (which coincides with the highest expression of *Nv*RARβ2 protein) and I found that the LE135-treatment significantly inhibited the tail regeneration process (Fig. 17Bi&ii) compared to DMSO alone (Fig. 17Ai&ii). The mean tail regenerate length in LE135-treated animals (0.38 ±0.09 mm) was significantly reduced ($p<0.01$) compared to DMSO-treated control regenerates (2.6±0.16 mm) after 21 days (Fig. 17C). Moreover, Western blotting demonstrated that LE135-inhibition of RARβ signaling led to a decrease in the expression of *Nv*RARβ2 protein at 21 days after amputation (Fig. 17D), suggesting a possible autoregulatory control for receptor expression in the newt, (as seen previously with mammalian RARβs) (de The et al., 1989).

An RARβ2-selective agonist (AC261066) inhibits tail regeneration

Previous experiments have shown that treatment of frog tadpoles with high levels of vitamin A (the precursor to RA) can lead to multiple limb structures growing from previously amputated tails (called homeotic transformation), indicating a severe disruption in proximal-distal patterning (Mahapatra and Mohantyhejmadi, 1994; Mohanty-Hejmadi et al., 1992). Conversely, it has been previously shown that vitamin A treatment inhibited tail regeneration in the adult newt, *N. viridescens* (Scadding, 1986). Since these experiments did not determine which receptor isoform may be involved in the aberrant effects of excessive or diminished vitamin A levels, I next aimed to determine whether the RARβ2-selective agonist, AC261066, would mimic either of these effects previously reported. Tails were again amputated from *N. viridescens*, AC261066 was

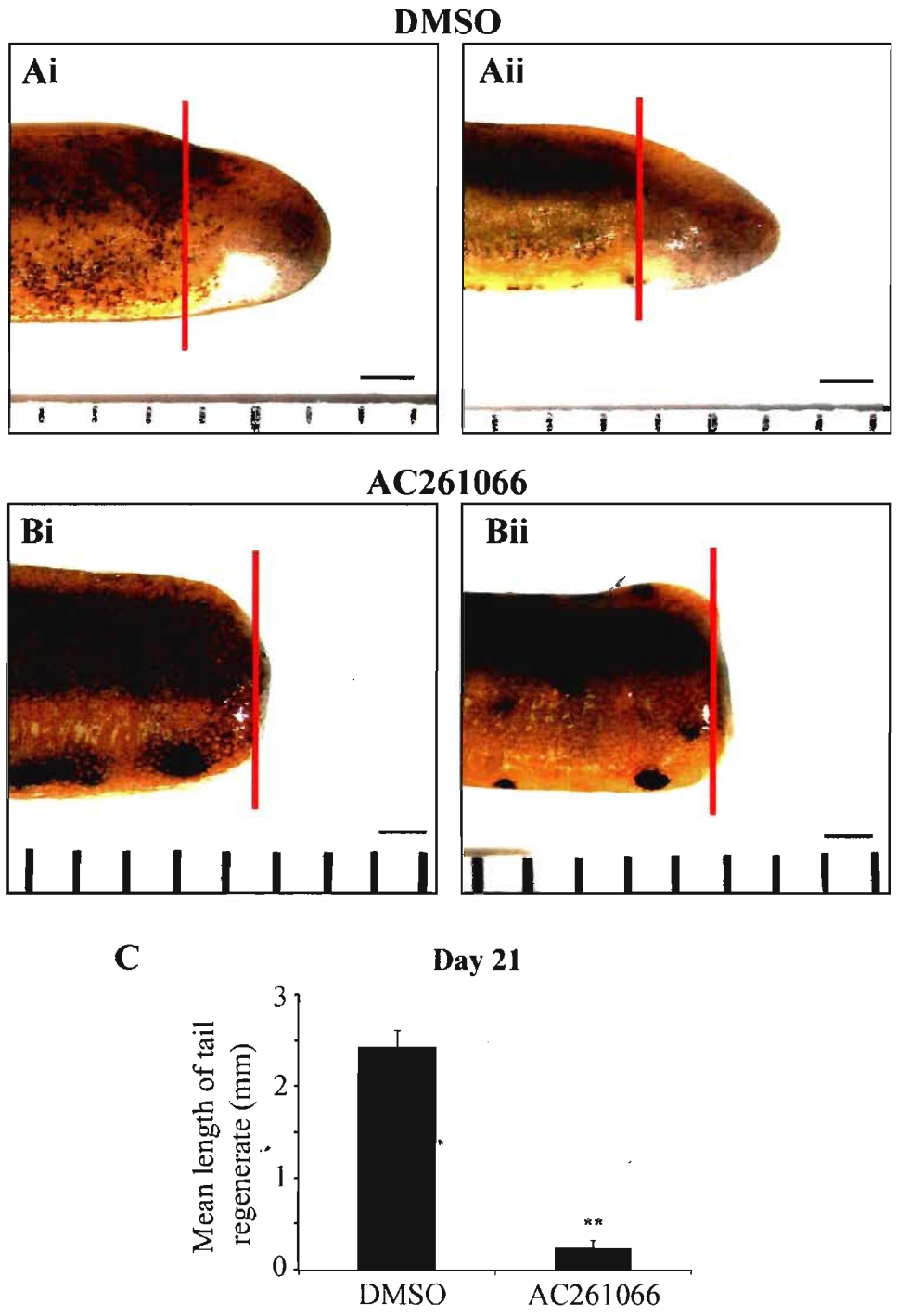

Figure 18. The RARβ2-selective agonist, AC261066, significantly reduces the length of tail regenerates. (Ai,ii) Two representative examples of newt tail regenerates after 21 days of immersion in the vehicle control DMSO (0.01% in dechlorinated water). The mean length of the regenerates was 2.44±0.18mm (n=6). (Bi,ii) Two representative examples of newt tail regenerates after 21 days of immersion in 10^{-6}M AC261066. The mean length of these AC261066-treated regenerates was 0.25±0.08 mm (n=8) and this is significantly less than the vehicle control group (C; student t-test, **p<0.01). All scale bars: 1 mm.

added by bath application at day 0, and the length of tail regenerates was measured at 21 days. Interestingly, AC261066-treatment significantly inhibited the tail regeneration process (Fig. 18Bi&ii) compared to DMSO controls (Fig. 18Ai&ii). These results indicate that both the RARβ2 agonist and the RARβ antagonist exerted similar effects on tail regeneration. The mean tail regenerate length in AC261066-treated animals (0.25 ±0.08 mm) was significantly reduced ($p<0.01$) compared to DMSO treated control regenerates (2.44±0.18 mm) after 21 days (Fig. 18C).

Interestingly, when these AC261066-treated newts were removed from the agonist at 21 days (time of analysis) and then placed back into normal pond water, tail regeneration commenced. Five weeks after removal from the AC261066, the tail had regenerated, albeit with an alteration in the dorsal-ventral patterning (Fig. 19B) compared to a normal tail regenerate (Fig. 19A). It would appear from Fig. 19B that a greater portion of the tail regenerate mass was contained in the dorsal region, compared to an equal distribution between the dorsal and ventral regions in the DMSO treatment (Fig. 19A).

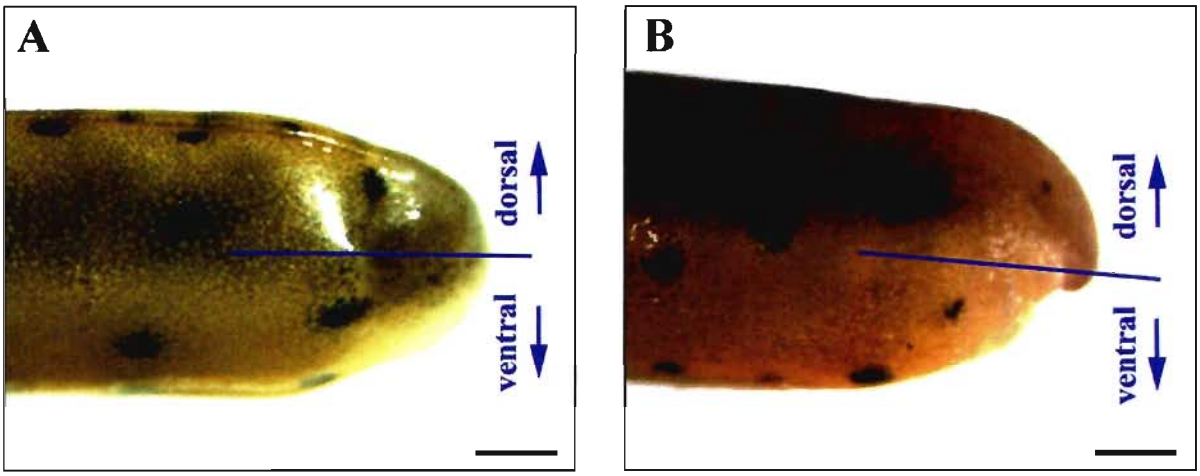

Figure 19. Delayed regeneration 5 weeks after agonist treatment shows disrupted patterning (A) Representative example of a newt tail regenerate after 21 days of immersion in dechlorinated tap water with DMSO. (Bi,ii) Representative example of a newt tail regenerate 5 weeks in dechlorinated tap water, after 21 days of immersion in 10^{-6}M AC261066. Note the abnormal tail regeneration with a larger portion of the regenerate mass in the dorsal region, compared to the ventral region. All scale bars: 2 mm.

2.05 Discussion

In this study, I have cloned a full length cDNA encoding the newt retinoic acid receptor β2 subtype (*Nv*RARβ2) and have characterized its spatial and temporal expression patterns in the regenerating tail and caudal spinal cord of adult newt, *Notophthalmus viridescens*. In addition, I have shown that interrupting RARβ signaling with a selective agonist or antagonist, resulted in the inhibition of normal tail regeneration in the adult newt.

Giguere et al. (1989) first reported the presence of a functional RAR receptor in the blastema of regenerating newt limb tissue. Though it was reported that this RAR was most similar to the β sub-type, it was later shown to be a chimera made up of two non-overlapping cDNA clones (Ragsdale, Jr. et al., 1989). The 3′ end of the clone covered most of the E and F domains, including the 3′ untranslated region, and was eventually determined to be a partial RARδ sequence. The 5′ clone, on the other hand, was more β-like and included a region equivalent to 155 amino acids covering the B, C, and D domains of what eventually would turn out to be a portion of the 448 amino acid *Nv*RARβ2 sequence that I have cloned in this study. However, prior to my study (in the absence of a fully cloned RARβ-type receptor), it was hypothesized over the years that newts do not possess an RARβ subtype (Maden and Hind, 2003). Hence, my results describe the first fully cloned newt RARβ subtype from regenerating newt tissue. The predicted amino acid sequence of this newt RARβ shares greater than 90% identity with all regions of many mammalian RARβ2 mRNAs.

Indirect evidence for a functional RARβ receptor came from previous studies in our lab by Dmetrichuk et al. (2005), who used the RARβ-selective antagonist to inhibit

RA-mediated outgrowth from newt spinal cord explants. Here, I have provided further evidence for a functional role for RARβ in newt spinal cord regeneration. The immunostaining experiments showed expression of an RARβ-like protein in the regenerating spinal cord, as well as the blastemal tissue of the regenerating newt tails.

It is important to note that the Western blots in this study used a custom-made antibody against the D domain (hinge region) of the *Nv*RARβ2 protein, and produced only one band at the predicted molecular weight. These data suggest that only one isoform of newt RARβ is present. The D (hinge) domain of the various mammalian isoforms of RARβ (1 to 5) are identical, but the isoforms would differ in their overall molecular weight. Given this information, I would predict that (if similar to mammals), the D domain of the different newt isoforms of RARβ would also be identical, and thus would all be detectable by our custom-made antibody. If multiple isoforms were indeed present in the regenerating newt tail, I would thus predict the presence of multiple bands, which did not occur. Though these data support the presence of one RARβ2 isoform, I can not entirely rule out the presence of other β isoforms from the Western blotting alone.

This newly identified *Nv*RARβ2 has an unusually long 5′-UTR of 795 bp, which is considerably longer than the 5′-UTR found in the mouse and human RARβ2 (~460 bp; (Zimmer et al., 1994). Although the 5′-UTR of *Nv*RARβ2 is ~350bp longer than the mouse and human RARβ2, it contains the sORFs preceding the mORF. These sORFs contain 'AUG' translational start sites that precede the 'AUG' for the mORF and can cause inhibition of downstream translation, thereby acting as a rate limiting factor in protein synthesis from the mORF (Zimmer et al., 1994). mRNAs that code for proteins involved in processes of cell growth and differentiation often contain these sORFs in the

5′UTR (Kozak, 1991). Since RA has been strongly implicated in cell growth and differentiation (Maden and Hind, 2003) and normally acts through nuclear receptor binding to transduce its signal, it is not surprising that *Nv*RARβ2 contains multiple sORFs in its 5′UTR. In the mouse RARβ2, it has been shown that mutations in the start/stop codons of the sORFs can result in altered regulation of RARβ2 in the heart and brain regions of developing embryos (Zimmer et al., 1994). Although the function of these sORFs of *Nv*RARβ2 was not determined in this study, it is quite likely that they exert some control over the expression of this receptor during regeneration.

I have shown here that both *Nv*RARβ2 mRNA and protein are expressed in the adult newt spinal cord and brain. Based on my immunofluorescent studies in newt tail regenerates, it appears that the highest levels of the receptor protein are expressed in the spinal cord and ependymal tube extending caudally into the blastema during the regeneration process. Corcoran et al. (2002) had previously postulated that the absence of (or below-threshold) expression of the RARβ2 receptor in the adult rat spinal cord, contributed to its inability to extend axons in response to injury. Indeed, even though all three RXRs and RARα were shown to be expressed and localized within the cytosol of neurons in uninjured adult rat spinal cord, no expression of RARβ was reported prior to, or at any time points examined after the spinal cord crush injury (Schrage et al., 2006). Conversely, in my study with the adult newt (which has spinal cord regeneration capabilities), I have demonstrated that both *Nv*RARβ2 mRNA and protein levels are not only present in the uninjured SC, but are then upregulated as a consequence of tail amputation. Increased expression occurred within the first 8 days after injury and continued to show higher levels throughout the first 21 days of regeneration. The time

course of this upregulation is consistent with previous studies on peripheral nerve regeneration in the rat, where protein levels of RARβ (as well as RARα and RXRα) were increased at 4, 7 and 14 days after sciatic nerve crush (Zhelyaznik and Mey, 2006). It is of importance to note that I have recently cloned the first reported newt RXR from the tail blastema of *N. viridescens* (termed *Nv*RXR; see Appendix 1). Interestingly, this *Nv*RXR is highly expressed at day 0 of tail amputation, but is down-regulated during the first 21 days of regeneration (opposite to what was shown with *Nv*RARβ2; Appendix 1). Future studies will be needed to determine the spatial distribution and function of this novel newt RXR in the process of tail regeneration.

Within the spinal cord, I have shown that *Nv*RARβ2 protein was localized to the ependymal cells and meningeal tissues surrounding the spinal cord in the non-regenerating tail. The *Nv*RARβ2 protein appears to be upregulated in the ependymal tube and bulb during the first 14 days after tail amputation with little expression in the blastemal mesenchyme. Ependymal cells of the spinal cord have been postulated to play an important early role in the regeneration of the caudal spinal cord of adult newts (Chernoff et al., 2003). By the third day post amputation, these cells have migrated and sealed off the lumen of the cut spinal cord, creating the terminal ependymal bulb (Chernoff et al., 2003), while the ependymal cells just rostral to this cut site proliferate and extend an ependymal tube into the blastema (Zhang et al., 2003). Stem cells within this population of ependymal cells will ultimately differentiate into glial cells, CNS neurons and peripheral ganglia, thereby restoring function (Chernoff et al., 2003). Whether signaling through *Nv*RARβ2 plays a role in these proliferating and

differentiating processes of the ependyma during newt tail regeneration, remains to be determined.

Other cell types involved in retinoid signaling through RARβ in the newt spinal cord after spinal cord injury (SCI) remain to be elucidated. For example, it is currently unclear where the ligand (all-*trans* RA) for this receptor is synthesized within the newt spinal cord, either before or after injury. Some of the earliest evidence for a role for retinoid signaling in SCI was provided by Mey et al. (2005) in the rat spinal cord, who demonstrated that RALDH2, the enzyme catalyzing the conversion of retinaldehyde to all-*trans* RA, significantly increased as a consequence of a contusion injury by day 4 post-injury, and then peaked at 8-14 days after the lesion. Before injury, RALDH2 was present in the meninges, whereas after lesioning, RALDH2 was upregulated in the meninges and colocalized with a population of oligodendrocyte precursors, thought to be derived from the meninges. These oligodendrocytes are postulated to migrate to the wound site and proliferate following SCI (Kern et al., 2007; Mey et al., 2005).

Zukor et al. (2011) have recently provided evidence for a role of meningeal cells in forming a permissive environment for axon regeneration in the newt after spinal cord transection injury. It would be interesting to determine if these newt meningeal cells were sites for all-*trans* RA synthesis. In mammalian development, meningeal cells are known to secrete RA (Shearer et al., 2003) and after SCI they are known to significantly increase the extent of RALDH2 distribution, indicating an increase in the production of RA (Mey et al., 2005). In the recently published newt model for spinal cord regeneration, Zukor et al. (2011) have proposed that an increase in RA production from the meningeal cells may act as a guidance cue for regenerating axons. It was also proposed by Zukor et al. (2011)

that in spinal cord transection in newts, meningeal cells are one of the first cell types to enter the lesion site. Since it is known that mesenchymal cells within the blastema can also produce all-*trans* RA (Maden, 1998), and since my experiments show RARβ2 expression in the meninges, this process of meningeal cell migration into the lesion may involve signaling though RARβ2, although future experiments would be needed to confirm this.

Our lab has already provided evidence that all-*trans* RA exerts chemotropic effects on regenerating neurites from newt spinal cord explants, and also provided evidence through the use of LE135, that this chemoattraction involves an RARβ-like receptor. It is evident from my work here that *Nv*RARβ2 protein is expressed early in the ependymal cells lining the central canal of the regenerating spinal cord, and so may be involved in guiding migration of these ependymal cells in response to RA. It is also interesting that the localization of *Nv*RARβ2 protein, which I have shown to be mainly cytoplasmic in cells of the wound epidermis at the tip of the blastema (an area known to produce RA) at day 21, appears to have a non-nuclear distribution in these same ependymal cells (Fig. 15Ai&Bi; red arrows), although without DAPI staining, I cannot determine this with complete confidence. This non-nuclear distribution might even suggest that the *Nv*RARβ2 is exerting non-genomic effects, possibly in RA-mediated chemoattraction (as has been shown for other retinoid receptors; Farrar et al., 2009). Interestingly, the RARβ has recently been implicated in a rapid, non-genomic response involving transmitter release at developing neuromuscular synapses in *Xenopus* cell cultures (Liao et al., 2004). Whether *Nv*RARβ2 is acting non-genomically in the

regenerating tail, or whether it is translocated to the nucleus at various stages, in order to transduce its signal, would also need further investigation.

The above results indicate that *Nv*RARβ2 may play a role in tail regeneration in the adult newt, possibly within the ependymal cells, meninges, and/or wound epithelium during the early post-amputation stages. In fact, bath treatment with the RARβ-selective antagonist, LE135, resulted in a significant inhibition of adult newt tail regeneration by 21 days. It is difficult to determine whether LE135 exerted its effects by inhibiting ependymal cell migration, mesenchyme proliferation, or whether it exerted its effects by inhibiting spinal cord regeneration. Inhibition of spinal cord regeneration alone might indeed be responsible, as there is strong evidence that regeneration of body parts depends on the nervous system, and denervation results in failure to regenerate. This is true for limb and tail regeneration of urodeles, including the newt (Singer, 1952). Further support for this hypothesis comes from preliminary work in our lab that found that local application of LE135 directly into the central canal of the spinal cord also inhibited tail regeneration (Clark, 2010). When LE135-soaked beads were implanted into the spinal cord immediately after tail amputation, the length of the tail regenerate was significantly inhibited after 21 days (although this inhibition was not as pronounced as my LE135 bath treatment condition). Further histological evidence suggested that the LE135 bead treatment negatively affected the growth of the ependymal tube. Interesting, if the LE135 bead treatment was delayed for 6 days after tail amputation, there was no significant effect on regenerate length at 21 days (Clark, 2010). This would indicate that there is a critical period of RARβ signaling (within the first 6 days PA) within and surrounding the

damaged caudal end of the spinal cord that appears to be required for normal tail regeneration.

One of the most remarkable effects of retinoids on regenerating systems is the homeotic transformation of tails into limbs in various species of frog tadpoles, which can be accomplished by treatment with high levels of all-*trans* RA and retinyl palmitate (an RA precursor) (Maden, 1993; Mohanty-Hejmadi et al., 1992). A similar effect has also been reported in frog tadpoles with the RAR pan-agonist, TTNPB, further implicating a role for RARs in this process (Maden and Corcoran, 1996). In the adult newt, *N. viridescens*, it has been shown that higher levels of RA can cause entire limb structures to grow from limbs amputated at the midforearm, producing an extra elbow joint (Maden, 1998). Taken together, these effects of RAR agonists have been interpreted as a re-specification of positional information along the appendage axis in a proximal direction. In this study I used the RARβ2-selective agonist, AC261066, to investigate whether stimulation of the *Nv*RARβ2 receptor protein could elicit respecification of tail blastema cells resulting in either homeotic transformation, or some form of respecification along the rostral-caudal axis during tail regeneration. Although somewhat unexpected, bath treatment with AC261066 for 21 days after tail amputation produced significant inhibition of tail regenerate length, similar to that seen with LE135. However, other studies have also shown that excess exogenous RA can actually inhibit tail regeneration, in the axolotl, *Ambystoma mexicanum*, and in the newt, *Notophthalmus viridescens* (Pietsch, 1987; Scadding, 1986). The previous effects of RA on re-specification of positional information may perhaps have resulted from RA acting on other RARs (besides the β subtype), that may also play some role in appendage regeneration. From

the results of this study, it would appear that there may be a critical level of *Nv*RARβ2-signaling that needs to occur for proper tail regeneration. Altering this signaling with either an RAR-selective antagonist or RARβ2-selective agonist severely inhibited this process.

Although AC261066 treatment did not result in respecification of positional information during tail regeneration after 21 days, an interesting phenomenon occurred after removal of the agonist. Within the first few weeks after being returned to normal pond water, the tail began to regenerate again, possibly due to a release of inhibition from AC261066. More importantly, 5 weeks after removal from AC261066, it was evident that the tail regenerate was altered in the dorsal-ventral plane. More specifically, a larger portion of the tail regenerate mass was located in the dorsal region of the tail, compared with the ventral region. It is difficult to explain this result, although it is well known that RA plays a role in the establishment of dorsal-ventral positional information (McCaffery and Drager, 1994; McCaffery et al., 1999). There is a concentration gradient of all-*trans* RA along the anterior-posterior axis, in addition to the proximal-distal axis in axolotl blastemas (although only studied in the limb regenerates). However, it is the RARδ2 isoform that has previously been implicated in playing a role in dorsal-ventral respecification during limb regeneration in newts (Pecorino et al., 1996). I can thus only speculate that the inhibition of *Nv*RARβ2 isoform may either have had an indirect effect in disrupting the RA gradient, or may have had an indirect effect on the signaling mediated by the RARδ2 isoform. Alternatively, it is also possible that the *Nv*RARβ2 isoform may play a specific, direct role in dorsal-ventral patterning during tail regeneration, but this remains to be determined.

In summary, I have cloned the first full-length RARβ2 cDNA from the adult newt, *N. viridescens*, an adult species that possesses extensive regenerative capabilities of the CNS, limbs and tail. I have also shown for the first time, that an RARβ2 is transcribed, and that this transcript is translated within an adult vertebrate spinal cord and that treatment with either an RARβ-selective antagonist or an RARβ2-selective agonist can inhibit newt tail regeneration. These studies support the previous hypothesis that RARβ2 is the key transducer of RA signaling during nerve regeneration, and further support the hypothesis that expression of RARβ2 is a marker for neurons capable of undergoing regeneration.

Chapter 3:

Developmental expression of a molluscan RXR and evidence for its novel, nongenomic role in growth cone guidance.

In manuscript form as:

Carter CJ, Farrar N, Carlone RL, Spencer GE (2010) Developmental expression of a molluscan RXR and evidence for its novel, nongenomic role in growth cone guidance. Developmental Biology 343:124-137.

N. Farrar contributed to Figures 5 and 6 of manuscript only (these correspond to Figs. 24 and 25 of thesis).

3.01 Abstract

It is well known that the vitamin A metabolite, retinoic acid, plays an important role in vertebrate development and regeneration. We have previously shown that the effects of RA in mediating neurite outgrowth, are conserved between vertebrates and invertebrates (Dmetrichuk et al., 2005; 2006) and that RA can induce growth cone turning in regenerating molluscan neurons (Farrar et al., 2009). In this study, we have cloned a retinoid receptor from the mollusc *Lymnaea stagnalis* (*Lym*RXR) that shares about 80% amino acid identity with the vertebrate RXRα. We demonstrate using Western blot analysis, that the *Lym*RXR is present in the developing *Lymnaea* embryo, and that treatment of embryos with the putative RXR ligand, 9-*cis* RA, or a RXR pan-agonist, PA024, significantly disrupts embryogenesis. We also demonstrate cytoplasmic localization of *Lym*RXR in adult central neurons, with a strong localization in the neuritic (or axonal) domains. Using regenerating cultured motorneurons, we show that *Lym*RXR is also present in the growth cones, and that application of a RXR pan-agonist produces growth cone turning in isolated neurites (in the absence of the cell body and nucleus). These data support a role for RXR in growth cone guidance and are the first studies to suggest a non-genomic action for RXR in the nervous system.

3.02 Introduction

Retinoic acid (RA) is the active metabolite of vitamin A and is well known to influence morphogenesis during vertebrate development (Maden and Hind, 2003; Maden, 2007). It can also act as a trophic factor and has been implicated in neurite outgrowth (Corcoran et al., 2000; Maden et al., 1998; Wuarin et al., 1990), and regeneration (Dmetrichuk et al., 2005) of the nervous system. Retinoic acid classically acts through nuclear receptors that act as transcription factors to affect downstream activation of various genes, including neurotrophins, cytokines, cell surface molecules (reviewed in Gudas, 1994; Mey and McCaffery, 2004) as well as specific genes involved in neurite outgrowth, such as NEDD9 (Knutson and Clagett-Dame, 2008) and neuron navigator 2 (Muley et al., 2008). The nuclear receptors responsive to RA include the retinoic acid receptors (RARs) and the retinoid X receptors (RXRs) and at least 3 classes of each have been identified (α, β and γ). RARs bind both all-*trans* and 9-*cis* RA isomers, whereas the RXRs (at least in vertebrates), bind only 9-*cis* RA (Heyman et al., 1992). There is evidence that both RARs and RXRs play a role in neurite outgrowth and/or neurite regeneration; RARβ plays a major role in the induction of neurite outgrowth from both embryonic (Corcoran et al., 2000) and adult (Dmetrichuk et al., 2005) spinal cord neurons, while RXR has been suggested to play a role in motor neuron innervation of limbs in mice (Solomin et al., 1998). Both RARs and RXRs are found in vertebrate nervous systems, but until recently, it was generally believed that non-chordates possessed only RXRs. However, evidence for putative RARs has now emerged from EST/genomic databases in annelids and molluscs (Albalat and Canestro, 2009), and a

molluscan RAR has now been cloned (Carter and Spencer, 2009; accession no. **GU932671**).

It has become increasingly evident that many effects of retinoic acid are conserved between vertebrate and invertebrate species. The presence of RA in invertebrates has been implicated by the presence of retinoic acid binding proteins in the insect (Mansfield et al., 1998) shrimp (Gu et al., 2002) and marine sponge (Biesalski et al., 1992). RA has also been detected in fiddler crab limb blastemas (Chung et al., 1998) and in the locust embryo (Nowickyj et al., 2008), suggesting a role in both limb regeneration and embryonic development. More recently, we have shown for the first time that RA is present in the invertebrate CNS (Dmetrichuk et al., 2008) and demonstrated that (in the absence of other neurotrophic factors), it induces neurite outgrowth as well as growth cone turning in cultured neurons of the mollusc, *Lymnaea stagnalis* (Dmetrichuk et al., 2006; Dmetrichuk et al., 2008; Farrar et al., 2009). The mechanisms underlying the neurotrophic and chemotropic effects of retinoic acid in *Lymnaea*, are, at present, largely unknown, though we have recently shown that the RA-induced growth cone turning involves a non-genomic mechanism that requires protein synthesis and calcium influx (Farrar et al., 2009).

In this study, we have cloned a RXR from the CNS of *Lymnaea* that demonstrates a high sequence homology with the vertebrate RXRα. Our aim was then to determine whether this *Lymnaea* RXR plays a role in either embryonic development and/or neuronal regeneration of central neurons in *Lymnaea stagnalis*.

3.03 Materials and Methods

Cloning of *L. stagnalis* RXR

Lymnaea stagnalis used in this study were laboratory bred and kept in aerated, artificial pond water and fed lettuce and NutraFin Max Spirulina fish food (Hagen). RT-PCR was performed on cDNA generated from total RNA extracted from the *Lymnaea* CNS. Briefly, reverse transcription was carried out with a mixture of poly A and random hexamer primers according to the iScript cDNA synthesis kit (BioRad). cDNA was then amplified with 40 pmol of forward (5'-CGA CAA AAG ACA GAG AAA CAG ATG YCA RTA YTG-3') and reverse (5'-GTC TCT GAA GTG TGG GAT TCT TTT NGC CCA YTC-3') degenerate primers. After 3 min of denaturation at 95°C, 35 cycles at 95°C for 30 sec, annealing at 55°C for 30 sec and elongation at 72°C for 1 min were performed with an Eppendorf Mastercycler Personal Thermocycler. Analysis of the product was carried out on 1% agarose gels in TAE buffer stained with ethidium bromide. Fragments of interest were excised from the gel and cloned into the pGemTEasy vector system (Promega). Sequencing was performed by GénomeQuébec (Montréal, Canada) using 3730xl DNA Analyzer systems from Applied Biosystems. Full-length cDNA was obtained by performing multiple rounds of 5'and 3' RACE with cDNA prepared from the same *Lymnaea* CNS preparations with the SMART RACE cDNA amplification kit (Clontech).

Antibodies

We designed antibodies against a synthetic peptide from the predicted 'hinge' region of the *Lymnaea* RXR covering the amino acid residues 183-198 between the DNA

binding domain (DBD) and ligand binding domain (LBD). This custom made *Lym*RXR antibody was produced in New Zealand white rabbits and affinity purified from the antisera by Pacific Immunology Corp. (Ramone, California, USA). In some Western blotting procedures, a commercial antibody against human GAPDH (Abcam Inc.) was used as a cytosolic fraction marker, and a commercial antibody against human actin (Sigma-Aldrich) was used as a control.

Lymnaea embryos

In order to investigate *Lym*RXR protein levels during *Lymnaea* development, egg masses were first incubated in pond water at 25°C and allowed to reach various stages of development, as described in Nagy and Elekes (2000). These stages included day 0 of embryogenesis (when egg mass is first laid and prior to first cleavage), the trochophore stage (approx 36 to 60 hrs of embryogenesis), the veliger stage (approx 60 to 96 hrs of embryogenesis), the adult-like stage just prior to hatching (96 to 192 hrs of embryogenesis) and hatchlings. When the embryos reached the desired stage, the capsules were removed from their gelatinous surroundings and total protein extracted and Western blotting performed, according to the protocol listed below for adult CNSs. These experiments were performed twice.

To determine if *Lym*RXR plays a role in *Lymnaea* development, embryos were incubated in a synthetic RXR agonist (PA024, a kind gift from Dr. H. Kagechika, Tokyo) and 9-*cis* RA (Sigma-Aldrich). At day 0 of embryogenesis (when egg mass is first laid), capsules were teased out of the gelatinous surroundings in which they were embedded, and maintained in pond water at 25°C for 30 hrs (until the end of the gastrulation stage).

This separation of the capsules increased probability of penetration of the agonist PA024 and 9-*cis* RA, while still allowing normal development of the egg inside the capsule (Creton et al., 1993). The RXR agonist PA024 (10^{-7}M), 9-*cis* RA (10^{-7}M), or DMSO (0.001%, vehicle control) were added to separate dishes of embryos at 30 hrs of embryogenesis (this was previously shown to be the most sensitive stage to disruption by RA; Creton et al., 1993). At days 6-7 of embryogenesis, embryos showing eye and/or shell malformations, or arrested development at the trochophore stage, were scored and compared with the DMSO control embryos. These experiments were also performed twice with incubation of embryos in RXR antagonists alone (PA452, 10^{-6}M; HX531, 10^{-6}M, both a kind gift from Dr. H. Kagechika, Tokyo) in the exact same manner as described above. Statistical analysis was comprised of multiple Fisher Exact tests that were then Bonferroni-Holm corrected.

Western Blotting

To investigate the expression of *Lym*RXR protein, the adult *Lymnaea* CNS (or whole embryos) were homogenized in lysis buffer containing 150mM NaCl, 50mM Tris HCl (pH7.5), 10 mM EDTA, 1% Trition X-100, 1mM PMSF and 0.01% Protease Inhibitor Cocktail (Sigma-Aldrich) with a PowerGen handheld homogenizer (Fisher Scientific). The homogenates were centrifuged 20,000 x g at 4°C for 30 minutes. 15μg of protein from each extract was separated on a discontinuous SDS-polyacrylamide gel (12% Resolving, 4% Stacking) and electroblotted onto a nitrocellulose membrane (BioRad). For embryo experiments, gels were electrophoresed in duplicate under identical conditions; one was stained with Commassie blue to ensure equal loading of

protein, and the other was subjected to Western blot analysis. The membranes were washed for 5 minutes in 1xPBS and then blocked in 1xPBS/0.1% Tween-20 (PBT) with 3% skim milk powder (w/v) for 1 hour. The membranes were then incubated with affinity purified *Lymnaea* RXR antibody at a dilution of 1/2500 in PBT/3% skim milk overnight at 4°C with gentle horizontal shaking. This was followed by 4 x 5 min washes at RT in PBT and incubation with a 1/15000 dilution of AlexaFluor 680 goat anti-rabbit secondary antibody (Invitrogen). After 4 x 5min washes in PBT and one wash in 1xPBS, the membranes were imaged with the LI-COR Odyssey Infrared Imaging System at 700nm wavelength.

To investigate the subcellular expression of *Lym*RXR in the *Lymnaea* CNS, as well as in embryos just prior to hatching, total protein from the cytoplasmic, membrane and nuclear compartments was isolated according to directions from the Qproteome Cell Compartment kit (Qiagen). These protein fractions were loaded onto a discontinuous SDS-polyacrylamide gel and *Lym*RXR was detected by Western blotting technique as previously described above. Anti-GAPDH (Abcam Inc.) was used as a cytosolic fraction marker and successful isolation of protein from all three compartments of the CNS was confirmed by staining for actin. These experiments were performed twice for embryos and four times for the adult CNS.

Immunostaining

For immunostaining, the CNSs isolated from the snails were fixed in 4% paraformaldehyde in PBS at 4°C overnight and washed in 10% sucrose/PBS for 2 hours, 20% sucrose/PBS for 2 hours, and then 30% sucrose/PBS overnight at 4°C. After

embedding the fixed CNSs in Optimal Cutting Temperature (O.C.T.) Compound (Tissue-Tek), serial 20μm sections were cut using a cryostat (Leica microsystems) and placed on Superfrost Plus slides (Fisher Scientific). For immunostaining of cultured neurons following outgrowth (24 to 36 hrs), cells were fixed in 4% paraformaldehyde in PBS at 4°C overnight. Form this point on, all immunostaining procedures were the same for CNSs and cultured neurons. The samples were washed in PBS and then permeablized in 0.3% Triton X-100 in PBS (PBT) for 20 min and blocked in 5% normal goat serum (NGS) in PBT for 1 hour at RT. The samples were then incubated with the primary *Lym*RXR antibody diluted 1:100 in blocking solution at 4°C overnight. As a control, preparations were also incubated only in blocking solution, without the primary antibody, at 4°C overnight. All samples were then washed in PBT 3 x 5 minutes and incubated in 1:500 dilution of Alexa Fluor 488 goat anti-rabbit secondary antibody (Invitrogen) in blocking buffer at RT for 2 hours. The samples were washed in 3 x 5 min in PBT and counterstained with DAPI for 2 min to visualize the nuclei. After a brief wash in PBS, the specimens were coverslipped with anti-fade Fluorosave mounting media (Calbiochem).

Cell culture procedures

All cell culture procedures were performed as described previously (Dmetrichuk et al., 2006; Farrar et al., 2009; Ridgway et al., 1991). Briefly, under sterile conditions, the central ring ganglia were isolated, subjected to a number of antibiotic washes and enzymatic treatment, and then pinned down in a dissection dish and bathed in high osmolarity (L-15 derived) Defined Medium (DM) (Ridgway et al., 1991). Using a pair of fine forceps, the connective tissue sheath surrounding the ganglia was removed and

identified Pedal A (PeA) motorneurons were individually extracted using gentle suction applied via a fire-polished pipette attached to a micro-syringe. The individual identified PeA somata were plated directly on poly-L-lysine coated dishes (onto a glass coverslip) containing brain-conditioned medium (CM) (Wong et al., 1981) and all-*trans* RA (10^{-7}M) to promote outgrowth. Cells were maintained in the dark at 22°C overnight. An inverted microscope (Zeiss Axiovert 200) was used for all phase and fluorescent imaging of cultured cells.

Growth cone assays

Growth cone assays were performed in an identical manner to those described in detail elsewhere (Farrar et al., 2009). Briefly, a pressure pipette (Eppendorf-Femtojet; 4-8μm) containing 9-*cis* RA (10^{-5}M), or the RXR agonist, PA024 (10^{-5}M or 10^{-6}M) was positioned 50 to 100 μm from an actively growing growth cone. Pressures between 5 and 12hPa were used to apply the agonists, while holding pressures of 1-2hPa were used during rest periods to prevent backflow of bath solution. Concentrations detected at the growth cone were likely 100-1000 times less than those present in the pipette (Lohof et al., 1992). Control experiments using the DMSO vehicle solution for the agonist (0.1%) were performed in the exact same manner. For isolated growth cone experiments, neurites were mechanically separated from the cell body using a sharp glass electrode (Farrar et al., 2009). In order to test whether the RXR agonist-induced turning was inhibited in the presence of RXR antagonists, PA024 was applied to the growth cones, either in the presence of bath-applied DMSO vehicle control (final bath concentration

0.01%), or in the presence of the RXR antagonists PA452 (final bath concentration 10^{-6}M) or HX531 (final bath concentration 10^{-6}M).

Growth cone behaviour in both intact and isolated neurites in response to drug application was monitored for at least one hour, and the maximum turning angle recorded. A one-way analysis of variance (1-way ANOVA) was performed on growth cone data sets, and a Tukey-Kramer *post-hoc* test was used to determine statistical significance. Results are expressed as mean ± standard error of the mean (SEM) and were deemed significant when $p<0.05$.

3.04 Results

Sequencing of *Lym*RXR

Using RT-PCR with degenerate primers designed from other known RXR sequences, we obtained an initial cDNA fragment from the CNS of *Lymnaea stagnalis*. A full-length RXR cDNA was elucidated by multiple rounds of 5' and 3' RACE from the initial cDNA clone. The final full-length cDNA we obtained was 1593bp, with a 1308bp major open reading frame that encodes for a 436aa RXR protein (we termed *Lym*RXR; accession no. **AY846875**). This *Lym*RXR has an overall amino acid identity of 97% with the RXR from a closely related mollusc, *Biomphalaria glabrata* (*Bg*RXR; accession no. **AAL86461**). Of the various vertebrate RXR subtypes, *Lym*RXR is most similar to the RXRα subtype. The predicted DNA-binding domain (DBD) of *Lym*RXR shares ~89% amino acid identity with the *Rattus norvegicus* RXRα (accession no. **NP_036937**), while the predicted ligand-binding domain (LBD) shares ~81% amino acid identity with rat RXRα (Fig. 20).

*Lym*RXR in the developing embryo

RA, acting as a transcriptional activator, is well known to play a role in vertebrate development. Our first aim following the identification of *Lym*RXR, was thus to determine whether the RXR protein was present in the developing *Lymnaea* embryo. *Lymnaea* embryogenesis is intracapsular, lasting about 8 days in total. There are three major developmental stages, defined as the trochophore stage (approx 36 to 60 hrs of embryogenesis,), veliger stage (60 to 96 hrs of embryogenesis) and the postmetamorphic

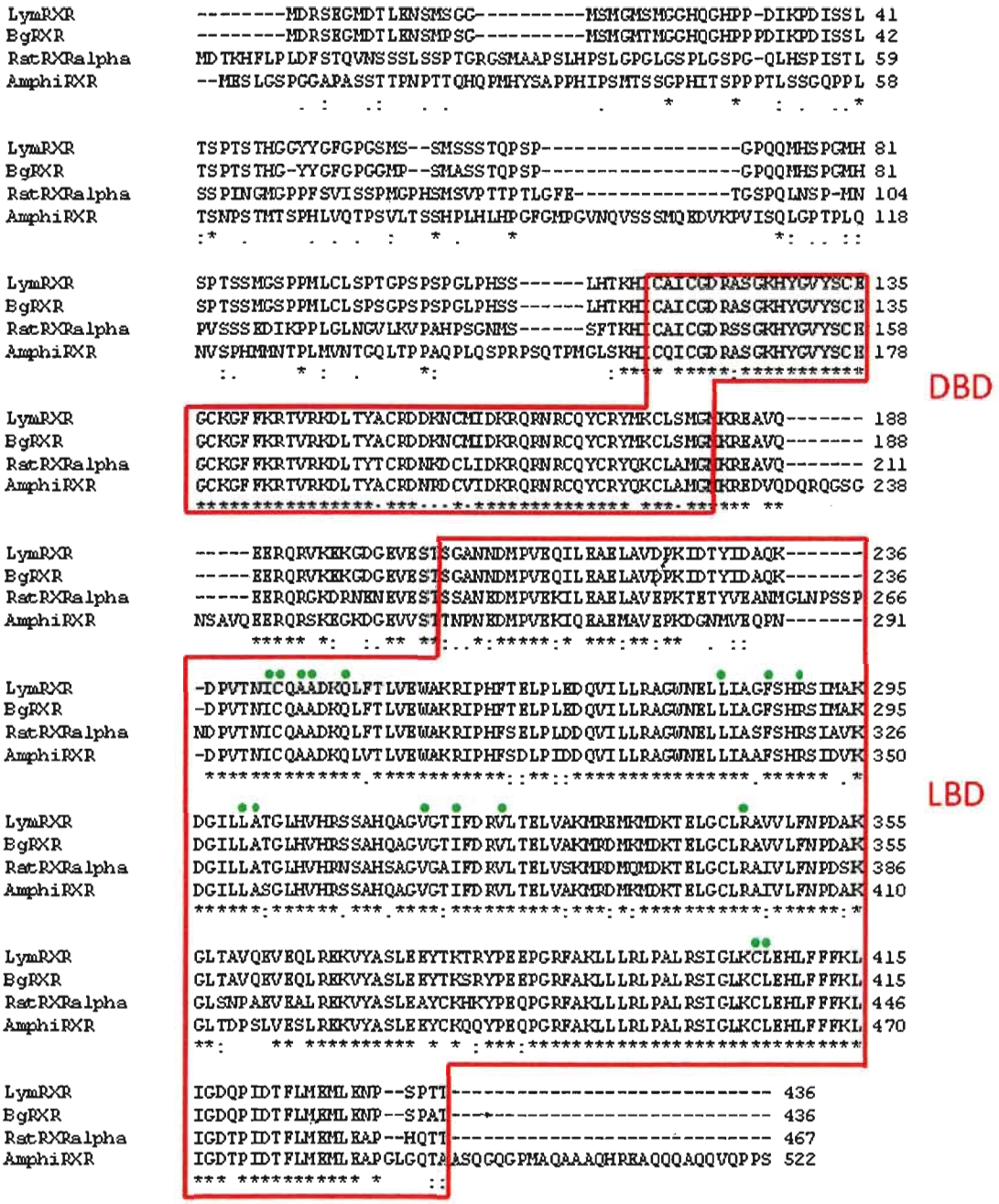

Figure 20. The *Lymnaea* RXR sequence. Multiple sequence alignment of the *Lymnaea stagnalis* RXR (LymRXR; accession no. **AY846875**), *Biomphalaria glabrata* RXR (BgRXR; accession no. **AAL86461**), *Rattus norvegicus* RXR alpha (RatRXRalpha; accession no. **NP 036937**) and the amphioxus, *Branchiostoma floridae* RXR (AmphiRXR; accession no. **AAM46151**) proteins. Note the high conservation of amino acids in the DNA-binding domain (DBD) and the ligand-binding domain (LBD). Amino acid residues reported to interact with the RXR natural ligand 9-*cis* RA (Egea et al., 2000) are indicated by green circles above the aligned sequences.

stage (96 hrs to hatching). It is during the veliger stage where ganglia are first detected (Nagy and Elekes, 2000) and many of the organs begin to develop (Meshcheryakov, 1972). Following hatching at about 8 days, the animal starts its juvenile, free-living existence.

A custom made antibody against a synthetic peptide from the 'hinge' region between the DBD and LBD was used to detect the *Lym*RXR protein during the various stages of embryogenesis. Western blot analysis of *Lymnaea* embryo total protein revealed a band of approximately 47 kDa in size, close to the predicted molecular weight of 48kDa (Fig. 21A). *Lym*RXR protein was present as early as the trochophore stage (approx 36 to 60 hrs) and was present in all subsequent stages studied, with its expression appearing maximal at the hatchling stage (Fig. 21A). RXR is typically known for its role as a nuclear hormone receptor and transcription factor. Thus, in order to determine its nuclear localization in cells of the *Lymnaea* embryo, total protein fractions were isolated from the cytoplasm, membrane and nucleus of embryos, immediately prior to hatching, using a Qproteome Cell Compartment kit (Qiagen). Western blot analysis showed a positive signal for RXR in the nuclear compartment of embryos, but also in the cytoplasmic and membrane compartments (Fig. 21B).

It is well documented that disruptions of RA signaling in vertebrates, either by inhibition of its synthesis, or by exogenous addition of RA, can lead to a wide array of developmental defects in limb, CNS and main body axis formation (Durston et al., 1989; Sive et al., 1990; Stratford et al., 1996). Creton et al., (1993) have also previously shown that RA disrupted embryogenesis in *Lymnaea,* mainly by affecting eye and shell development. Having determined that RXR is present in the embryo, we next

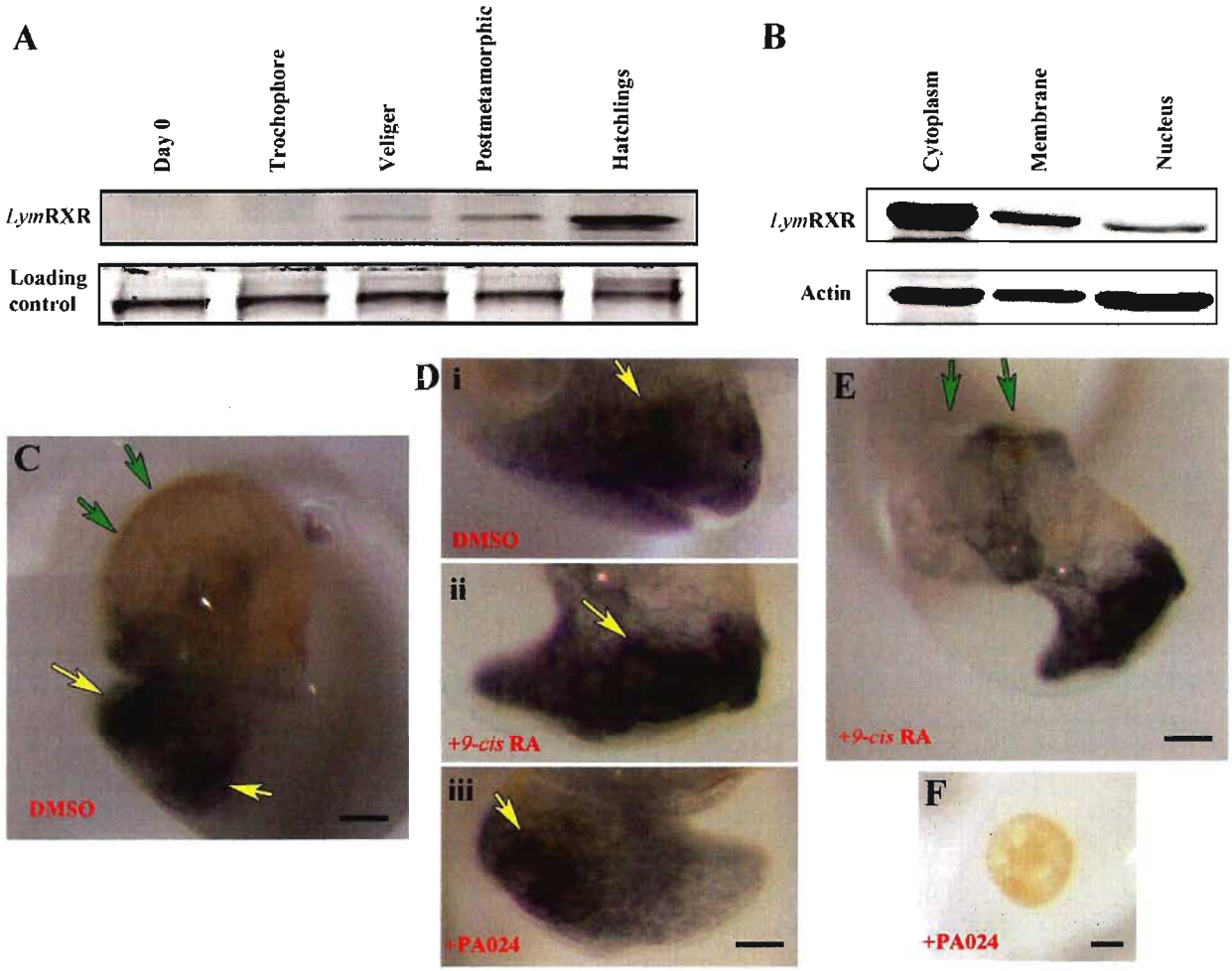
A
Day 0
Trochophore
Veliger
Postmetamorphic
Hatchlings
LymRXR
Loading control
B
Cytoplasm
Membrane
Nucleus
LymRXR
Actin
C
DMSO
D
i
DMSO
ii
+9-cis RA
iii
+PA024
E
+9-cis RA
F
+PA024
G
% showing eye defects
%
DMSO
9-cis RA
PA024
H
% showing shell malformations
%
DMSO
9-cis RA
PA024
J
% halted at trochophore stage
%
DMSO
9-cis RA
PA024

Figure 21. Embryonic RXR plays a role in *Lymnaea* development. (A) Western blot analysis at five different stages of *Lymnaea* embryogenesis revealed its presence as early as the trochophore stage, and showed maximal expression at hatching. A commassie blue stain of the acrylamide gel, prior to transfer, was used as a loading control. (B) Western blot analysis performed on subcellular fractionations of embryos, using the *Lym*RXR antibody, showed a signal in the cytoplasmic, membrane and nuclear compartments. Actin staining as a control also showed staining in all three compartments. (C) DMSO (0.001%) added to the *Lymnaea* embryos as a vehicle control, did not affect development. All of the animals showed normal eye and shell development (compared to embryos in the absence of DMSO). Green arrows indicate the outline of the normally developed shell, and yellow arrows indicate the presence of both eyes. Scale bar: 200μm. (Di) Representative image of a control embryo in DMSO showing the clear presence of an eye (yellow arrow) (ii) Representative example of an under-developed eye, reduced in size (yellow arrow), following incubation in the natural RXR ligand, 9-*cis* RA (10^{-7}M); (iii) Representative example of an embryo missing an eye (yellow arrow indicates where eye should be located) following incubation in the synthetic RXR agonist PA024 (10^{-7}M); Scale bar (Di-iii): 150μm (E) Green arrows indicate malformation of the shell following incubation in 9-*cis* RA (10^{-7}M); Scale bar: 200μm (F) PA024 halted some embryos at the trochophore stage. Scale bar: 100μm. For graphs (G) through (J), 9-*cis* RA (n=40) and PA024 (n=40) treatments were compared to the DMSO (n=40) treatment (* $p<0.05$, ** $p<0.01$).

aimed to determine whether known RXR agonists/ligands would disrupt the normal pattern of development in *Lymnaea*. We also used eye and shell formation as indicators of normal growth because these are easily visualized and characterized using light microscopy, shortly after the veliger stage. Eyes normally become pigmented at the end of the veliger stage (at about 96 hrs) and the shell extends over the visceral masses just a few hours later (Nagy and Elekes, 2000).

Lymnaea embryos were maintained within their capsules, but were removed from their gelatinous surroundings. Capsuled embryos were treated with a synthetic RXR pan-agonist, PA024 (10^{-7} M; n = 40), the putative RXR ligand, 9-*cis* RA (10^{-7}M; n = 40), and DMSO as the vehicle control (0.001%; n = 40). These treatments were started at the gastrula stage (30 h) and continued for the next 5 days of embryonic development. In the presence of DMSO, both shell (Fig. 21C) and eye (Fig. 21C, Di) development appeared normal. However, we found that treatments with 9-*cis* RA and PA024 produced defects in both eye (Fig. 21Dii-iii, G) and shell formation (Fig. 21E, H) in a significant number of embryos. Eye defects included either missing eyes (Fig. 21Diii), or those noticeably reduced in size (Fig. 21Dii). Interestingly, PA024 displayed a higher number of abnormalities than 9-*cis* RA, including a number of embryos that exhibited halted development at the trochophore stage (Fig. 21F, J).

Similar experiments were next performed with incubation of embryos in RXR antagonists, in order to determine the effect of inhibiting RXR signaling during embryogenesis. Incubation in the RXR antagonist, HX531 (10^{-6}M), produced shell defects in all embryos (48 of 48 embryos; 100%), but not in eye development (0 of 48 embryos; 0%). Interestingly, incubation in the RXR antagonist, PA452 (10^{-6}M), did not

produce any observable defects in either eye or shell development (0 of 44 embryos; 0%; data not shown).

Together, these data strongly suggest a role for RXR in *Lymnaea* development.

_Lym_RXR is present in the adult CNS

We have previously shown that both all-*trans* RA and 9-*cis* RA exert trophic and tropic effects on adult CNS neurons of *Lymnaea* (Dmetrichuk et al., 2006; Dmetrichuk et al., 2008), but little is known of the underlying cellular and molecular mechanisms. We next aimed to determine whether RXR expression is maintained following the embryonic stages and specifically, to determine whether it is present in the adult (non-regenerating) CNS. Western blot analysis of adult *Lymnaea* CNS total protein again revealed a band of approximately 47 kDa in size (Fig. 22A). Using the same *Lym*RXR-specific antibody, we next performed immunohistochemistry on frozen sections of acutely isolated *Lymnaea* CNSs (n=30). Immunoreactivity was detected in neurons of all central ganglia. There was strong immunoreactivity in the neuropil and nerve bundles radiating from the brain, suggesting staining of the axonal tracts (Fig. 22B, D). Interestingly, there was little to no apparent staining of RXR (traditionally considered to be a nuclear receptor) in the nuclear region of the neurons, given that there was no RXR signal overlapping with the nuclear DAPI staining (Fig. 22C). Some ganglia also showed strong punctuate-like staining around the periphery of the ganglia (Fig. 22D), which may have been due to RXR immunoreactivity of glial networks and cell bodies in the neural sheath. Control CNS sections with no primary antibody added (n=6) demonstrated no immunostaining (Fig. 22E).

In order to confirm the neuritic localization of RXR, immunofluoresence was also performed on acutely isolated axons. During cell isolation from the intact ganglia, axonal segments up to ~200 μm in length can be acutely isolated, removed from the cell body and then plated in cell culture (Spencer et al., 2000). We showed that *Lym*RXR immunostaining was indeed present in the acutely isolated axons in culture (n = 3 of 3; Fig. 22F), which confirmed the above observation that RXR is present in the neuritic processes of neurons in the intact, adult CNS.

To further identify the neuronal compartmentalization of *Lym*RXR in the adult CNSs, we isolated total protein fractions from the cytoplasm, membrane and nucleus of the adult *Lymnaea* CNS using a Qproteome Cell Compartment kit (Qiagen). In Fig. 22G, Western blot analysis showed a positive signal for RXR in the cytoplasmic and membrane compartments, but not in the nucleus. Successful isolation of protein in the nuclear fraction was confirmed by staining for actin, which is now well known to reside in the nucleus (Fig 22J) (Bettinger et al., 2004; Franke, 2004). Anti-GAPDH was also used as a control on the same protein fractions and as expected, GAPDH showed only positive immunoreactivity in the cytoplasmic compartment (Fig. 22H). In order to further confirm the absence of nuclear RXR in the adult CNS cellular fractions, two additional CNS samples were again run, but this time in parallel with embryonic tissue. In the CNS fractions, the RXR was present in both cytoplasmic and membrane compartments, but was again absent in the nuclear compartment (data not shown), whereas the embryonic fractions revealed nuclear RXR (as seen in Fig. 21B).

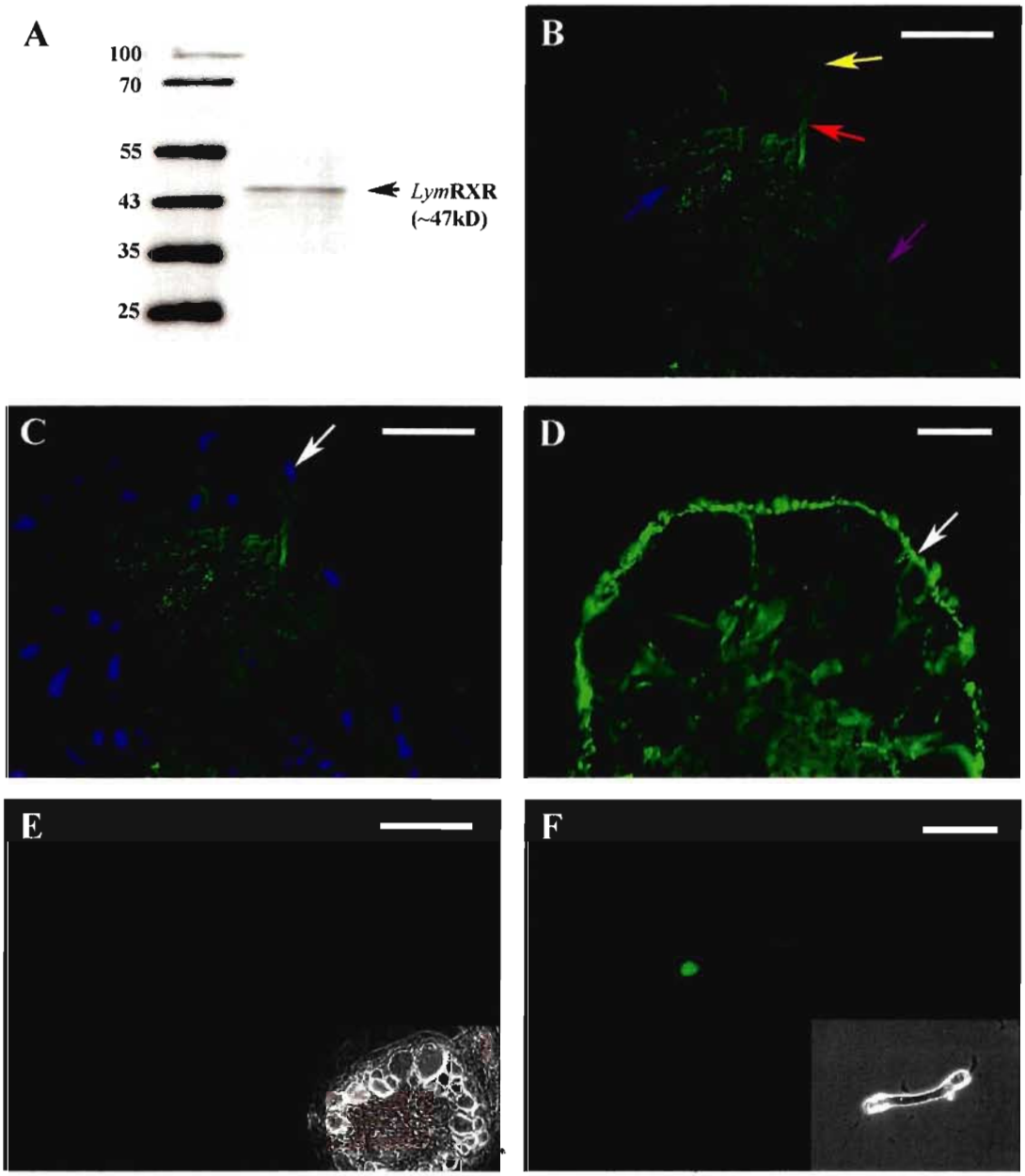
A
100
70
55
43
35
25
LymRXR
(~47kD)
B
C
D
E
F
G
LymRXR
Cyt
Mem
Nuc
H
GAPDH
Cyt
Mem
Nuc
J
ACTIN
Cyt
Mem
Nuc

Figure 22. Cytoplasmic localization of *Lym*RXR in the adult, non-regenerating nervous system.

(A) Western blot analysis of total protein extracted from the *Lymnaea* CNS showed a band near 47 kDa that closely matches the predicted molecular weight of *Lym*RXR from our cloned sequence. (B) and (C) *Lym*RXR immunoreactivity was detected in the neurons of ganglia of the CNS (Visceral ganglion shown), primarily in the cytoplasm of the cell body (yellow arrow), axons (red arrow), neuropil (blue arrow) and nerve bundles radiating from the brain (purple arrow). Note the absence of RXR staining in the nuclei, stained blue using DAPI (C; white arrow). Scale bars: 100μm. (D) Some ganglia (Right Pedal ganglion shown) produced strong punctuate-like staining near the periphery (white arrow). Scale bar: 50μm. (E) Control staining was also performed under the same conditions, only in the absence of the primary *Lym*RXR antibody. No immunostaining was visible (inset is a phase-contrast image of the same ganglia). Scale bar: 100μm. (F) Acutely isolated axons from the *Lymnaea* CNS, plated *in vitro,* also displayed strong immunoreactivity. Inset is a phase-contrast image of the same axon. Scale bar: 30μm. (G) Western blot performed on subcellular fractionations using the *Lym*RXR antibody, showed a signal in the cytoplasmic (Cyt) and membrane (Mem) compartments, but not in the nuclear (Nuc) compartment. (H) GAPDH is an abundant glycolytic enzyme in cytoplasm, and a GAPDH antibody, used as a control, showed signal only in the cytoplasmic compartment of the same samples. (J) Actin staining served as a positive control to demonstrate successful isolation of protein from the nuclear compartment.

_Lym_RXR is present in the neurites and growth cones of regenerating cultured neurons

Retinoic acid is known to promote neurite regeneration in many species, including neurons from *Lymnaea* (Dmetrichuk et al., 2006; Dmetrichuk et al., 2008). Our next aim was to determine the localization of RXR immunofluorescence in regenerating central neurons in culture. PeA motorneurons were individually isolated from the intact ganglia and given 24-36 hours to regenerate in cell culture (Fig. 23Ai). Following outgrowth, cells were then fixed and stained with the *Lym*RXR antibody. RXR immunoreactivity was visualized in the cell body of every cultured PeA neuron, whether it was actively regenerating neurites or not (n = 96 of 96). In the neurons that displayed outgrowth (n = 35), RXR immunoreactivity was observed in the majority of neurites (Fig. 23Aii), though there appeared to be a differential distribution of the RXR signal in the neurites of some cells. Figure 23Bii illustrates an example of a neurite emanating from a cell body that displayed strong immunoreactivity over most of its length, while another neurite from the same cell body showed very little RXR staining. Furthermore, while most of the growth cones located at the tips of the neurites, demonstrated positive immunoreactivity for RXR (n = 95 of 102), there were some neurites that displayed little, if any RXR staining along the neurite leading to the growth cone. Immunostaining of the RXR was evident in the central or C-domain of the growth cones, but very little to no staining was evident in the peripheral or P domain (lamellipodia and filopodia; Fig. 23Cii). Control regenerating PeA neurons, under the same staining conditions except in the absence of primary antibody, did not demonstrate RXR immunoreactivity (n = 6; data not shown).

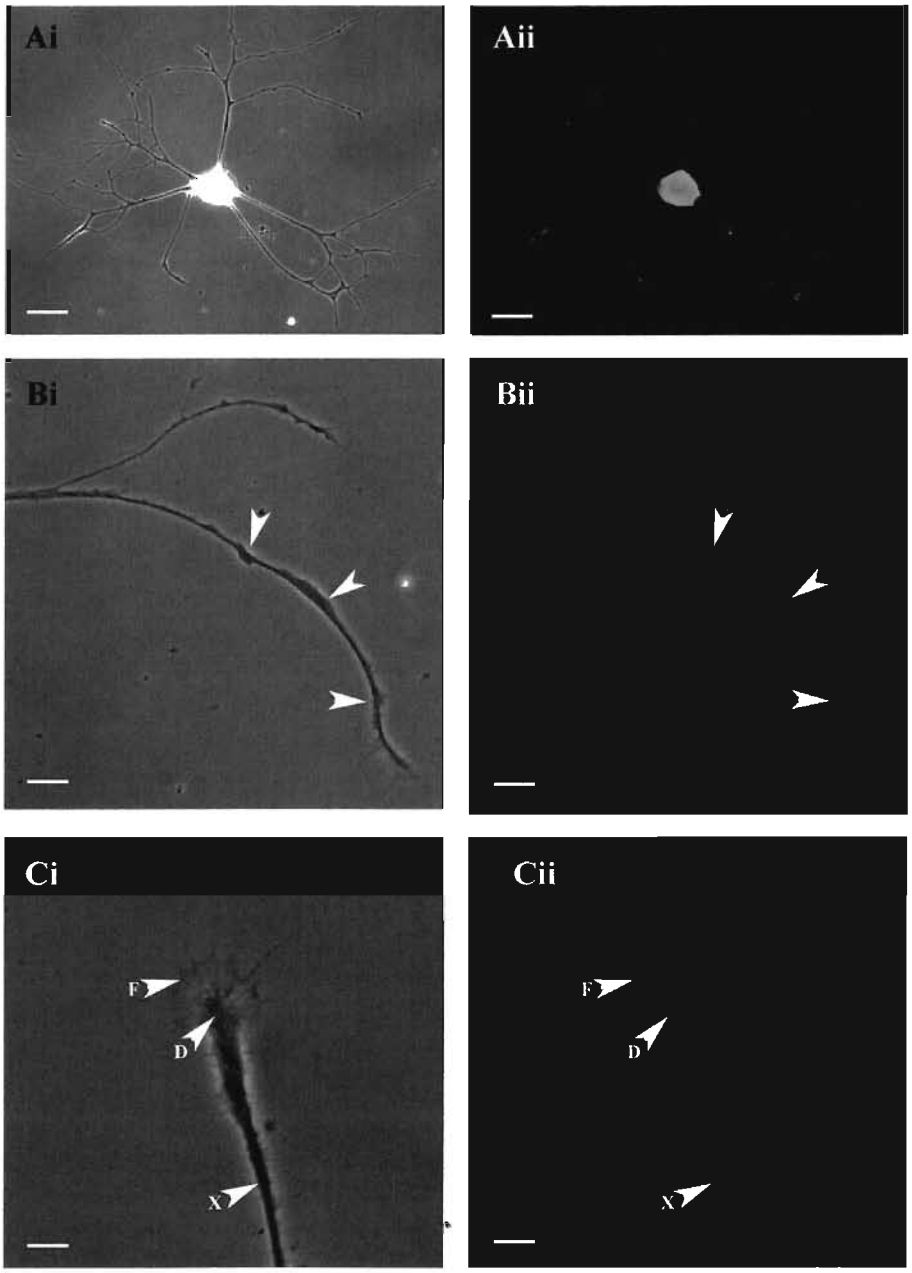

Figure 23. *Lym*RXR is present in the neurites and growth cones of regenerating motorneurons *in vitro*. (Ai) Phase-contrast image of a cultured *Lymnaea* Pedal A neuron at 48 hrs in CM, with regenerated neurites. (Aii) Immunostaining of the same PeA cell with *Lym*RXR antibody revealed a signal in the cytoplasm of the cell body and the regenerating neurites. Scale bars Ai-ii: 50μm. (Bi) Phase-contrast image of two neurites from the same cell. (Bii) Immunostaining with the *Lym*RXR antibody showed differential staining in the two branches. White arrows indicate staining of one branch, while the other branch displayed little, to no staining (red arrow). Scale bars Bi-ii: 20μm. (Ci) Phase-contrast image of a PeA growth cone *in vitro*. (Cii) Immunostaining with the *Lym*RXR antibody showed a signal in the neurite leading to the growth cone (X), in the central domain of the growth cone (D), but no staining in the lamellipodia and filopodia (F). Scale bars Ci-ii: 10μm.

An RXR agonist induced growth cone turning

We have previously shown that retinoic acid (both all-*trans* and 9-*cis* isomers) can induce positive growth cone turning of regenerating *Lymnaea* growth cones (Dmetrichuk et al., 2006; Dmetrichuk et al., 2008; Farrar et al., 2009). We have also shown that this growth cone turning is dependent on protein synthesis and calcium influx (Farrar et al., 2009). Because we had demonstrated that this turning response occurred in isolated growth cones and involved a localized, non-genomic mechanism, we had not previously investigated a role for the retinoid receptor. However, having now determined that the RXR is present in the regenerating growth cones and neurites, we next investigated whether it was involved in the localized growth cone turning response to RA.

We have previously reported growth cone turning toward 9-*cis* RA in VF neurons (Dmetrichuk et al., 2008). However, 9-*cis* RA was applied again in this study, in order to directly compare its effects on PeA growth cone behaviour, with those of a RXR agonist. Here, we showed that 9-*cis* RA produced attractive growth cone turning of intact PeA neurites with an average turning angle of 24.8 ± 7° (n = 6; Fig. 24Ai-iii). We next pressure applied the RXR pan-agonist PA024, on to the PeA growth cones, to determine whether it would mimic the growth cone turning induced by 9-*cis* RA. Indeed, PA024 induced positive growth cone turning of intact neurites with a mean angle of 30.6 ± 4.0° (n = 14; Fig. 24Bi-iii). As PA024 is dissolved in DMSO, control experiments with DMSO in the pipette were also performed and were shown not to produce positive growth cone turning (-16.9 ± 8.3°; n = 7; Fig. 24Ci-iii). Statistical analysis revealed that growth cone turning toward the RXR agonist PA024, was significantly different from the

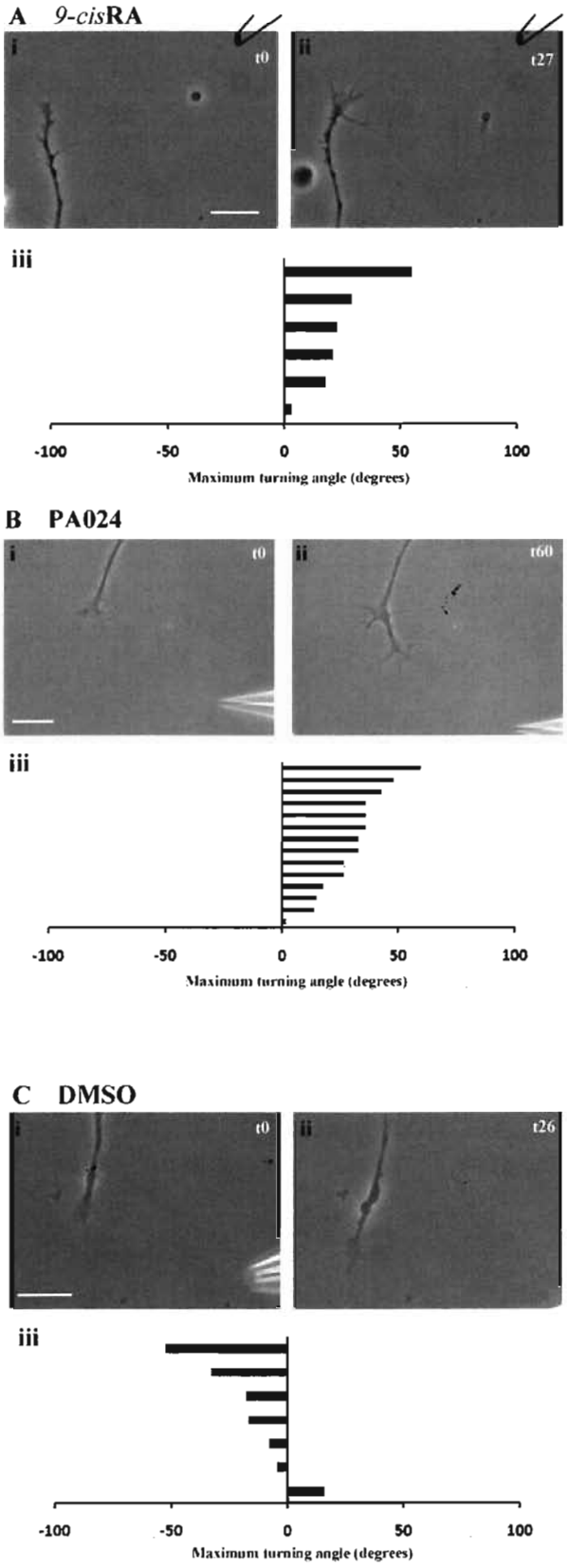
A 9-cisRA
i
t0
ii
t27
iii
-100
-50
0
50
100
Maximum turning angle (degrees)
B PA024
i
t0
ii
t60
iii
-100
-50
0
50
100
Maximum turning angle (degrees)
C DMSO
i
t0
ii
t26
iii
-100
-50
0
50
100
Maximum turning angle (degrees)

Figure 24. Intact PeA growth cones turn toward the RXR agonist. (Ai-ii) Representative example of a PeA growth cone turning toward 9-*cis* RA (i: 0 mins; ii: 27 mins after start of application). Approximate pipette location is indicated. Scale bar: 30μm. (Aiii) Histogram depicts maximum turning angle of intact growth cones to 9-*cis* RA and each bar represents one growth cone. Positive values represent a turn toward the pipette and negative values a turn away from the pipette. (Bi-ii) Representative example of a PeA growth cone turning toward the RXR pan-agonist PA024 (i: 0 mins, ii: 60 mins after start of application). Scale bar: 30μm. (Biii) Histogram depicts maximum turning angle of intact growth cones to PA024 and each bar represents one growth cone. Positive values represent a turn toward the pipette and negative values a turn away from the pipette. (Ci-ii) Representative example of a PeA growth cone that did not turn toward DMSO (vehicle control) (i: 0 mins, ii: 26 mins after start of application). Scale bar: 30μm. (Ciii) Histogram depicts maximum turning angle of intact growth cones to DMSO and each bar represents one growth cone. Positive values represent a turn toward the pipette and negative values a turn away from the pipette.

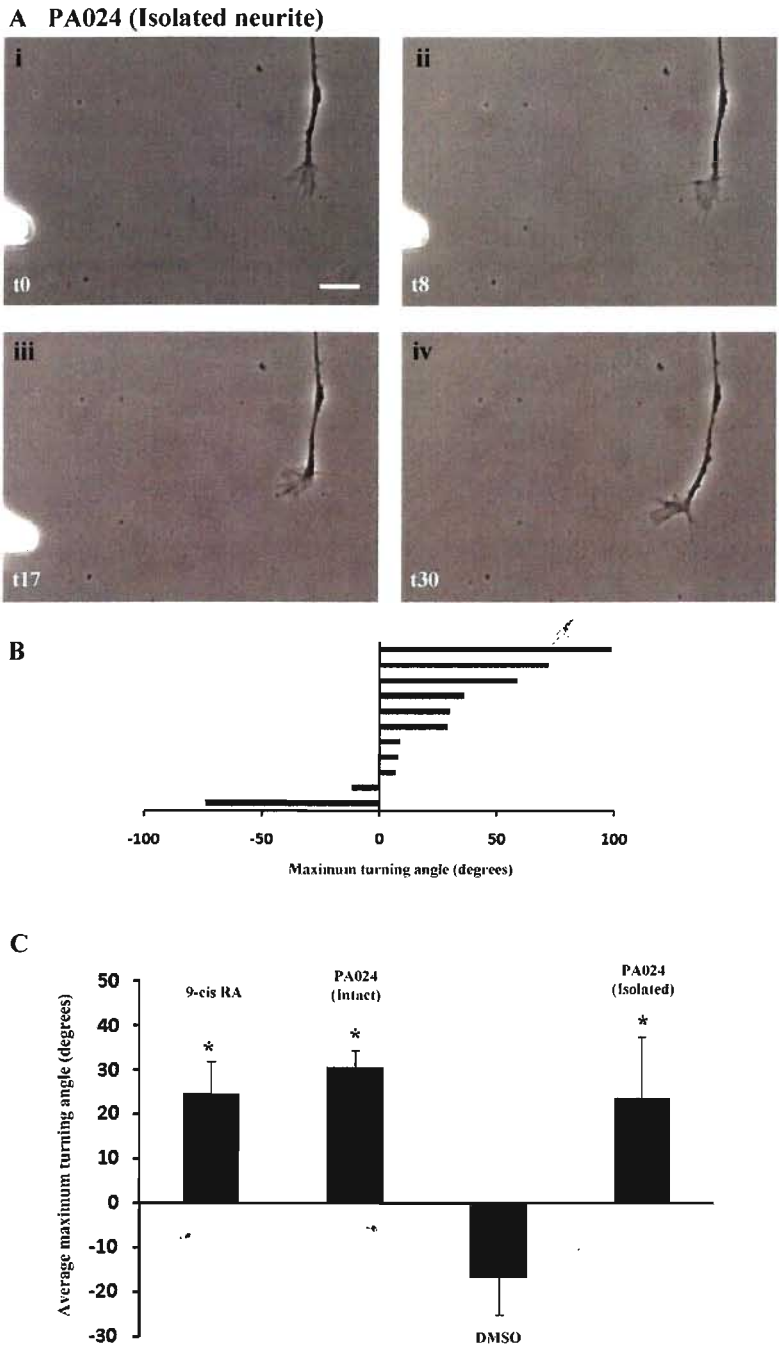

Figure 25. Isolated PeA growth cones turn toward the RXR agonist. Neurites were physically isolated from the cell bodies and the RXR agonist PA024 was applied to the isolated growth cones. (A) Representative example of an isolated growth cone turning toward PA024 (i) before PA024 application and following (ii) 8 mins, (iii) 17 mins and (iv) 30 mins of PA024 application. Scale bar: 25μm. (B) Histogram depicts maximum turning angle of isolated growth cones to PA024 and each bar represents one growth cone. Positive values represent a turn toward the pipette and negative values a turn away from the pipette. (C) Summary graph of mean growth cone turning angles under all conditions. Error bars represent standard error of the mean (S.E.M.). * $p<0.05$ when compared to DMSO controls.

DMSO control ($p < 0.05$), but was not significantly different from growth cone turning toward 9-*cis* RA.

We previously showed that neurites physically transected and isolated from their cell body could also turn toward RA, demonstrating that a local mechanism was involved. We next aimed to determine whether the RXR agonist would also induce turning in growth cones of transected neurites, physically isolated from their cell body. Once again, PA024 induced attractive growth cone turning (Fig. 25A) with a mean angle of 23.9 ± 13.8° (n = 11; Fig. 25B), which was not significantly different from that produced by PA024 in intact neurites (data summarized in Fig. 25C). These data suggest that RXR, located in neurites and growth cones of regenerating neurons, plays a novel, non-genomic role in RA-induced growth cone turning, at least in *Lymnaea* PeA motorneurons.

The RXR agonist-induced growth cone turning is inhibited in the presence of an RXR antagonist

We next aimed to determine whether we could block the RXR agonist-induced growth cone turning in the presence of a RXR antagonist. First of all, we showed that application of the RXR agonist PA024 (10^{-6}M) to intact PeA growth cones in the presence of the vehicle control (DMSO; 0.01%) produced growth cone turning (Fig. 26Ai-ii) with a mean angle of 36.3 ± 8.7° (n = 7; Fig. 26B). We next applied the RXR agonist PA024 (10^{-6}M) in the presence of the RXR antagonist PA452 (final bath concentration 10^{-6}M). In the presence of the RXR antagonist PA452, the mean turning angle in response to application of the agonist, was significantly reduced to 3.3 ± 10.3° (n = 9; $p < 0.05$; Fig. 26E). However, despite the overall reduced mean turning angle, 6 of

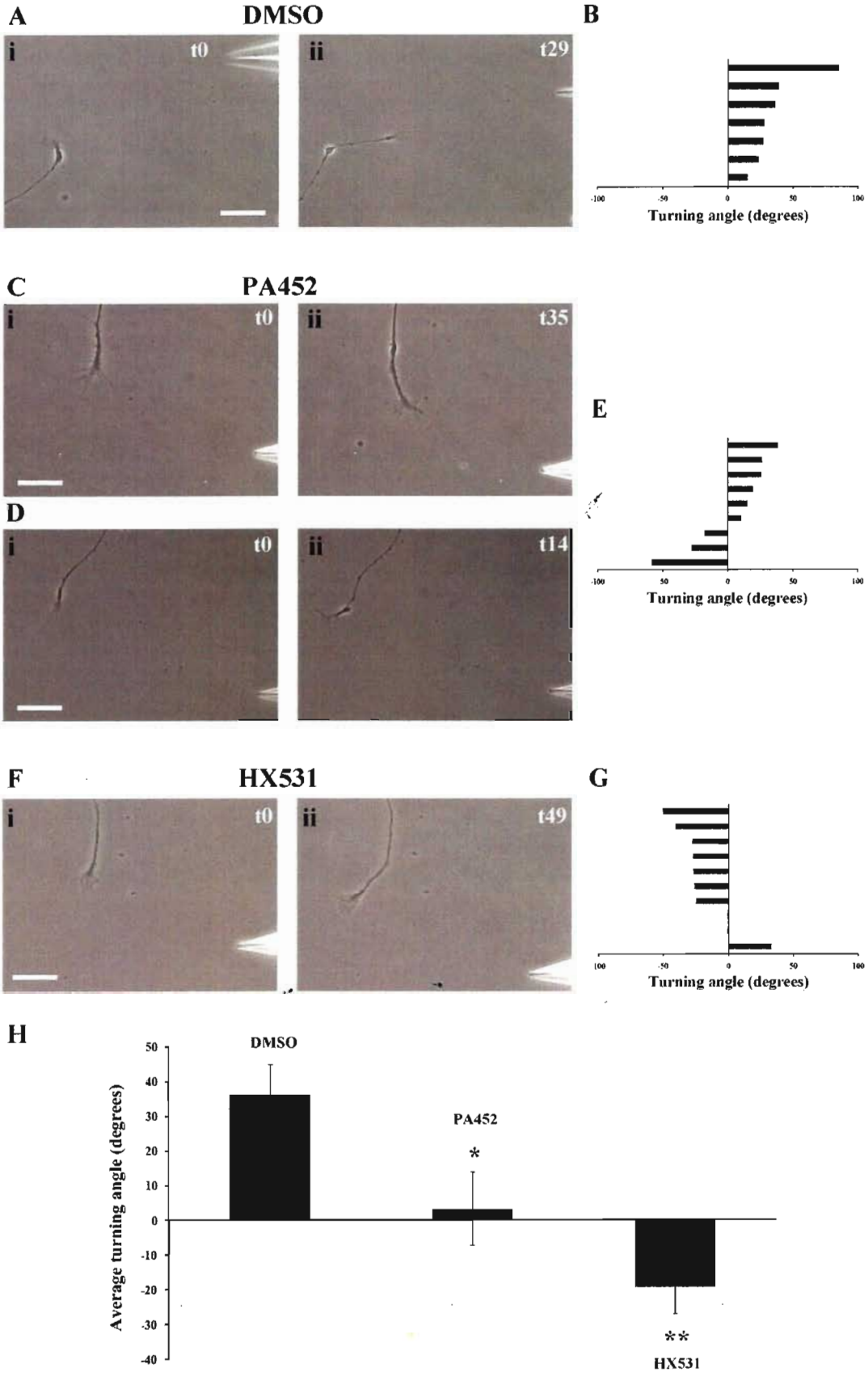
A
DMSO
i
t0
ii
t29
B
-100
-50
0
50
100
Turning angle (degrees)
C
PA452
i
t0
ii
t35
D
i
t0
ii
t14
E
-100
-50
0
50
100
Turning angle (degrees)
F
HX531
i
t0
ii
t49
G
100
-50
0
50
100
Turning angle (degrees)
H
Average turning angle (degrees)
50
40
30
20
10
0
-10
-20
-30
-40
DMSO
PA452
*
**
HX531

Figure 26. The agonist-induced growth cone turning is inhibited by RXR antagonists. The RXR agonist, PA042 was pressure applied (10^{-6}M) to intact PeA growth cones, in the presence of either DMSO (vehicle), or RXR antagonists in the bath. (A) An example of a growth cone that turned toward the RXR agonist PA024, in the presence of bath-applied DMSO (0.01%). i) Before application of PA024 and ii) following 29 mins of application. Note that the growth cone continued to grow in the direction of the pipette. Scale bar: 30 μm. B) Histogram depicts turning angles of intact growth cones to PA024 in the presence of DMSO, and each bar represents one growth cone. C) Representative example of a growth cone that turned toward PA024 in the presence of bath-applied RXR antagonist, PA452 (10^{-6}M). i) before application of PA024 and ii) following 35 mins of application. Scale bar: 30μm. D) Representative example of a growth cone that turned away from PA024 in the presence of bath-applied RXR antagonist, PA452 (10^{-6}M). i) before application of PA024 and ii) following 14 mins of application. Scale bar: 30μm. E) Histogram depicts turning angles of intact growth cones in response to PA024 in the presence of the RXR antagonist PA452. F) Representative example of a growth cone that turned away from PA024 in the presence of bath-applied RXR antagonist, HX531 (10^{-6}M). i) before application of PA042 and ii) following 49 mins of application. Scale bar: 30μm. G) Histogram depicts turning angles of intact growth cones to PA024 in the presence of the RXR antagonist HX531. H) Summary graph of mean growth cone turning angles in response to PA042, in the presence of either DMSO or RXR antagonists. Error bars represent standard error of the mean (S.E.M.). * $p<0.05$ and ** $p<0.01$, when compared to DMSO controls.

the 9 growth cones maintained a positive turn toward the RXR agonist in the presence of PA452 (Fig. 26Ci-ii), with an average turning angle of 22.5 ± 4.0°. The remaining 3 growth cones turned away from the pipette (Fig. 26Di-ii), with a mean turning angle of -35± 12.3° (n = 3).

We next chose to use a different RXR antagonist, HX531, to determine whether we could block the agonist-induced growth cone turning. In these experiments, we recorded the growth cone turning angle in response to application of the RXR agonist, in the presence of HX531 (10^{-6}M). This time, the growth cone turning toward PA024 was completely abolished in 9 of the 10 growth cones tested (Fig. 26Fi-ii). The mean turning angle in the presence of HX531 was -19.4 ± 7.5°, away from the pipette (Fig. 26G), which was significantly different from the turning angle in DMSO ($p < 0.01$; Fig. 26H). We also confirmed that the turning of isolated PeA growth cones toward the RXR agonist was abolished in the presence of HX531 (n = 4 of 4; data not shown).

In summary, these data suggest that RXR, located in neurites and growth cones of regenerating neurons, plays a novel, non-genomic role in RA-induced growth cone turning, at least in *Lymnaea* PeA motorneurons.

3.05 Discussion

In this study, we have cloned a full-length RXR from the mollusc, *Lymnaea stagnalis*, and have shown that this retinoid receptor is present in the developing embryo, as well as in the non-regenerating, adult CNS, where it was found in the neuritic domains of central neurons. Using regenerating cultured motorneurons, we have provided evidence that it plays a role in the chemotropic response of growth cones to retinoic acid.

RXRs are highly conserved members of the steroid/retinoid family of nuclear hormone receptors and have been identified in species ranging from the phylogenetically oldest metazoan phylum, (the sponge), to mammals (Mangelsdorf et al., 1992). Interestingly, the RXR from *Lymnaea* (a lophotrochozoan, non-chordate mollusc and true invertebrate outside of the chordate lineage) shows higher amino acid identity with the rat RXRα than the RXR from *Polyandrocarpa*, a urochordate species and closest living relative of the vertebrates (Borel et al., 2009). Furthermore, it has previously been shown that a molluscan RXR (from *Biomphalaria glabrata*; *Bg*RXR) functionally interacts with vertebrate RXR binding partners, strongly suggesting that retinoid signaling may be shared between the lophotrochozoan branch of the protostomes, and the deuterostomes (which contain the chordate branch).

RXRs from mammals have been studied most extensively, and it has been shown that they can form homodimers, heterodimers or even homotetramers, and regulate target gene expression when bound with their proposed ligand, 9-*cis* RA (Kersten et al., 1995). Interestingly, the amino acids in mouse RXR that interacted with 9-*cis* RA (Egea et al., 2000) are all perfectly conserved in the *Bg*RXR sequence (Bouton et al., 2005) as well as in our *Lym*RXR sequence. The *Bg*RXR can also transactivate transcription when treated

with exogenous 9-*cis* RA (Bouton et al., 2005). Though there is evidence that invertebrate RXRs, like the vertebrate RXRs, bind 9-*cis* RA (Kostrouch et al., 1998), a recent study showed that both 9-*cis* and all-*trans* RA isomers bind with similar affinities to the locust RXR (Nowickyj et al., 2008). All-*trans* RA also up-regulates RXR mRNA in the marine sponge *Suberites domuncula* (Wiens et al., 2003) and increases the abundance of RXR mRNA in blastemas during limb regeneration in the fiddler crab *Uca pugilator* (Chung et al., 1998). We have recently shown using HPLC and MS, that both 9-*cis* and all-*trans* RA isomers are present in the *Lymnaea* CNS (Dmetrichuk et al., 2008), and so we cannot rule out that both isomers may be natural ligands for *Lym*RXR.

RXR expression in the developing embryo

Our results indicate that RXR expression occurred in *Lymnaea* embryos as early as the trochophore stage and continued through the postmetamorphic stage, reaching maximal expression at hatching (juvenile form). We do not know whether this expression occurred in the nervous system, or whether it was associated with other organs. However, demonstration of RXR expression at the veliger stage correlates with the first ultrastructural detection of cerebral and pedal ganglia (Nagy and Elekes, 2000). However, at this developmental stage, the authors detected only 2 to 3 cells per ganglia, and only a small number of axon profiles, with no evidence of filopodial processes or developing synapses. In the later stages of embryonic development (postmetamorphic, adult-like stage), when we observed increased RXR expression, Nagy and Elekes (2000) observed the whole central ring ganglia and neuropil densely packed with axon profiles, though there was no evidence of glia or the neural sheath. Interestingly, the authors proposed that

the absence of the neural sheath during these stages would facilitate trophic and/or hormonal influences in the developing ganglia, which we propose may include trophic or tropic support provided by RA. By hatching, at which stage we saw maximal RXR expression, Nagy and Elekes (2000) demonstrated that the CNS had significantly increased in size, with enlarged neuropil and more axon profiles, as well as the first evidence of glia and a neuronal sheath. In summary, we found that RXR is expressed in our *Lymnaea* embryos prior to the metamorphic stage, which is thought to be the time when the neuropil is undergoing substantial reorganization, likely indicating a period of substantial migration and reorganization of axons (Nagy and Elekes, 2000). It is quite feasible therefore, that the RXR plays a role in *Lymnaea* nervous system development.

Creton et al (1993) have previously demonstrated that application of 10^{-7}M RA during the gastrulation stage of *Lymnaea* embryos, produced only eye defects (no shell or CNS deformations), and only in 15% of embryos. In our study, both eye and shell deformations were found following incubation in 10^{-7}M 9-*cis* RA and PA024. Though not explicitly stated, we presume that the isomer used in the previous studies was all-*trans* RA, possibly explaining the difference in teratogenicity observed. If this is indeed the case, it might suggest that 9-*cis* RA is a more potent teratogen in *Lymnaea* than all-*trans* RA. It should be noted however, that in vertebrates, 9-*cis* RA activates RARs, in addition to RXRs. It is thus possible that 9-*cis* RA might also be activating an RAR. We believe this unlikely, as despite our recent cloning of an RAR in *Lymnaea*, we have not yet been able to detect it in the early embryonic stages of development (Carter and Spencer, 2009). This suggests that if the RAR is indeed present, it is likely at much lower levels than the RXR. In support of our hypothesis that 9-*cis* RA is likely acting via the

RXR , the effects of 9-*cis* RA were closely mimicked by PA024, which was developed as a RXR-selective agonist (Ohta et al., 2000). The demonstration that the RXR was present in the nuclear compartments of embryonic protein fractions, strongly suggests that the teratogenic effects of the RXR agonist and 9-*cis* RA were likely mediated via genomic actions of the RXR. However, we were unable to distinguish cellular localization of the RXR in specific tissues of the embryo, and as its presence was also shown in cytoplasmic and membrane compartments, we cannot rule out the possibility of non-genomic effects during embryogenesis.

Cytoplasmic localization of RXR, and its role in growth cone turning behaviour

Though we could not determine where in the *Lymnaea* embryo the RXR was specifically expressed, we were able to clearly determine the expression and sub-cellular localization of RXR in neurons of the adult CNS. We found that *Lym*RXR protein was localized to the cytoplasm and membrane of adult neurons, and staining in the neuropil strongly suggested localization in the axonal tracts. This axonal staining was further confirmed following immunostaining of acutely isolated axonal segments from the CNS, plated in culture. These findings were interesting, since RXR traditionally acts as a ligand-activated transcription factor and would thus be expected to show nuclear localization. Some nuclear receptors, including steroid and thyroid hormone receptors can, however, shuttle between the nucleus and cytoplasm (DeFranco, 1997; Kaffman and O'Shea, 1999). RXRα also shuttles between the nucleus and cytoplasm (either in the absence or presence of its ligand 9-*cis* RA), and can also act as a shuttle for the orphan receptor TR3, a process stimulated by 9-*cis* RA (Lin et al., 2004). 9-*cis* RA was also

found to enhance nuclear translocation of RXRα in COS-7 cells, by means of association with importinβ bound to a RXRα nuclear localization signal (NLS). Phosphorylation of a conserved serine/threonine in the NLS of nuclear receptors inhibits their ability to translocate to the nucleus, and if threonine is mutated into aspartic acid in human RXRα, nuclear localization is significantly hindered (Sun et al., 2007). Our *Lym*RXR protein shares an identical NLS with the human RXRα, suggesting that phosphorylation of this threonine in *Lym*RXR may play a role in its cytoplasmic localization.

In embryonic cultured rat hippocampal neurons, RXR isoforms exhibited differential nuclear and cytoplasmic staining. All RXR isoforms except RXRβ2, were shown to be present in the cytoplasm, but RXRα was the only RXR isoform that was expressed in the axonal compartment (Calderon and Kim, 2007). RXRα was also evident in the axonal compartment of newly regenerating axons following sciatic nerve crush injury (Zhelyaznik and Mey, 2006), possibly supporting a role for RXR in neural regeneration. In our regenerating adult *Lymnaea* neurons, RXR immunoreactivity was found in most of the neuritic processes, though some differential distribution between neurites of the same cell was observed. The cellular distribution of RXRα has also been shown to be time-dependent during regeneration in acutely isolated rat spinal cord tissue, varying between dendritic and nuclear localization, depending on days following surgery (Schrage et al., 2006). Interestingly, these authors also determined the presence of retinoid receptors in the cytoplasm of neurons and glia cells in the *non-injured* spinal cord, similar to our observations of *Lym*RXR distribution in the non-regenerating CNSs.

Having demonstrated neuritic localization of *Lym*RXR, both in non-regenerating and regenerating neurons, we next demonstrated that a RXR pan-agonist, applied to the growth cones of cultured PeA motorneurons, induced growth cone turning and mimicked the growth cone response to 9-*cis* RA (and all-*trans* RA seen previously; Dmetrichuk et al., 2008). We should note however, that this RXR pan-agonist was designed for the vertebrate RXR and we have no knowledge of its binding affinity to the *Lym*RXR, (though our *Lym*RXR shows over 80% homology to the LBD of vertebrate RXRα and the 9-*cis* RA-interacting amino acids are 100% conserved). Likewise, both RXR antagonists used in this study were designed against the vertebrate RXR, yet our data show that both antagonists significantly reduced the growth cone turning response to the RXR agonist. Interestingly, the results with the RXR antagonist PA452 were more ambiguous than with the antagonist HX531. In the presence of PA452, even though the overall mean turning angle was significantly reduced compared to controls, the RXR agonist was still able to induce a positive turning response in 6 of the 9 growth cones tested. This was not the case with HX531, where only 1 of 10 growth cones showed any positive turning response to the RXR agonist. In 9 of the 10 growth cones, the attractive turning was completely abolished in HX531. It appears, therefore, that HX531 is a more effective antagonist for the *Lym*RXR than PA452, though the reason for this is not known. This is also supported by our finding that HX531 produced some teratogenic effects during *Lymnaea* embryogenesis, whereas PA452 had no obvious effect.

Together with our evidence that *Lym*RXR is localized in neurites and growth cones, our data showing RXR agonist-induced growth cone turning (that is subsequently inhibited in the presence of an RXR antagonist), strongly implicate a role for RXR in

regeneration and growth cone guidance. In support of this conclusion, Zhelyaznik and Mey (2006) recently showed that RXRα transcript and protein levels were up-regulated after sciatic nerve crush injury in rats. Furthermore, they demonstrated that the increase in RXRα immunoreactivity after injury did not occur in the degenerating nerve stump, but was observed in regenerating axons. This led the authors to propose that regulation of RXRα was connected with processes related to axon growth.

As mentioned previously, an RAR has also recently been cloned from the *Lymnaea* CNS (Carter and Spencer, 2009). We do not yet know whether this receptor also exists outside the nucleus, and thus cannot rule out the possibility that the RXR may be acting in conjunction with the RAR to produce growth cone turning. We also have not yet determined whether the endogenous retinoid isomers might be activating other parallel pathways (such as direct interactions with enzymes) to produce growth cone turning, and so the exact contribution of RXR activation in the turning response produced by 9-*cis* and all-*trans* RA is yet to be determined.

A non-genomic role for RXR in growth cone turning

A significant finding of our current study is that the RXR agonist also produced growth cone turning of isolated growth cones, in the absence of the cell body and nucleus, suggesting a novel, non-genomic role in growth cone steering. There are a number of reports in the literature of RA exerting non-genomic actions. Some of these involve activation of messengers such as ERK1/2 and RSK (Aggarwal et al., 2006), and direct binding with PKC (Ochoa et al., 2003). Other reports implicate non-genomic actions of RARs. For example, RA rapidly enhanced spontaneous acetylcholine release

at developing neuromuscular synapses in *Xenopus* cell culture and an RARβ agonist alone mimicked this effect (Liao et al., 2004). Another study demonstrated RARα in rat hippocampal dendrites and demonstrated a non-genomic role in translational control of GluR1 (Poon and Chen, 2008). The activation of phosphatidylinositol-3-kinase during RA-induced differentiation of neuroblastoma cells is also proposed to occur via non-genomic actions of the RAR (Masia et al., 2007). Though there are no previous reports of non-genomic actions of RXR in the CNS, RXRs were recently shown to exert non-genomic effects in human platelets (Moraes et al., 2007). RXRα and RXRβ were present in the cytosolic and membrane fractions of the platelets and (despite the lack of a nucleus) the proposed RXR ligand, 9-*cis* RA, inhibited platelet aggregation. It was determined that the platelet RXR bound to the G protein $Gq_{/11}$, and that this association was strengthened within 3 minutes of 9-*cis* RA stimulation. This led the authors to propose that the RXR-$Gq_{/11}$ binding event induced by 9-*cis* RA prevents $Gq_{/11}$ from activating Rac and the subsequent aggregation-dependant pathways (Moraes et al., 2007). Though we have previously shown a role for protein synthesis and calcium influx in the non-genomic actions of RA in *Lymnaea* growth cone turning, where and how the RXR may be involved in this signaling pathway, is currently unknown.

In summary, we have cloned the first retinoid receptor in the mollusc *Lymnaea stagnalis*, and demonstrated its presence and potential role during embryonic development. Significantly, we have demonstrated a cytoplasmic and neuritic localization for *Lym*RXR, both in non-regenerating adult CNSs, as well as in regenerating motorneurons *in vitro*. Finally, we have shown that *Lym*RXR is present in regenerating

growth cones, and provide the first evidence that RXR may play a novel, non-genomic role in mediating the chemotropic effects of RA.

Chapter 4:

Cloning of a novel, non-chordate retinoic acid receptor and its role in invertebrate development.

4.01 Abstract

Retinoic acid signaling in vertebrates is mediated by two classes of nuclear receptors, the retinoid X receptors (RXRs) and the retinoic acid receptors (RARs). Despite less being known about RA signaling in invertebrates, some effects of RA are conserved between vertebrates and invertebrates, though the RARs are thought not to exist in non-chordate invertebrates. However, invertebrates have been shown to contain both isomers of retinoic acid (9-*cis* RA and all-*trans* RA), even though the all-*trans* RA does not bind to the RXRs (at least in vertebrates). This raises the interesting question as to why invertebrates possess the all-*trans* RA isomer, if it has no RAR to bind to.

In this study, I have fully cloned the very first invertebrate, non-chordate RAR from the pond snail, *Lymnaea stagnalis (Lym*RAR*)*, and have studied its distribution and expression in the developing embryo, adult CNS, as well as regenerating cultured neurons. I then determined a functional role for this novel RAR in invertebrate development, and showed that RAR antagonists can disrupt embryonic development. These data strongly suggest that the role of the invertebrate RAR is conserved with the known roles of RARs in vertebrates. Interestingly, the expression pattern of the *Lym*RAR in non-regenerating neurons of the adult *Lymnaea* CNS, showed a non-nuclear distribution. This was also the case in the regenerating cultured neurons, where *Lym*RAR expression was also found in the growth cones. These findings indicate that the *Lym*RAR may also play a non-genomic role in RA-mediated chemoattraction, as shown for the *Lym*RXR.

Overall, this is the first study to fully clone and show functional expression of a non-chordate, invertebrate RAR, and sheds light on why invertebrates may possess the all-*trans* RA isomer.

4.02 Introduction

In the previous chapter, I cloned an invertebrate RXR from *L. stagnalis* and, together with N. Farrar, provided the first evidence that this RXR may play a role in mediating the chemotropic effects of RA on cultured *Lymnaea* neurons (Carter et al., 2010). Specifically, we demonstrated that a RXR-selective pan-agonist mediated growth cone turning, which was not significantly different from the turning produced by the natural ligand, 9-*cis* RA (Carter et al., 2010). I then showed that this RXR-agonist-induced growth cone turning was prevented in the presence of two different RXR antagonists, providing compelling evidence for an important role of the RXR. However, it has not yet been determined whether the RXR actually mediates the 9-*cis* RA-induced growth cone turning (Dmetrichuk et al., 2008), which is the natural ligand for RXR, at least in vertebrates.

Interestingly, the vertebrate RAR ligand, all-*trans* RA is also known to produce growth cone turning in *Lymnaea* neurons, and its role as both a neurotrophic and chemotropic factor in *Lymnaea* has been well documented (Dmetrichuk et al., 2006; Dmetrichuk et al., 2008). Despite the evidence for the presence and function of this all-*trans* RA isomer in the *Lymnaea* CNS (Creton et al., 1993; Dmetrichuk et al., 2006; Dmetrichuk et al., 2008), in addition to some other invertebrates (Nowickyj et al., 2008), a full-length RAR has never been cloned from any non-chordate, invertebrate species.

In vertebrates, RA signaling involves binding to the nuclear receptors, RXR and RAR. The active ligands for the RARs include both all-*trans* RA and 9-*cis* RA, whereas 9-*cis* RA acts as the ligand for RXRs. RXR is a promiscuous partner that can heterodimerize with many different receptors including RAR, thyroid receptor (TR),

Vitamin D receptor (VDR) and peroxisome proliferator-activated receptor (PPAR). RXR is also found in almost all metazoan species from insects to nematodes, including the non-metazoan marine sponge, *Suberites domuncula* (Simoes-Costa et al., 2008). Conversely, RAR is only known to partner with RXR to mediate RA-signaling.

The machinery responsible for RA metabolism includes the enzymes responsible for RA synthesis, called retinaldehyde dehydrogenases (ALDH1a, formerly RALDH), and the enzyme responsible for RA degradation (Cyp26). Until recently, ALDH1a, Cyp26, and RAR were only described in chordates, and the presence of these three genes was thought to be an important step for the innovation of the chordate body plan (Fujiwara and Kawamura, 2003). Most studies investigating the action of all-*trans* RA (e.g. on patterning embryonic axes) have thus almost exclusively used chordates. For example, after removal of RA from the diet of quail embryos (with a vitamin A deficient diet), the posterior hindbrain fails to develop normally (Maden, 2002). In mouse embryos, knocking out RALDH2, one of the enzymes that synthesize all-*trans* RA, causes neural tube defects, a reduction in the trunk region and defects to specific organs such as the heart (Niederreither et al., 1999). Conversely, treatment with higher levels of exogenous all-*trans* RA resulted in abnormal development of the caudal midbrain and anterior hindbrain regions in zebrafish embryos (Hill et al., 1995), and was also shown to significantly alter neural cell shape and polarity in developing rat sympathetic ganglia (Chandrasekaran et al., 2000).

Until recently, all-*trans* RA signaling was thought to be a vertebrate innovation. Recent studies with invertebrate chordates have revealed evidence for RA signaling machinery throughout the chordate lineage, including the invertebrate chordate species

cephalochordates (*Branchiostoma floridae*) and the urochordates (*Ciona intestinalis*). Together with the vertebrates, the cephalochordates and urochordates belong to the deuterostomes, a sub-taxon of the bilateria branch (see Fig. 27). Vertebrates possess three different RARs (α, β and γ) and three different RXRs (α, β and γ), whereas cephalochordates and urochordates have a single representative of each type of receptor. The only non-chordate, deuterostome RAR identified to date (predicted through genome screening) belongs to the sea urchin *Strongylocentrotus purpuratus*.

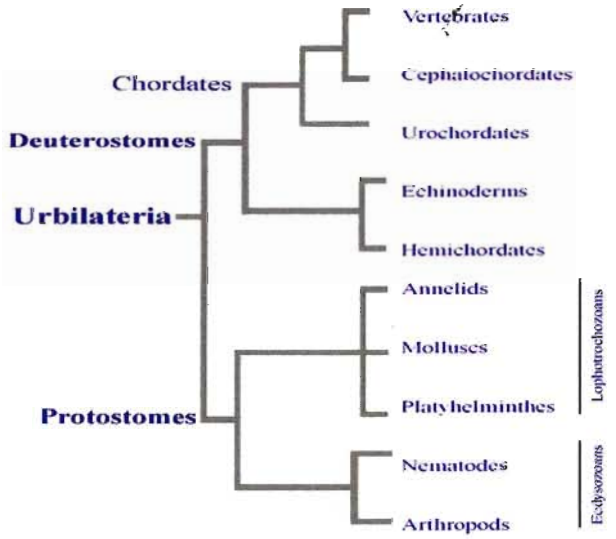

Figure 27. Tree diagram of the bilaterians

The other subtaxon of the bilateria branch is the protostomes, and this includes species such as molluscs and annelids (which belong to lophotrochozoans), and nematodes, crustaceans, and insects (which belong to ecdysozoans). Recently, genome screening of various protostomes has predicted the presence of an ancestral RAR in the annelid, *Capitella capitata*, and in the mollusk, *Lottia gigantea*. These predicted RAR sequences are the first evidence of an RAR in the protostome branch of bilaterians, but

neither of these sequences has been cloned, nor has the presence and/or role of the RAR protein been determined. To date, no RARs have been fully cloned from any protostome species.

The main aim of this study was to determine whether an RAR exists in the invertebrate, non-chordate protostome, *Lymnaea stagnalis*, and if so, to attempt to clone the full mRNA sequence and determine whether the RAR plays a similar role as it does in vertebrates.

4.03 Materials and Methods

Cloning of *L. stagnalis* RAR

All of the animals used in this study were laboratory-bred in aerated artificial pond water and were kept on a diet consisting of romaine lettuce and NutraFin Max Spirulina fish food (Hagen). Total RNA was isolated from the *Lymnaea* CNS using a PowerGen handheld homogenizer (Fisher Scientific) and purified according to the Norgen Total RNA isolation kit (Norgen Biotek Corp, Thorold, ON). Reverse transcription was carried out with a mixture of poly A and random hexamer primers according to the iScript cDNA synthesis kit (BioRad). Amplification was carried with 40 pmol of forward (5'-GTS AGY TCC TGT GAG GGC TGC AAG-3') and reverse (5'-GWA CAC GTT CAG CHC CTT TAA CGC-3') degenerate primers generated from conserved areas of the closest related species where an RAR had been identified. After 3 min of denaturation at 95°C, 30 cycles at 95 °C for 40 sec, annealing at 55 °C for 30 sec, and elongation at 72 °C for 30 sec, were performed with an Eppendorf Mastercycler Personal Thermocycler. The product was analysed on a 1.2% agarose gel containing ethidium bromide in TAE buffer. Bands of interest were excised from the gel according to MoBio gel purification kit and cloned into a pGemTEasy vector (Promega). Sequencing of the inserts was performed by GénomeQuébec (Montréal, Canada) using a 3730xl DNA Analyzer system from Applied Biosytems. From a partial RAR-like sequence, a full-length cDNA was generated from multiple rounds of both 5′ and 3′ RACE according to the SMART RACE cDNA amplification kit (Clontech).

Antibodies

From the full-length amino acid sequence for *Lymnaea* RAR, I designed antibodies against a synthetic peptide from a predicted 'hinge' region (AVRNDRNKKRKQKPES) covering the amino acid residues 188-203 located between the DNA binding domain (DBD) and ligand binding domain (LBD). The custom-made antibody was generated in New Zealand white rabbits by Pacific Immunology Corp. (Ramone, CA, USA) and was affinity-purified from the crude antisera. Commercial antibodies against human GAPDH (Abcam Inc.) and human actin (Sigma-Aldrich) were used as a cytosolic fraction marker and a control for the nuclear compartment, respectively.

***Lymnaea* embryos**

In order to investigate *Lym*RAR protein levels during *Lymnaea* development, egg masses were first incubated in pond water at 25°C and allowed to reach various stages of development, as described in Nagy and Elekes (2000). These stages included day 0 of embryogenesis (when egg mass is first laid and prior to first cleavage), the trochophore stage (approx 36 to 60 hrs of embryogenesis), the veliger stage (approx 60 to 96 hrs of embryogenesis), the adult-like stage just prior to hatching (96 to 192 hrs of embryogenesis) and hatchlings. When the embryos reached the desired stage, the capsules were removed from their gelatinous surroundings, total protein was extracted and Western blotting was performed, as described in the next section for adult CNSs. However, *Lym*RAR signals were not detected in early stages of embryogenesis, so

Western blotting was only performed on late veliger/metamorphosis stage embryos (approx. 84-108 h of embryogenesis).

Western Blotting

To investigate the expression of *Lym*RAR protein, adult *Lymnaea* CNSs (or whole embryos at the late veliger/metamorphic stage of development) were homogenized in lysis buffer containing 150mM NaCl, 50mM Tris HCl (pH7.5), 10mM EDTA, 1% Triton X-100, 1mM PMSF and 0.01% Protease Inhibitor Cocktail (Sigma-Aldrich) with a PowerGen handheld homogenizer (Fisher Scientific). The homogenates were centrifuged 20,000 x g at 4°C for 30 minutes. 15µg of protein from each extract was separated on a discontinuous SDS-polyacrylamide gel (12% Resolving, 4% Stacking) and electroblotted onto a nitrocellulose membrane (BioRad). The membranes were washed for 5 minutes in 1xPBS and then blocked in 1xPBS/0.1% Tween-20 (PBT) with 3% skim milk powder (w/v) for 1 hour. The membranes were then incubated with affinity purified *Lymnaea* RAR antibody at a dilution of 1/1000 in PBT/1% skim milk overnight at 4°C with gentle horizontal shaking. This was followed by 4 x 5 min washes at room temperature in PBT and incubation with a 1/15000 dilution of Alexa Fluor 680 goat anti-rabbit secondary antibody (Invitrogen). After 4 x 5min washes in PBT and one wash in 1xPBS, the membranes were imaged with the LI-COR Odyssey Infrared Imaging System at 700nm wavelength.

To investigate the subcellular expression of *Lym*RAR in the *Lymnaea* CNS, total protein from the cytoplasmic, membrane and nuclear compartments was isolated according to directions from the Qproteome Cell Compartment kit (Qiagen). Briefly,

20mg of CNS tissue (which equates to approximately 15 adult *Lymnaea* CNSs) was isolated and immediately placed into a 2ml centrifuge tube with 500µL of the manufacturer's buffer solution (CE1) that contains a protease inhibitor. The tissue was disrupted on the lowest speed with a PowerGen homogenizer (Fisher Scientific) for only 5 sec. The tissue was further disrupted by centrifugation for 2 min at 4°C in a QIAshredder homogenizer tube (Qiagen). After end-over-end mixing at 4°C for 10 min and centrifugation, the resulting supernatant should primarily contain cytosolic proteins. By sequential addition of other different extraction buffers to a cell pellet, proteins in other different cellular compartments can be selectively isolated by this method. Equal amounts of cytoplasmic, membrane, and nuclear fractions were loaded onto a discontinuous SDS-polyacrylamide gel (12% Resolving, 4% Stacking) and *Lym*RAR was detected by Western blotting technique as described above. Anti-GAPDH (Abcam Inc.) was used as a cytosolic fraction marker and successful isolation of protein from all three compartments of the CNS was confirmed by staining for actin. These experiments were performed three times.

Immunostaining

For immunostaining, the CNSs isolated from adult snails were fixed in 4% paraformaldehyde in PBS at 4°C overnight. For *Lymnaea* embryos, the capsules from egg masses at the late veliger stage were teased out of the gelatinous surroundings and washed in distilled water. The capsules were then fixed in 4% paraformaldehyde in PBS at 4°C overnight. Both fixed embryo capsules and CNSs were then washed in 10% sucrose/PBS for 2 hours, 20% sucrose/PBS for 2 hours, and then 30% sucrose/PBS

overnight at 4°C. After embedding the fixed embryonic capsules and CNSs in Optimal Cutting Temperature (O.C.T.) Compound (Tissue-Tek), serial 20μm sections were cut using a cryostat (Leica microsystems) and placed on Superfrost Plus slides (Fisher Scientific). For immunostaining of cultured neurons following outgrowth (24 to 36 hrs), cells were fixed in 4% paraformaldehyde in PBS at 4°C overnight. From this point on, all immunostaining procedures were the same for embryo capsules, adult CNSs, and cultured neurons. The samples were washed in PBS and then permeablized in 0.3% Triton X-100 in PBS (PBT) for 20 min and blocked in 3% normal goat serum (NGS) in PBT for 1 hour at RT. The samples were then incubated with the primary *Lym*RAR antibody diluted 1:50 in blocking solution at 4°C overnight. As a control, different preparations were incubated only in blocking solution, without the primary antibody, at 4°C overnight. All samples were then washed in PBT 3 x 5 minutes and incubated in 1:500 dilution of Alexa Fluor 488 goat anti-rabbit secondary antibody (Invitrogen) in blocking buffer at RT for 2 hours. The samples were washed for 3 x 5 min in PBT and after a brief wash in PBS, the specimens were coverslipped with anti-fade Fluorosave mounting media (Calbiochem).

Lymnaea embryonic development

To determine if *Lym*RAR plays a role in *Lymnaea* development, embryos were incubated in a synthetic RAR pan-agonist (TTNPB, Tocris Bioscience), a synthetic RAR pan-antagonist (LE540, a kind gift from H. Kagechika, University of Tokyo), a synthetic RARβ-selective antagonist (LE135, Tocris Bioscience), all-*trans* RA (Sigma-Aldrich), and DMSO as a control. At day 0 of embryogenesis (when egg mass is first laid),

capsules were teased out of the gelatinous surroundings in which they were embedded, and maintained in pond water at 25°C for 30 hrs (until the end of the gastrulation stage). This separation of the capsules increased probability of penetration of the agonists and antagonists while still allowing normal development of the egg inside the capsule (Carter et al., 2010; Creton et al., 1993). The RAR pan-agonist TTNPB (10^{-6}M and 10^{-5}M), the RAR pan-antagonist LE540 (10^{-6}M), the RARβ-selective agonist LE135 (10^{-6}M and 10^{-5}M), all-*trans* RA (10^{-6}M), or DMSO (0.001%, vehicle control) were added to separate dishes of embryos at 30 hrs of embryogenesis (this was previously shown to be the most sensitive stage to disruption by RA; Creton et al., 1993; Carter et al., 2010). The specific concentrations of agonist and antagonists used in these experiments were chosen partly on advice from Dr. Hiroyuki Kagechika (University of Tokyo, Japan) who developed LE540 and LE135, and from previous transactivation experiments (Pignatello et al., 1999; Umemiya et al., 1997). At days 6-7 of embryogenesis, embryos showing eye and/or shell malformations, or arrested development at the trochophore stage, were scored and compared with the DMSO control embryos. Statistical analysis was comprised of multiple Fisher Exact tests that were then Bonferroni-Holm corrected.

4.04 Results

Sequencing of a *Lymnaea* RAR

In my search for an invertebrate RAR gene, I first designed degenerate primers utilizing sequences for putative RAR genes of two species (*Lottia gigantean* and *Capitella capitata*) outside of the deuterostome lineage, that were previously discovered through surveys of genomic databases (Albalat and Canestro, 2009). Using these primers, I obtained an initial cDNA fragment from the CNS of *Lymnaea stagnalis*. Multiple rounds of 5′ and 3′ RACE from this initial fragment generated a full-length RAR cDNA that was 2280 bp, with a 1434 bp open reading frame that encodes for a 478 amino acid RAR protein (termed *Lym*RAR; accession no. GU932671). This *Lym*RAR has an overall amino acid identity of 55% with the vertebrate RARβ from *Homo sapiens,* although similar identity is also seen with RARα and RARγ from other vertebrates such as *Xenopus laevis* (54% identity and 55% identity respectively). Interestingly, the *Lym*RAR shows higher amino acid identity to vertebrate RARs than to the invertebrate chordate RARs. For example, it shares only 51% amino acid identity with the invertebrate chordate RARs from *Ciona intestinalis* (CionaRAR) and the amphioxus, *Branchiostoma floridae* (AmphioxusRAR). As is commonly seen with other nuclear receptors, the most conserved regions in the *Lym*RAR protein sequence are the predicted DNA-binding domain (DBD), which shares 85% amino acid identity with the DBD of *Homo sapiens* RARβ (accession no. NP_990657), as well as the predicted ligand-binding domain (LBD), which shares 58% amino acid identity with the LBD of *Homo sapiens* RARβ (Fig. 28).

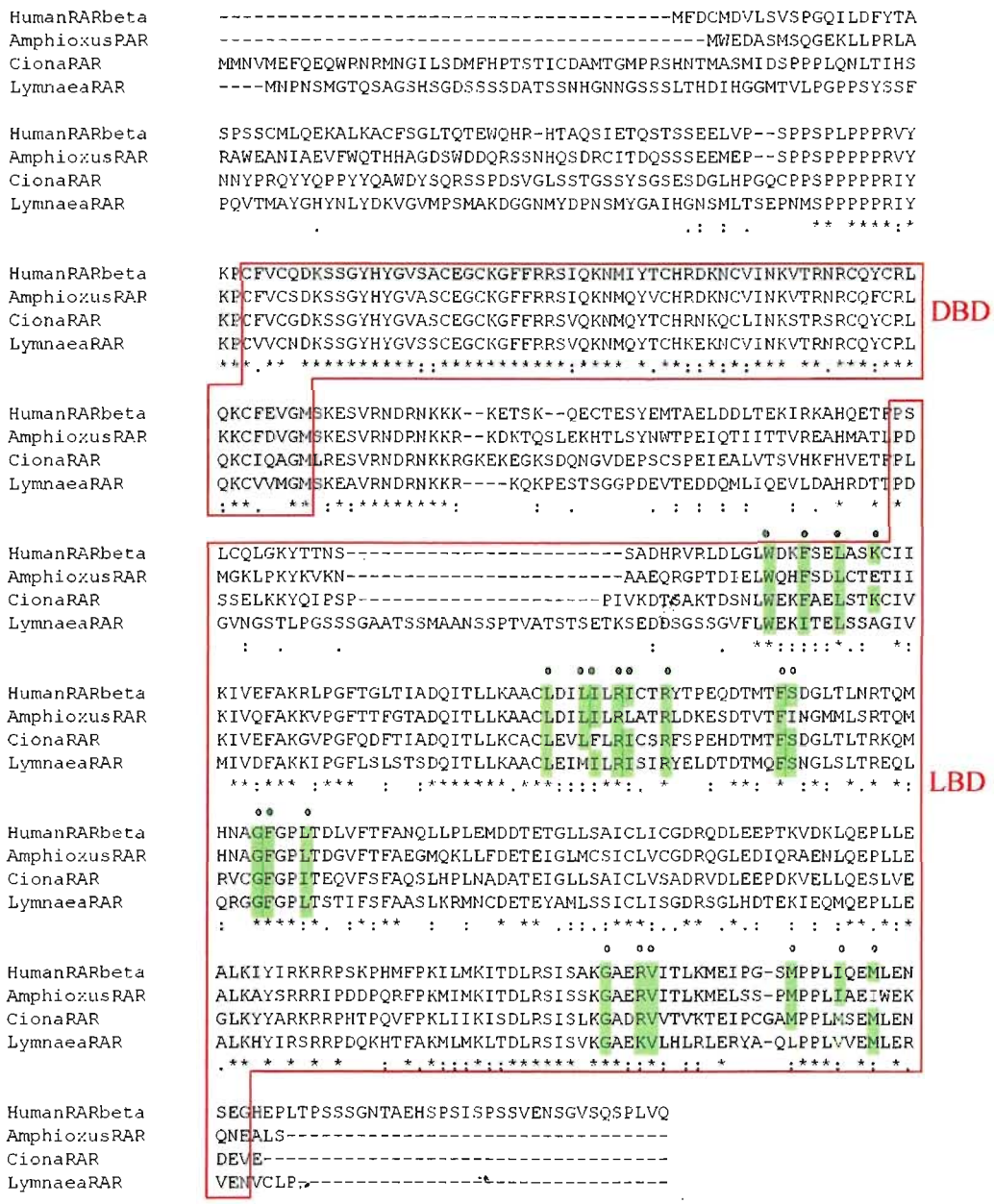

Figure 28. The *Lymnaea* RAR sequence. Multiple sequence alignment of the *Homo sapiens* RAR (HumanRARbeta; accession no. BAH02279), the cephalochordate amphioxus (an invertebrate chordate) RAR of *Branchiostoma floridae* (AmphioxusRAR; accession no. AAM46149), the urochordate tunicate (also an invertebrate chordate) RAR of *Ciona intestinalis* (CionaRAR; accession no. NP_001072037), and *Lymnaea stagnalis* RAR (LymnaeaRAR; accession no. ADF43963). The conserved DNA-binding domain (DBD) and ligand-binding domain (LBD), regions that are common to all retinoid receptors, are outlined in red. Amino acid positions that are implicated to be in direct contact with all-*trans* RA are indicated by a green circle above. Exact matches to human RARbeta are shaded green.

The only invertebrate, non-chordate RARs that I can compare with *Lym*RAR are from the predicted RAR sequences from *Lottia giantia* and *Capitella capitata* (previously mentioned above). *Lym*RAR shares 61% amino acid identity with the predicted RAR from the annelid, *Capitella capitata*, and 65% identity with the closest related RAR, that was predicted from the mollusc, *Lottia gigantea*.

Conservation of LBD residues

Previous studies have identified specific amino acids in the ligand binding pocket (LBP) of vertebrate RARs that are implicated in having direct contact with RA (Renaud et al., 1995). Table 1 shows these amino acids of the LBP with a comparison of aligned protostome and deuterostome RAR sequences, and reveals a significant degree of conservation between the two branches of bilaterians. In fact, of the fourteen sites that are shown in Table 1, the number of amino acids in the closest related non-chordate RAR (from *C. intestinalis*) that are conserved with the human RARs (α, β and γ) is twelve, whereas this number is only ten in the amphioxus RAR, nine in *L. gigantea* RAR and eight in the *C. capitata* RAR. Interestingly, the number of conserved amino acids between the human RARs and my newly found invertebrate, non-chordate *Lymnaea* RAR is ten. Thus, the RAR from *L. stagnalis* displays a high conservation of direct ligand binding residues with human RARs, one that is comparable to that of the amphioxus RAR, a receptor that has previously been found to bind, and be activated by, the RAR ligand all-*trans* RA.

Table 2 lists other known amino acid sites that have recently been found in mouse to directly interact with all-*trans* RA (Escriva et al., 2006). When comparing *L. stagnalis*

and amphioxus RARs with the mouse RARs, the *L. stagnalis* RAR has seven of the twelve amino acids conserved, while the amphioxus RAR has eight amino acids conserved. Of the amino acids that are not perfectly conserved with mouse RARs, the *Lymnaea* RAR contains three conservative amino acid substitutions, while the amphioxus contains two. Although not conclusive, the evidence provided here from Tables 1 and 2, show a similar degree of conservation between the *Lym*RAR and AmphiRAR with the human and mouse RARs.

In summary, although there is currently no direct experimental evidence to suggest that RAR may be a functional receptor for all-*trans* RA in protostomes, it is at least plausible that the RAR of *L. stagnalis* might bind the endogenous ligand, all-*trans* RA.

_Lym_RAR in the developing embryo

Given our previous finding of the presence of *Lym*RXR in the *Lymnaea* embryo during various stages of development, my first aim here was to determine whether the newly found *Lym*RAR was also present at various developmental stages in *Lymnaea*. A custom-made antibody against a synthetic peptide from the 'hinge' region between the DBD and LBD was used to detect the *Lym*RAR protein in frozen sections of *Lymnaea* embryos at the late veliger stage (Fig. 29). I chose this stage of development for the immunostaining since this is the earliest developmental stage with which I could detect a positive signal with Western blotting (Fig. 29C). Immunoreactivity was detected in various regions of the *Lymnaea* embryo, but stronger signals were seen within the shell

Table 1. Conservation of residues contacting all-*trans* RA in the LBD of RARs. Depicted below are the amino acid residues that are known to contact RA in the ligand binding pocket of human RARγ. Other metazoan RARs are aligned with the human RARs in order to show conservation of these RA-interacting residues. Amino acids marked red are exact matches to RARγ and boxes shaded blue are the amino acid positions of human RARγ that are known to interact with the carboxylate moiety (-COOH) of RA. The asterisk (*) above Met272 indicates the position where there is a difference between Human RARγ, RARα and RARβ (modified from Campo-Paysaa et al., 2008).

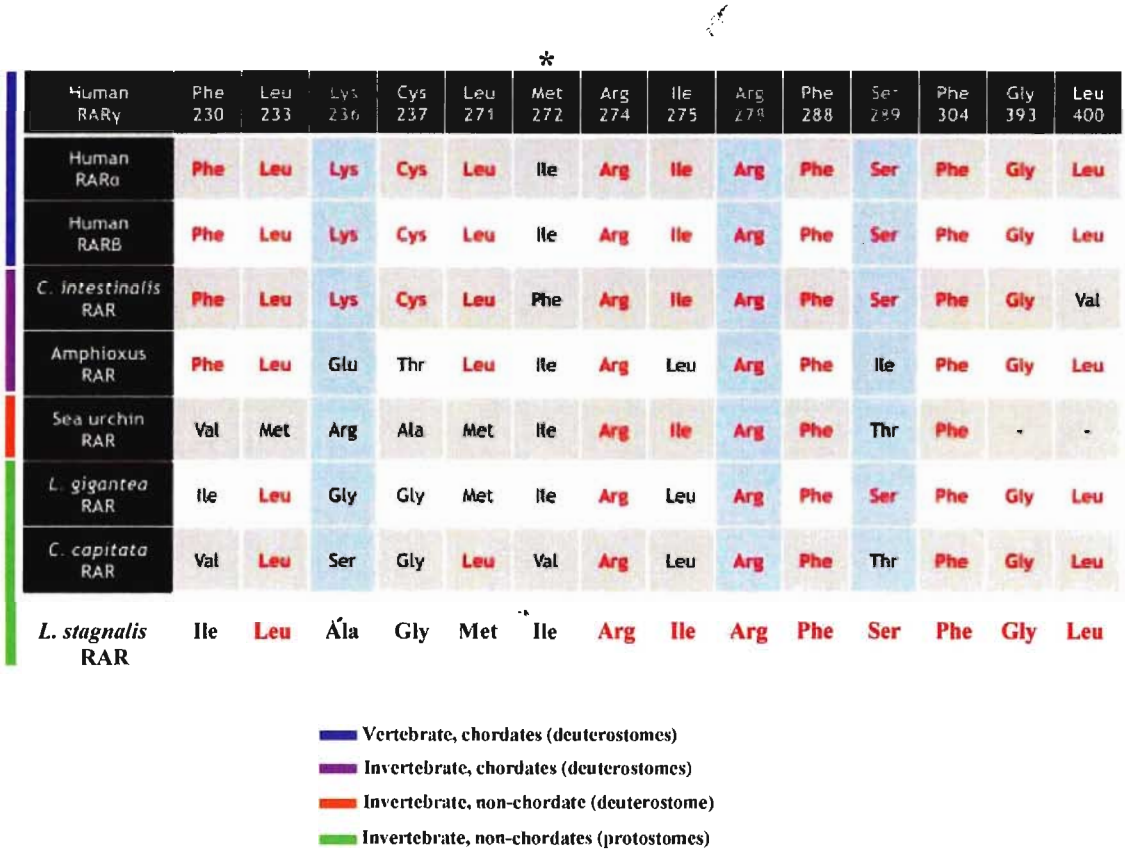

Table 2. Conservation of additional residues that have recently been implicated in contacting all-*trans* RA in the LBD of RARs. Depicted below are additional amino acid residues that are implicated in having direct contact with RA in the ligand binding pocket of mouse RARs. Other metazoan RARs are aligned with the mouse RARs in order to show conservation of these RA-interacting residues. Amino acids marked red are exact matches to mouse RARγ and blue amino acids are exact matches to either mouse RARβ or RARα (modified from Escriva et al., 2006). The asterisk (*) above Ala234 and Ala397 indicates the positions where there is a difference between the mouse RARγ, RARα and RARβ. The symbol (ǂ) indicates a conserved amino acid substitution (information for this table is taken partly from Escriva et al., 2006).

RARγ(mouse)	Phe(201)	Trp(227)	*Ala(234)	Cys(237)	Leu(268)	Gly(303)
RARα(mouse)	Phe	Trp	Ser	Cys	Leu	Gly
RARβ(mouse)	Phe	Trp	Ala	Cys	Leu	Gly
AmphiRAR	Leuǂ	Trp	Cys	Thr	Leu	Gly
LymRAR	Thr	Trp	Ser	Gly	Leu	Gly
RARγ(mouse)	Leu(307)	Arg(396)	*Ala(397)	Met(408)	Ile(412)	Met(415)
RARα(mouse)	Leu	Arg	Val	Met	Ile	Met
RARβ(mouse)	Leu	Arg	Val	Met	Ile	Met
AmphiRAR	Leu	Arg	Val	Met	Ile	Ileǂ
LymRAR	Leu	Lysǂ	Val	Leuǂ	Valǂ	Met

region (white arrows; Fig. 29Ai). One of the structures within the shell region resembled an early neural cell (as seen in Croll et al., 1996) with a long process emanating from the cell body (Fig. 29Aii). The only other clearly recognizable structure that displayed strong *Lym*RAR immunoreactivity was the lining of the pharynx/esophagus (yellow arrows; Fig. 29Bi,Bii) which appears in the shell region of the *Lymnaea* embryo. Western blot analysis of *Lymnaea* embryos total protein revealed a band of approximately 52 kDa in size, which matches the molecular weight predicted from the full ORF (Fig. 29C). However, as mentioned above, I was only able to detect *Lym*RAR protein by Western blotting in the latter stages of embryogenesis. The Western blot shown in Figure 29C is from embryos taken near the late veliger/metamorphic stage.

_Lym_RAR plays a role in embryonic development

Having previously shown a role for RXR in *L. stagnalis* embryogenesis, I next aimed to determine whether the same is true for the newly cloned RAR. Previously, both RXR agonists and antagonists were shown to disrupt various aspects of embryonic development (Carter et al., 2010) and so here, I again tested the effects of both agonists and antagonists of the RAR, as well as the known RAR ligand, all-*trans* RA (with DMSO controls). Specifically, I aimed to determine whether these treatments would disrupt the normal pattern of development in *Lymnaea*, and again, used eye and shell formation as indicators of normal growth, as these are easily visualized and characterized using light microscopy, shortly after the veliger stage.

Lymnaea embryos were maintained within their capsules, but were removed from their gelatinous surroundings. Capsuled embryos were treated with one of the

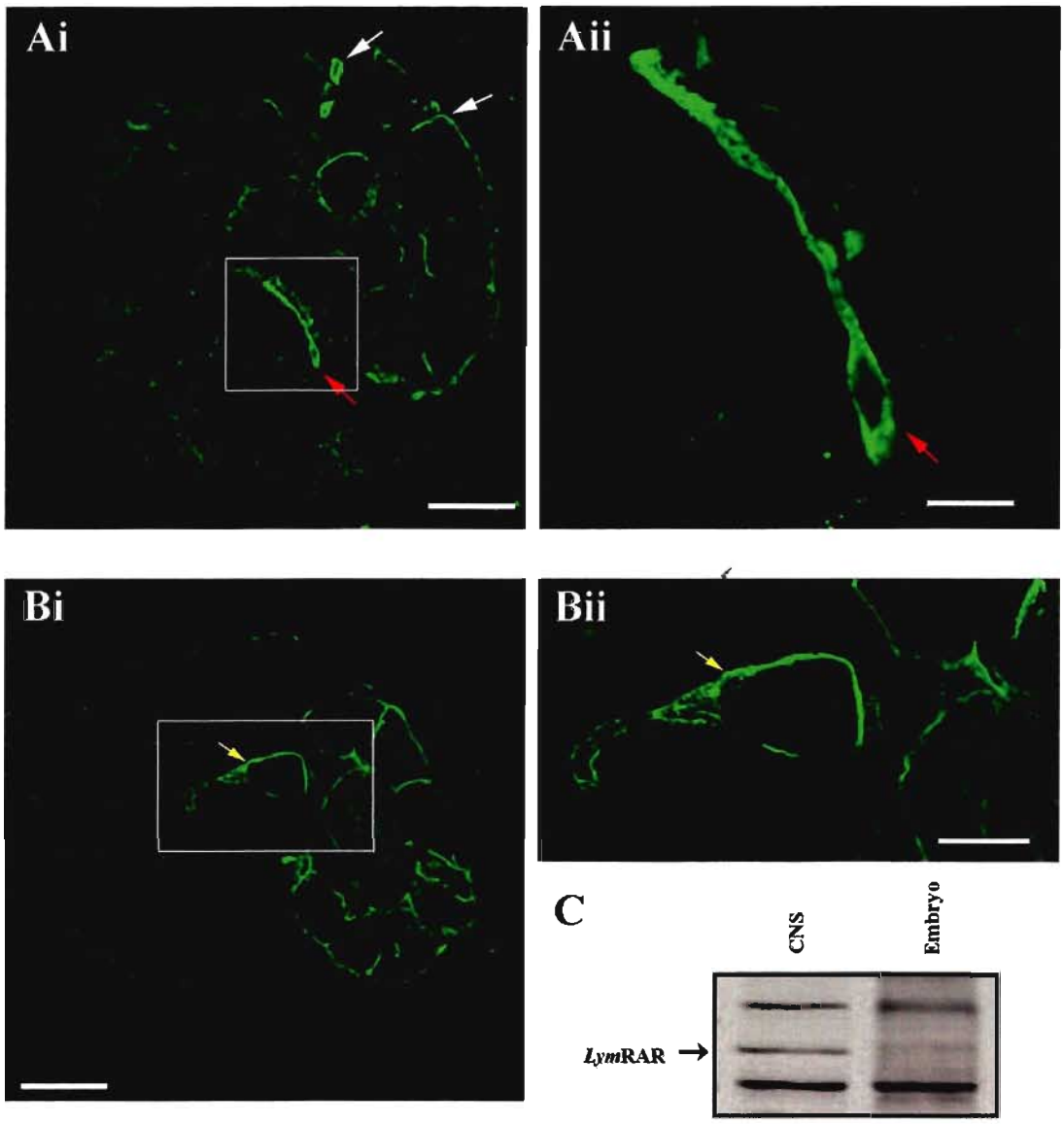

Figure 29. *Lym*RAR immunoreactivity in the developing embryo. (Ai) A section of a *Lymnaea* embryo at the late veliger stage of development shows more intense immunoreactivity for RAR in the shell region (white arrows) and at the interface between the shell and the foot region (red arrow). Scale bar: 100μm (Aii) Upon higher magnification of the boxed region of Ai, the structure shown by the red arrow appears to be a cell body with a long process emanating from it. Given the size and shape, this may be an early nerve cell (as seen in Croll et. al., 1996). Scale bar: 20μm (Bi) Another structure in the shell region that shows RAR immunoreactivity (yellow arrow) appears to be the pharynx/esophagus of the embryo. Scale bar: 100μm (Bii) Higher magnification of the boxed region in Bi reveals strong staining around the inner lining of this putative pharynx/esophagus (yellow arrow). Scale bar: 20μm. (C) Western blot indicating the presence of the *Lym*RAR in the late-stage embryo (as well as in the adult CNS for comparison).

following: a synthetic RAR pan-agonist, TTNPB (10^{-6}M, n = 40; 10^{-5}M, n = 42), a synthetic RAR pan-antagonist, LE540 (10^{-6}M, n = 35), an RARβ-selective antagonist, LE135 (10^{-6}M; n=27), the RAR ligand, all-*trans* RA (10^{-6}M; n = 24), or DMSO as the vehicle control (0.001%; n = 40). These treatments were started at the gastrula stage (30 h) and continued for the next 5 days of embryonic development. In the presence of DMSO, both shell and eye development appeared normal (Fig. 30A). However, I found that treatment with the antagonist LE135 (10^{-6}M; Fig. 30B), as well as the ligand all-*trans* RA (Fig 31A,B), produced defects in both eye and shell formation in a significant number of embryos (Fig. 32B,C). Eye defects included either missing eyes (Fig. 31A), or those noticeably reduced in size (not shown). Interestingly, TTNPB did not display any eye or shell abnormalities at 10^{-6}M (Fig. 31C) compared to all-*trans* RA at the same concentration (Fig. 31B), although increasing the TTNPB concentration to 10^{-5}M produced complete lysis of all embryos after 12 hours of treatment (Fig 31D), similar to the effects seen with 10^{-6}M LE540 and 10^{-5}M LE135 treatments (Fig. 30D, 32A). Together, these data strongly suggest a role for RAR in *Lymnaea* development.

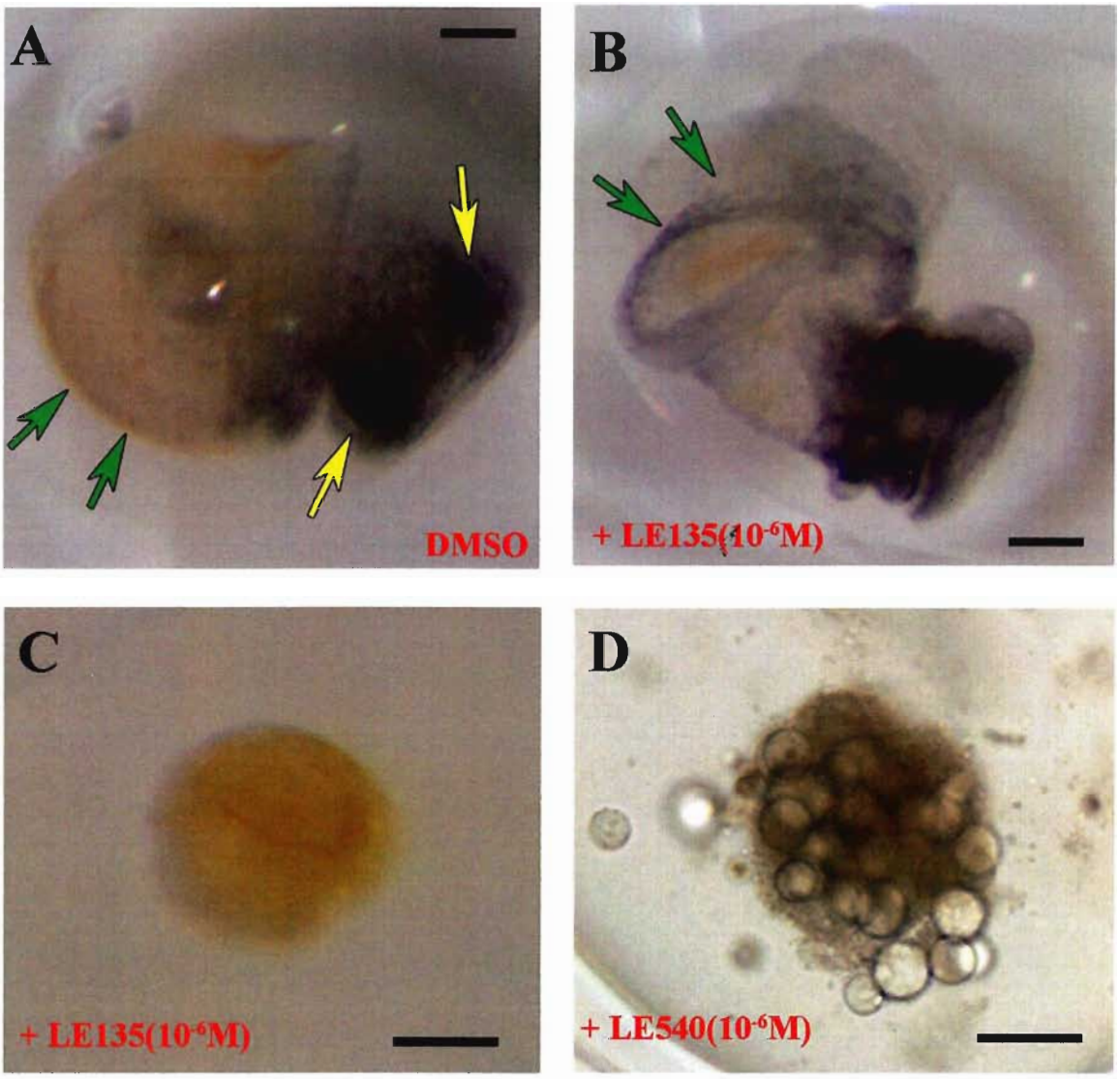

Figure 30. RAR-selective antagonists inhibit *Lymnaea* development.
(A) Representative example showing that addition of DMSO (0.001%) to *Lymnaea* embryos (as a vehicle control), did not affect development. All of the animals showed normal eye and shell development (when compared to embryos that were not treated with DMSO; not shown). Green arrows indicate the outline of the normally developing shell, and yellow arrows indicate the presence of both eyes. Scale bar: 200μm. (B) Representative example of a *Lymnaea* embryo incubated in the RARβ-selective antagonist LE135 (10^{-6}M). Green arrows indicate malformation of the shell. Scale bar: 200μm (C) Representative example of a halted embryo at the trochophore stage following incubation in LE135 (10^{-6}M). Scale bar: 100μm. (D) In some of the conditions, the halting of embryogenesis was due to early lysis of the normal spherical embryonic structure. This example was treated with RAR pan-antagonist, LE540 (10^{-6}M). Scale bar: 100μm.

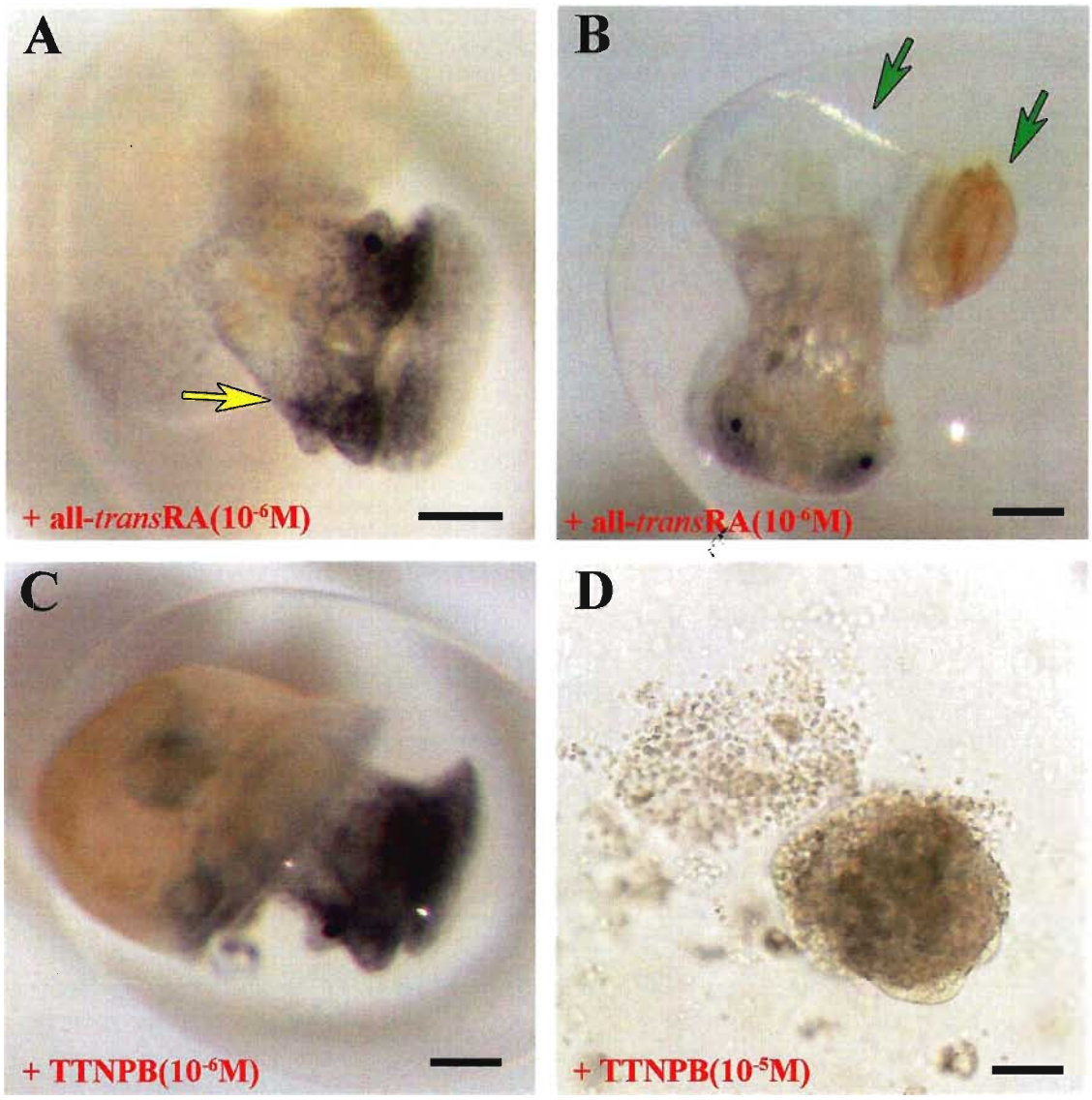

Figure 31. An RAR-selective agonist can inhibit *Lymnaea* development.
(A) Representative example of a *Lymnaea* embryo missing an eye (yellow arrow indicates where eye should be located) following incubation in all-*trans* RA (10^{-6}M); Scale bar: 200μm. (B) Treatment of embryos with all-trans RA (10^{-6}M) also caused malformations of the shell (green arrows); Scale bar: 200μm. (C) All of the animals showed normal eye and shell development when incubated in the RAR pan-agonist, TTNPB (10^{-6}M). Scale bar: 200μm. (D) When the concentratration of TTNPB was increased to 10^{-5}M, it resulted in complete lysis in 100% of the *Lymnaea* embryos early in development. Scale bar: 80μm.

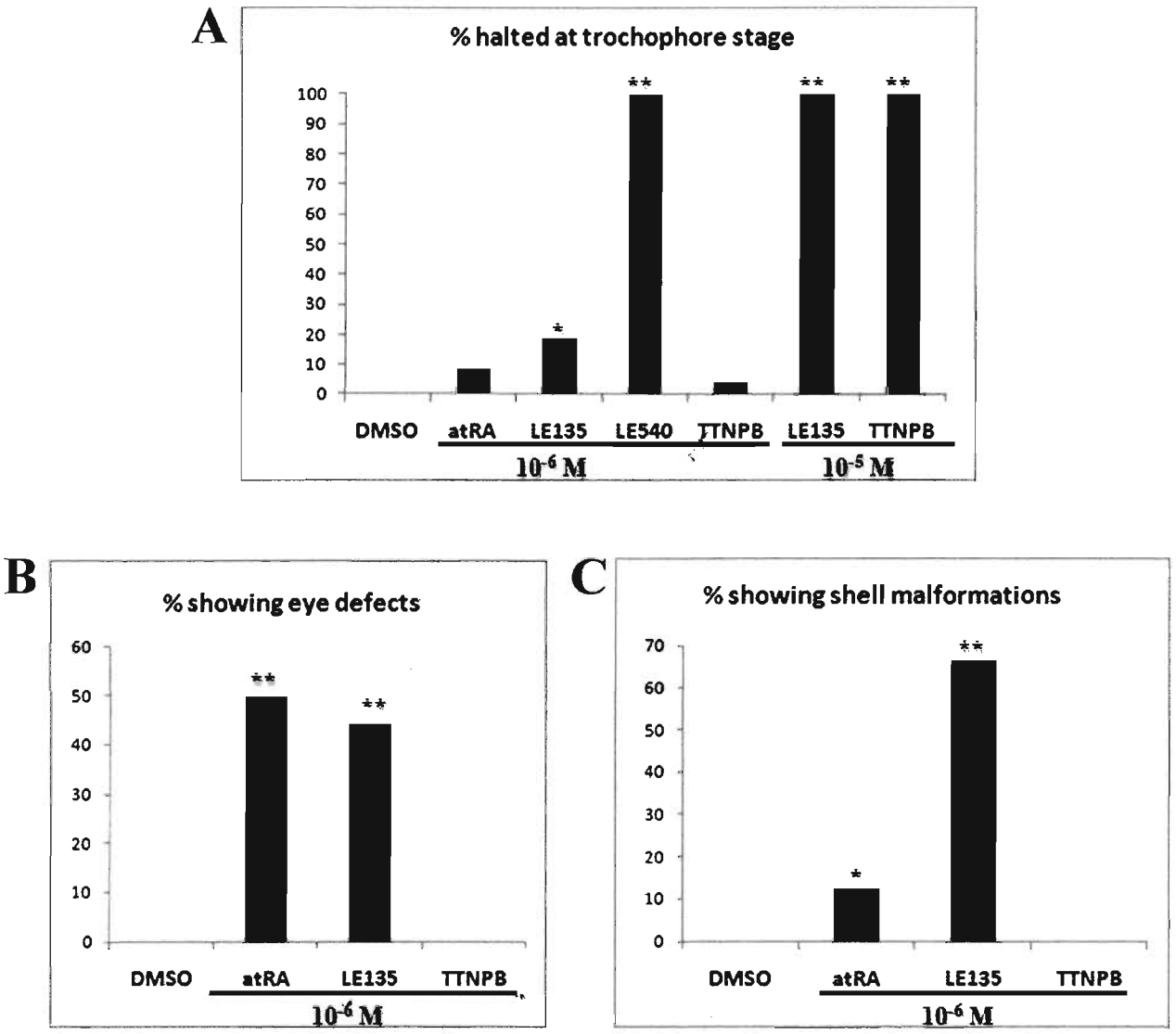

Figure 32. RAR agonists and antagonists cause varying degrees of abnormalities in *Lymnaea* development. Embryos were treated with RAR agonists and antagonists at different concentrations and the % of embryos halted at the trochophore stage (A), % with eye defects (B) and % with shell formations (C) are shown graphically above. All-*trans* RA (all-*trans* RA; n=24), LE135 (10^{-6}M; n=27), LE135 (10^{-5}M; n=32), LE540 (n=35), and the RAR-selective agonist TTNPB (10^{-6}M; n=40; 10^{-5}M; n=42) treatments were compared to the DMSO (n=40) treatment (* $p<0.05$, ** $p<0.01$).

***Lym*RAR is expressed in the adult CNS**

Recently, it has been shown that all-*trans* RA can exert both trophic and tropic effects on adult CNS neurons of *L. stagnalis* (Dmetrichuk et al., 2005). As these adult neurons of *Lymnaea* can respond to the RAR ligand, all-*trans* RA, my next aim was to determine the localization and expression of the *Lym*RAR in the adult CNS of *L. stagnalis*. Western blot analysis of the adult *Lymnaea* CNS total protein revealed a band of approximately 52 kDa in size (as shown previously in Fig. 29C). Using the same *Lym*RAR-specific antibody, I next performed immunohistochemistry on frozen sections of acutely isolated *Lymnaea* CNSs (n=22). Immunoreactivity was detected in neurons of all ganglia of the CNS. Specifically, the signal appeared to be located in the cytoplasmic region (Fig. 33B; yellow arrow) and axonal tracts (Fig. 33B; red arrow) of the central neurons, as well as in the neuropil (Fig. 33A; blue arrow). There was also strong immunoreactivity in the sheath surrounding the ganglia (Fig. 33B). This sheath immunoreactivity may have been due to RAR immunoreactivity of glial networks and cell bodies in the neural sheath, though this has not been conclusively demonstrated. Interestingly, there was little to no apparent staining of RAR (traditionally considered to be a nuclear receptor) in the nuclear region of the neurons (Fig. 33B; white arrow). Control CNS sections with no primary antibody added (n=8) demonstrated no immunostaining (Fig. 33D).

To further identify the neuronal compartmentalization of *Lym*RAR, I next isolated total protein fractions from the cytoplasm, membrane and nucleus of the *Lymnaea* CNS

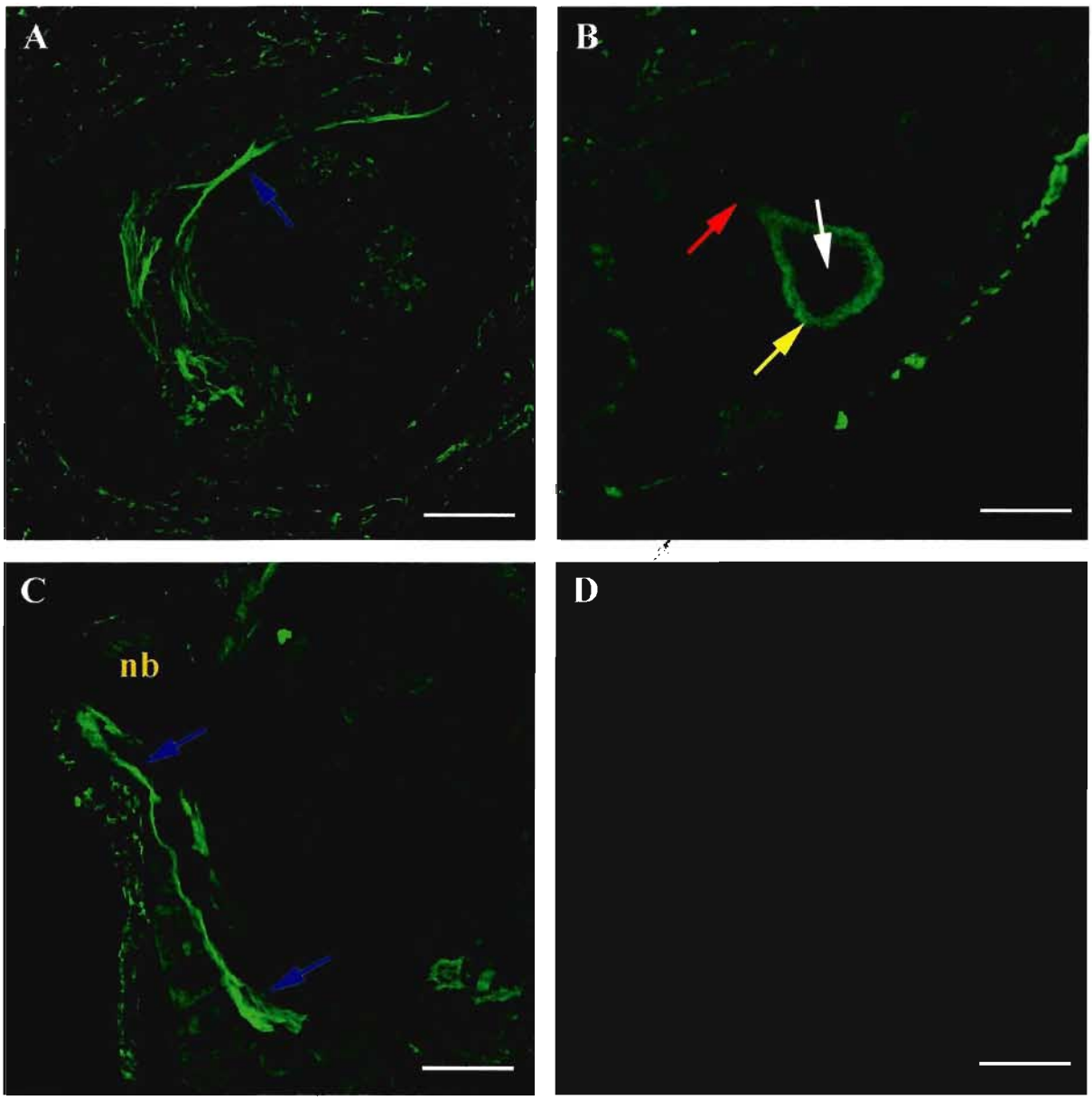

Figure 33. Cytoplasmic localization of *Lym*RAR in the adult, non-regenerating nervous system. (A) and (B) *Lym*RAR immunoreactivity was detected in the neurons of ganglia of the CNS (Visceral ganglion shown), primarily in the cytoplasm of the cell body (yellow arrow), axons (red arrow) and neuropil (blue arrow). Note the absence of RAR staining in the area that contains the nucleus (B; white arrow). Scale bars: A=100μm, B=50μm. (C) Immunoreactivity was also observed in axon tracts of the neuropil (blue arrows) that extend into a nerve bundle (nb) that connects to an adjacent ganglion. Scale bar: 80μm (D) Control staining was also performed under the same conditions, only in the absence of the primary *Lym*RAR antibody. Scale bar: 200μm.

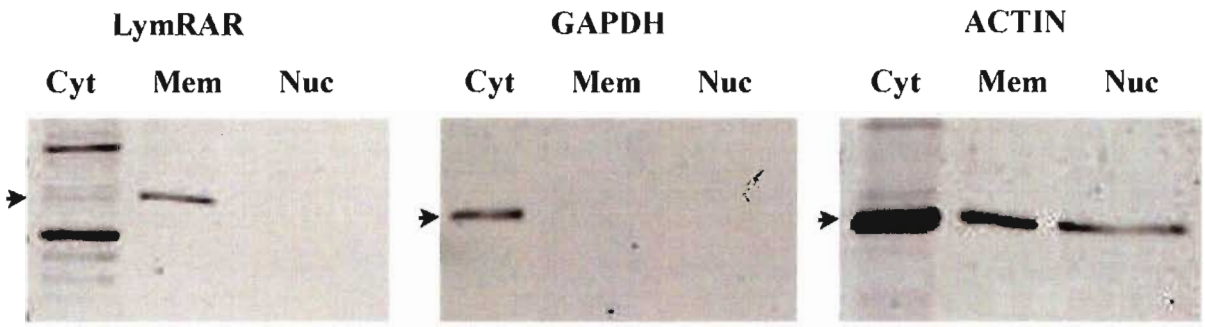

Figure 34. *Lym*RAR does not appear to be present in the nuclear fraction. Western blot performed on subcellular fractionations using our custom made *Lym*RAR antibody displayed a weak signal at the predicted molecular weight (arrow) in the cytoplasm (Cyt) and membrane (Mem) compartments, but was absent in the nuclear (Nuc) compartment. The abundant cytoplasmic enzyme GAPDH was used as a control and showed signal only in the cytoplasmic compartment of the same samples. Actin staining was used as a control to demonstrate successful isolation of protein from the nuclear compartment.

using a Qproteome Cell Compartment kit (Qiagen). In Fig 34, Western blot analysis shows a positive signal for RAR in the cytoplasmic and membrane compartments, but not in the nucleus. Anti-GAPDH was used as a control on the same protein fractions and as expected, GAPDH showed positive immunoreactivity only in the cytoplasmic compartment. The actin control demonstrated successful isolation of protein from all three compartments.

_Lym_RAR is present in the neurites and growth cones of regenerating cultured neurons

Previously, our lab has shown that the all-*trans* RA isomer can not only induce neurite outgrowth from cultured *Lymnaea* neurons, but can also exert a chemoattractive effect on the growth cones of these same neurons (Dmetrichuk et al., 2006). Despite not knowing whether all-*trans* RA is the natural ligand for this novel *Lym*RAR, I aimed to determine the presence and distribution of this *Lym*RAR in regenerating central neurons in culture. Pedal A (PeA) motor neurons were individually isolated from the intact ganglia and given 24-36 hours to regenerate in cell culture. Following outgrowth, these cells were then fixed and stained with the custom-made *Lym*RAR antibody. RAR immunoreactivity was visualized in the cell body of every cultured PeA neuron, whether it was actively regenerating neurites or not (n = 38 of 38). In the neurons that displayed outgrowth (n = 18), RAR immunoreactivity was observed in the majority of neurites (Fig. 35Ci; red arrows). Most of the growth cones located at the tips of the neurites also demonstrated positive immunoreactivity for RAR (Fig. 35Bi,Ci; white arrows). Interestingly, a closer look at the cell body of these neurons (Fig. 35Ai) revealed

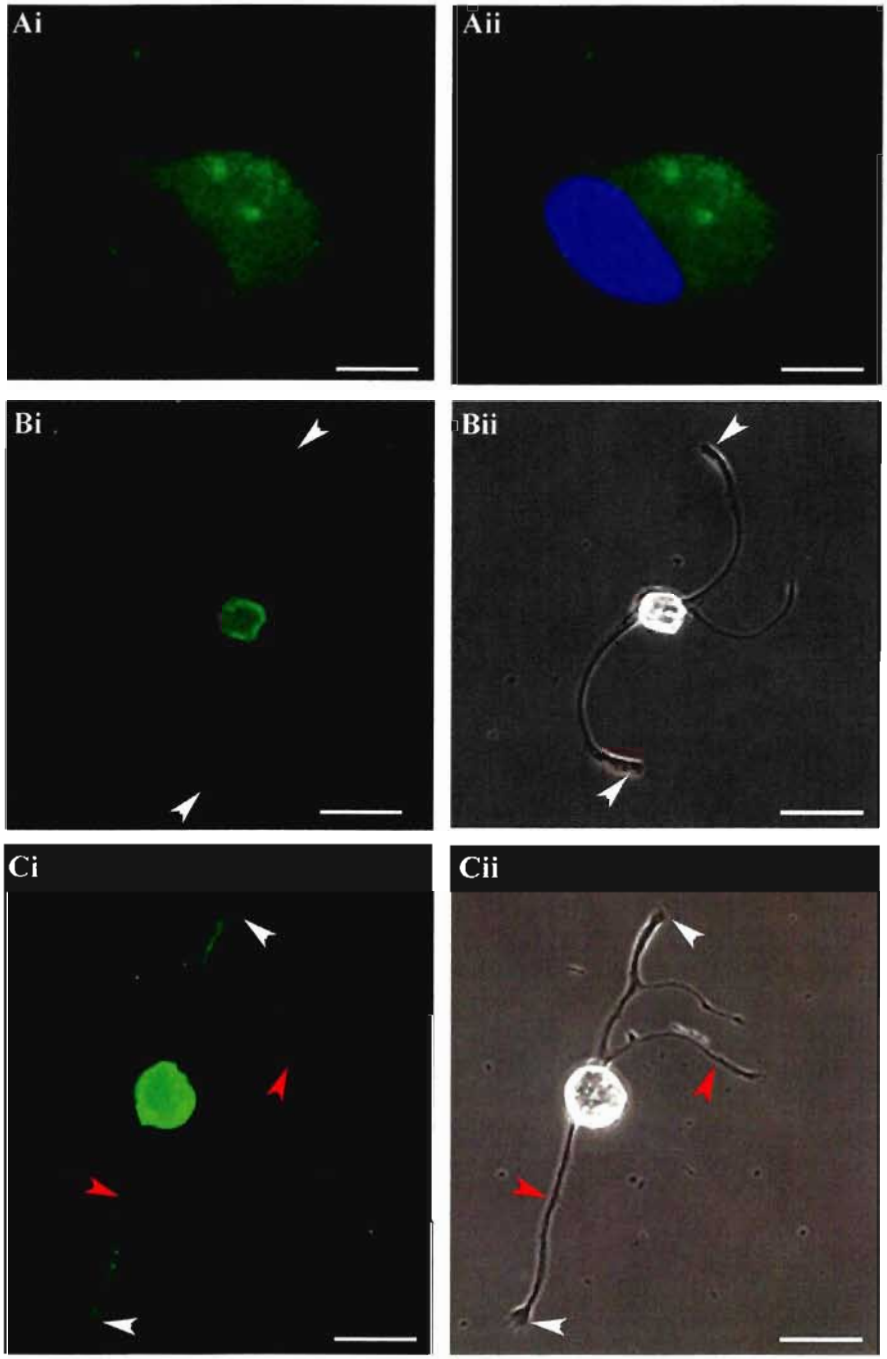

Figure 35. *Lym*RAR is present in the neurites and growth cones of regenerating motorneurons *in vitro*. (Ai,ii) Immunostaining of a cultured PeA cell with *Lym*RAR antibody revealed a signal in the cytoplasm of the cell body. Note the reduced RAR staining in the nucleus stained with DAPI. (Aii; blue) Scale bars: 10μm. (Bi) Immunostaining with the *Lym*RAR antibody showed staining in the cell body and in the growth cone domains (white arrows) (Bii) Phase-contrast image of the same PeA cell. Scale bars Bi-ii: 50μm. (Ci) Immunostaining with the *Lym*RAR antibody also showed a signal in some neurites (red arrows) leading to the growth cones (white arrows) (Cii) Phase-contrast image of the same PeA cell. Scale bars Ci-ii: 40μm.

immunofluorescence in the cytoplasmic region (Fig 35Ai), as indicated by the lack of RAR signal in the nuclear region stained with DAPI (Fig. 35Aii). Control regenerating PeA neurons, under the same staining conditions except in the absence of primary antibody, did not demonstrate RAR immunoreactivity (n = 6; data not shown).

4.05 Discussion

In this study, I have cloned a full-length RAR cDNA from the mollusc, *L. stagnalis* and have shown that this retinoid receptor is present in the embryo and in non-regenerating adult CNS, where it was found in the neuritic domains of the central neurons. Using regenerating cultured motor-neurons, I have revealed evidence for strong non-nuclear staining of RAR in the cytoplasm, neurites and growth cones. This finding is similar to the expression pattern of RXR of these same PeA motor neurons (Carter et al., 2010).

This newly identified *Lym*RAR is the first full-length RAR cloned from any non-chordate invertebrate species, and more importantly, from a species outside of the deuterostome lineage. This protostome RAR shares high homology with the only other molluscan RAR that was recently predicted from screening the genome of the mollusc *Lottia gigantea*. *Lym*RAR has an overall amino acid identity of 66% with *L. gigantea* RAR and approximately 55% with other vertebrate RARs of all types (α, β and γ). The similar homology of *Lym*RAR with all three vertebrate RAR classes is not surprising since the mollusc, *L. stagnalis*, may only contain a single copy of RAR, similar to the single copy of amphioxus RAR. There is increasing evidence that the three known vertebrate RAR subtypes arose through two periods of genome duplications, one before the split of agnathans (e.g. hagfish), and one before the split of cartilaginous fishes (Escriva et al., 2006).

I have also cloned a full-length RALDH cDNA (now known as Aldh1a) from the CNS of *L. stagnalis* (Appendix II). After the initial conversion of retinol to retinaldehyde, the Aldh1a enzyme irreversibly transforms retinaldehyde to RA. The Aldh1a enzyme was

initially thought to be a chordate innovation until the recent discovery of Aldh1a in cephalochordates, urochordates and hemichordates (Canestro et al., 2006), and later discovered through the help of genome sequencing in the lophotrochozoans, including two predicted Aldh sequences in the mollusc *L. gigantea*. My cloning of an Aldh1a and an RAR in *L. stagnalis*, along with the detection of all-*trans* RA in the CNS (Dmetrichuk et al., 2008) further supports a putative role for all-*trans* RA and its signaling machinery in *Lymnaea,* and also indicates an ancient origin of RAR and the Aldh1a enzymes, at least in the common ancestor of the bilaterians. We have not yet discovered the RA-catabolizing enzyme Cyp26 from *L. stagnalis*, but recent evidence has uncovered genes that are predicted to code for Cyp26 enzymes from the non-chordate, protostome species *L. gigantea* and *Capitella sp*. (Albalat and Canestro, 2009).

The ligand-binding domain (LBD) of most nuclear receptors, including RAR, is made up of an anti-parallel, three-layered, helical sandwich consisting of 12 helices. These helices form a hydrophobic ligand-binding pocket (LBP), and studies with vertebrate RARs show that the LBD consists of approximately 250 amino acids. It has been determined through studying the crystal structure of RARγ, that there are approximately 25 amino acids localized in the LBD of the RAR that make direct contact with the known ligand all-*trans* RA (Escriva et al., 2006; Renaud et al., 1995). Most of these predicted sites are shown in Figure 28 (green circles above sequence), and there is close to complete homology between *Lym*RAR and the vertebrate RARβ sequence at these same sites. Although we have not provided any direct evidence for all-*trans* RA binding with *Lym*RAR, there are functional studies that provide strong evidence from invertebrate chordates (cephalochordates and urochordates) and invertebrate non-

chordates (echinoderm species), that retinoid receptors can activate transcription in the presence of all-*trans* RA (Escriva et al., 2002; Nagatomo and Fujiwara, 2003). More recently, work by Campo-Paysaa et al. (2008) has predicted that the protostome RAR from the mollusc *L.gigantea* might bind all-*trans* RA providing *in silico* evidence from conserved amino acids within the LBD. Our lab has provided evidence that all-*trans* RA is present in the *Lymnaea* CNS (Dmetrichuk et al., 2008), which, together with this new evidence for expression of RAR and Aldh1a in the *Lymnaea* CNS, suggests that a good portion of the machinery is present for all-*trans* RA-signaling.

I have shown using Western blotting of *Lymnaea* embryo total protein near the late veliger/metamorphosis stage (approx. 84-108 h of embryogenesis), the presence of *Lym*RAR at the predicted molecular weight of 52 kDa. I was unable to detect a *Lym*RAR signal during earlier stages, possibly because RAR expression is below the detectable limits of my Western blotting procedure. There are other bands present (as shown in Figure 29C), and although I cannot conclude what these other bands are, they may represent cross-reactions of our custom-made *Lym*RAR antibody with other proteins, or they may be other isoforms of RAR. Multiple isoforms of RAR in our model system seems unlikely since in the few non-chordate species where RAR has been reported, there has only been one form of the receptor found in each species. Future work should include an immunizing peptide blocking experiment as a control to neutralize the custom-made *Lym*RAR antibody during Western blotting. In this way, the staining specific for the epitope of the *Lym*RAR antibody should be absent from the blot, and any bands that remain should be considered non-specific. Interestingly, the *Lym*RAR antibody-treated

membrane compartment in Figure 34 displays only one solid band at the predicted molecular weight of *Lym*RAR.

Previously, when we investigated the presence of *Lym*RXR in the embryo, we were unable to determine whether the signal was occurring in the nervous system or in other organs of the embryo. With the *Lym*RAR antibody, I thus performed immunohistochemistry on *Lymnaea* embryos at the later veliger stage of development (approx. 84-96 h of embryogenesis) to localize the expression. Early in this veliger stage, FMRFamide-reactive cells begin to form some of the first elements of the nervous system, and their presence remains into the later stages of *L. stagnalis* development (Croll and Voronezhskaya, 1996). These FMRFamide-reactive cells are thought to form the scaffold upon which the central ganglia and interconnecting pathways later develop. These cells are specifically referred to as Early FMRFamide-like immunoreactive Anteriorly Projecting (EFAP) cells, and can be further classified by position as central, left, or right (c-, l-, and r-) EFAP cells. The first ganglia (that will eventually circle the esophagus) may begin to appear within this time frame, but it is difficult to view them using light microscopy (Nagy and Elekes, 2000). In this study, I detected a strong *Lym*RAR signal in what appears to be a cell body with an elongated process emanating from it. The size and location of this cell are very similar to that seen with the l- and r-EFAP cells. I also detected staining in what appear to be thin processes extending across the embryo which may correspond to fibers projecting from early embryonic neurons as seen in Croll and Voronezhskaya (1996). The other staining I observed was around the lining of what appears to be the pharynx/esophagus. Again, these could be nerve fibers, but without any staining specific for nervous tissue, these hypotheses are speculative.

Therefore, in the absence of any neural-specific marker, I am unable to conclude the exact localization of the RAR within neural tissue at this time. My main aim here was, however, to show the presence of *Lym*RAR in the developing embryo.

In Chapter 3, I demonstrated that exposure of *L. stagnalis* embryos at the gastrula stage (approx. 30 h of embryogenesis) to 9-*cis* RA (10^{-7} M) caused specific developmental defects including eye defects, shell malformations and in some extreme cases, even halted development. The occurance of each of these defects increased when exposed to the RXR agonist PA024 alone (at the same concentration as the 9-*cis* RA isomer). Although all-*trans* RA was also shown to cause similar effects in *L. stagnalis* embryos at 10^{-6} M (Creton et al., 1993), there was no previous evidence for an RAR in non-chordates, so no synthetic RAR agonist or antagonists were previously used to investigate these all-*trans* RA-mediated effects. In this study, 10^{-6} M all-*trans* RA (typically a vertebrate RAR ligand) was also found to cause eye and shell malformations but the synthetic RAR pan-agonist, TTNPB, at 10^{-6} M did not have any effects on *L. stagnalis* embryogenesis. However, at 10^{-5} M, TTNPB caused complete lysis of 100% of the embryos after only 12 hours of treatment. This result could suggest that TTNPB does not bind as efficiently with the *Lym*RAR as it has been shown to in vertebrates, where it is effective at concentrations as low as 10^{-8} M (Pignatello et al., 2002). Interestingly, an RARβ-selective antagonist, LE135, was found to cause eye and shell malformations at 10^{-6} M, but treatment with an RAR pan-antagonist, LE540, caused complete lysis of the embryos after 12 hours. This result is not surprising since my examination of the *Lym*RAR sequence has revealed that it does not show strong similarity towards one

specific subtype of RAR, but instead displays some similarities to all three vertebrate subtypes.

It is also possible that in *L. stagnalis*, all-*trans* RA may exert its effects through *Lym*RXR. Though the vertebrate RXR does not show binding affinity for all-*trans* RA, there is evidence from other invertebrates (e.g. locust embryos) that RXRs can bind both 9-*cis* and all-*trans* RA with similar affinities (Nowickyj et al., 2008). However, *Lym*RXR shares a higher amino acid similarity with the LBD of vertebrate RXRα than the locust RXR (data not shown), suggesting that *Lym*RXR is more likely to share binding affinities with vertebrate RXRs. In addition, there is supporting evidence that arthropods (such as locusts) do not possess an RAR (Albalat and Canestro, 2009; Campo-Paysaa et al., 2008; Simoes-Costa et al., 2008) so the locust RXR may have a different binding affinity for all-*trans* RA than *Lym*RXR, as their functional roles may be very different.

From the immunostaining of the *L. stagnalis* embryos, I could not get a clear picture of the exact localization of the *Lym*RAR signal, especially in the region of the nervous system, given the lack of a specific neural tissue marker. However, staining of the adult *L. stagnalis* CNS revealed *Lym*RAR signals in the cytoplasm and axons of neurons, with strong staining in the axonal tracts of the neuropil. Surprisingly, the nuclear region of the neurons shows little, if any, staining of *Lym*RAR. In fact, Western blot experiments revealed no discernable RAR signal in the nuclear compartment, but the *Lym*RAR protein was present in the cytoplasmic and membrane compartments of acutely isolated CNSs. These data mirror my previous findings with the *Lym*RXR, which also showed a non-nuclear distribution in the acutely isolated *Lymnaea* CNS. Again, these findings are interesting since RARs (like RXRs) have been classically defined as 'nuclear

receptors' and have been shown to regulate gene expression by binding to RA-response elements (RAREs) in the regulatory regions of direct target genes in the nucleus (Maden, 2007). Recently, however, there have been a number of reports of non-nuclear localization of RARs (Maghsoodi et al., 2008; Schrage et al., 2006) and there is also evidence of RARs (specifically RARα) shuttling between the nucleus and cytoplasm as a result of nerve injury (Schrage et al., 2006). Although we cannot rule out that the *Lym*RAR may translocate to the nucleus upon injury or in the presence of specific ligands, the presence of *Lym*RAR in the cytoplasm and axons may indicate a non-genomic role for *Lym*RAR.

It has been demonstrated in regenerating neurons of the adult *L. stagnalis* CNS, that local application of all-*trans* RA can induce growth cone turning (Dmetrichuk et al., 2006). Although the exact mechanism for this growth cone turning was not determined, the presence of *Lym*RAR in the vicinity of the growth cone may shed some light on a possible non-genomic mechanism involving *Lym*RAR. In fact, our lab has already provided evidence that this all-*trans* RA-mediated growth cone turning can occur in isolated neurites (without the cell body that contains the nucleus), and is dependant on local protein synthesis and calcium influx (Farrar et al., 2009). Other studies in vertebrates have also provided strong evidence supporting non-genomic roles of RAR in the nervous system. RARβ has been implicated in a rapid, non-genomic response involving transmitter release at developing neuromuscular synapses in *Xenopus* cell cultures (Liao et al., 2004). Also, RARα has been implicated in a non-genomic role as an RNA binding protein that directly regulates translation of glutamate receptor subunits in a RA-gated manner in dendrites (Poon and Chen, 2008). Immunostaining of our

regenerating adult *Lymnaea* neurons resulted in *Lym*RAR signals in the neuritic processes, including the growth cones. Although the presence of *Lym*RAR in the growth cones, along with the previous work showing all-*trans* RA-mediated growth cone turning (Dmetrichuk et al., 2006) suggests a chemotropic effect involving *Lym*RAR, future work is required to provide evidence for this. Interestingly, preliminary work by C. Rand in our lab has indeed shown evidence that the RAR pan-antagonist, LE540, can abolish both all-*trans* and 9-*cis* RA mediated turning.

In summary, I have cloned the first, full-length RAR cDNA from a non-chordate species and have provided the first evidence that it may play an important role in non-chordate embryonic development. This work thus provides evidence for an important conservation of the role of RARs between vertebrate and invertebrate species. As with the *Lym*RXR, we have also shown that *Lym*RAR has a cytoplasmic and neuritic localization in both regenerating and non-regenerating adult CNS neurons. The presence of *Lym*RAR in regenerating growth cones suggests a possible mechanism for all-*trans* RA-mediated turning, possibly in conjunction with *Lym*RXR. Future work is needed to elucidate whether *Lym*RAR and *Lym*RXR are indeed working in conjunction with each other.

5. Conclusions

The overall aim of this thesis was to first identify novel retinoid receptors present in specific vertebrate and invertebrate species, and to then investigate their expression patterns and functional roles. From the invertebrate species, *Lymnaea stagnalis*, I cloned a novel RXR and then showed for the first time that this receptor was important during molluscan development and (together with N. Farrar) in axon guidance. Furthermore, I cloned the very first invertebrate, non-chordate RAR and provided evidence for its conserved functional role in development.

In the vertebrate species, *N. viridescens*, I was the first to clone a full-length RARβ subtype. Although human, rat and mouse contain an RARβ, it was previously thought that newts did not possess the β subtype (Maden and Hind, 2003). I also showed for the first time in any adult vertebrate CNS, that an RARβ2 can be transcriptionally active in the adult brain and spinal cord. This was the first demonstration of a full-length RARβ2 in a vertebrate species capable of regenerating many anatomical structures and organs, such as the CNS, limbs and tail.

Role of *Nv*RARβ2 in newt tail regeneration

Previous studies had found a strong correlation between axonal regeneration and expression of RARβ2 receptors in developing mammals. For example, embryonic mouse spinal cord tissue extended neurites after application of RA *in vitro*, and this corresponded well with the expression of RARβ2. However, tissue from adult mouse spinal cord did not regenerate neurites after application of RA and did not show an upregulation of RARβ2. If the adult spinal cord tissue was then transfected to over-express RARβ2, prolific neurite

outgrowth occurred (Corcoran et al., 2002). These previous studies strongly suggest that the ability of adult spinal cord to regenerate is highly dependent on expression levels of RARβ2.

In this study, I investigated the expression of a novel RARβ2 receptor in a species capable of spinal cord regeneration. In particular, I investigated its role in both tail and spinal cord regeneration in the adult newt, *N. viridescens*. After the first seven to eight days of tail regeneration, I found that the expression levels of RARβ2 mRNA and protein increase. These data indicate that RARβ2 is transcriptionally and translationally upregulated in response to tail regeneration. I have shown with immunostaining that RARβ2 expression is present in the spinal cord during the tail regeneration process. However, whether the upregulation of RARβ2 occurred only in the spinal cord, or whether it occurred in the regenerating peripheral nerves, or non-neural regenerate tissue of the tail blastema, is currently unknown. Expression of RARβ2 in the regenerating spinal cord following tail amputation corresponds well with the previous findings of Dmetrichuk et al. (2005). Our lab had previously shown that all-*trans* RA was capable of inducing directed neurite outgrowth from cultured newt spinal cord explants and that the RARβ-selective antagonist, LE135, could inhibit this regenerative response (Dmetrichuk et al., 2005). I have now shown in this study that the RARβ receptor subtype is not only important for spinal cord regeneration, but also for whole tail regeneration, as LE135 significantly reduced the length of tail regeneration compared to controls. The importance of the β2 subtype was studied by treating newts undergoing tail regeneration with the RARβ2-selective agonist, AC261066. Interestingly, this agonist treatment induced similar effects to the RARβ antagonist, (although it is well documented that both increased and decreased levels of RA can interrupt physiological processes). The only other literature pertaining to the effects of RAR agonists on tail regeneration involved the use of high

levels of exogenously applied retinol palmitate (Vitamin A; a precursor of RA which is a RAR pan-agonist). Specifically, Scadding (1986) showed that retinol palmitate caused an inhibition of tail regeneration in the newt *N. viridescens*, which is a similar result to that found in my study with the RARβ2-selective agonist. Likewise, in the closely related axolotl, *Ambystoma mexicanum*, all-*trans* RA treatment also inhibited overall growth of the tail regenerate by some 73% (Pietsch, 1987). Conversely, in frog tadpoles, increased levels of retinol palmitate caused aberrant regeneration by inducing numerous hindlimbs to regenerate from the cut site (Maden, 1993). It is not clear why the effects on these tadpoles were different from those in adult newt. However, despite these previous contradictory findings, my studies on the novel RARβ2 receptor in the adult newt strongly suggest that there may be a critical level of receptor signaling involved in normal tail regeneration. That is, alteration of its actions with either selective agonists or antagonists has profound downstream effects. Taken together, these results provide strong evidence for a crucial role for RARβ2 signaling in newt tail regeneration.

Non-nuclear distribution of the novel retinoid receptors in the CNS of *Lymnaea stagnalis*

Most previous studies on RA-mediated regeneration of the nervous system have been conducted in vertebrate systems, and little is known about the role of retinoid receptors in the invertebrate nervous system. Previous work from our lab has shown that both 9-*cis* and all-*trans* RA isomers are present in the CNS of the mollusc, *Lymnaea stagnalis*, and that both can exert neurotrophic and chemotropic effects on adult molluscan neurons (Dmetrichuk et al., 2006; Dmetrichuk et al., 2008; Farrar et al., 2009).

However, despite these observed physiological effects of RA, no retinoid receptors had previously been identified in this mollusc.

In this study, I have cloned the first retinoid receptor from the CNS of *L. stagnalis*. First, I identified a full-length RXR (*Lym*RXR), and then I determined that it shares high homology with the vertebrate RXRα isoform. Whereas other molluscan RXRs had previously been cloned, no full-length invertebrate, non-chordate RAR had ever been cloned. Despite the absence of any cloned RAR cDNA from the invertebrate non-chordates, its natural ligand, all-*trans* RA, had been shown to exert numerous morphogenic effects in invertebrates. For example, all-*trans* RA exerts morphogenic effects in the marine sponge (Imsiecke et al., 1994), disrupts limb regeneration in the fiddler crab (Hopkins and Durica, 1995) and produces developmental defects in molluscs (Creton et al., 1993), to name but a few. In this study, I cloned the first full-length invertebrate non-chordate RAR, a finding that may ultimately explain the means by which all-*trans* RA may be exerting its varied effects in numerous non-chordates.

In looking at the distribution of the *Lym*RXR and *Lym*RAR, I found that both of these (traditionally "nuclear") receptors were located in non-nuclear domains. This was the case for both the non-regenerating CNS as well as the regenerating adult neurons in culture. Interestingly, this suggests that both the *Lym*RXR and *Lym*RAR may have the potential to act in a non-genomic manner, although I cannot rule out the possibility that under certain circumstances they may translocate from the cytoplasm to the nucleus, as has been shown for other retinoid receptors (Park et al., 2010; Schrage et al., 2006; Yasmin et al., 2005).

My discovery of *Lym*RXR expression in the growth cones of actively regenerating neurites suggested that it may be playing a novel, non-genomic role in RA-mediated growth cone guidance. Dmetrichuk et al (2006) had previously shown that RA could induce growth cone turning in isolated neurites, in the absence of the nucleus. In Carter et al. (2010) we demonstrated that RXR agonists could also induce growth cone turning of isolated neurites, and as such, the RXR was likely mediating a non-genomic role in axon guidance. This is the first demonstration of a non-genomic role for RXR in the nervous system of any species. I then went on to confirm the role of RXR, by specifically showing that the RXR pan-antagonists, HX531and PA452, inhibited the PA024-induced growth cone turning.

Once the *Lym*RAR was cloned, the immunostaining studies also provided evidence for its presence in regenerating neurites and growth cones. This finding makes it plausible that the RAR may also be exerting non-genomic effects, as it has been shown to do in previous vertebrate studies. A colleague, Christopher Rand, now has preliminary evidence that *Lym*RAR is also involved in mediating RA-induced growth cone guidance. In particular, he has shown that the RAR pan-antagonist, LE540, significantly reduces the all-*trans* and 9-*cis* RA-induced growth cone turning in neurons from *L. stagnalis* (unpublished observations). However, whether *Lym*RAR is also mediating its effects in a non-genomic manner (as does the *Lym*RXR) has yet to be determined.

A conserved role for the invertebrate retinoid receptors in development

Both RXRs and RARs are well known to play important roles in the development of vertebrates (Niederreither and Dolle, 2008), but less is known about their specific roles

in non-chordate development, especially in the case of the RARs. In this study, I showed that both *Lym*RXR and *Lym*RAR are expressed in *L. stagnalis* embryos. Although I was specifically able to show that *Lym*RXR was present in the nuclear compartment in embryos, I was unable to distinguish whether the embryonic expression of either receptor was localized to the nervous system. However, with the use of selective RXR and RAR agonists and antagonists, I provided compelling evidence that both retinoid receptors play a role in *Lymnaea* development. This is the first evidence for a role of either an RXR or an RAR in the development of an invertebrate, non-chordate species.

Do the invertebrate receptors act together, and are they isomer specific?

The data presented here, for this non-chordate species implicate a role for both RXR and RAR in very similar processes of development as seen in many chordate species. Interestingly, the data also showed that the *Lym*RXR and *Lym*RAR have similar distribution expressions in the adult *Lymnaea* CNS. Even though vertebrate RXRs and RARs are well known to heterodimerize in order to bind to DNA and affect gene expression, I have no evidence that the same event is taking place in *Lymnaea.* The evidence for RXR/RAR heterodimers comes primarily from studies in vertebrate systems, mainly due to the fact that there are very few invertebrate RARs known, and of these, all have previously been found in chordates. However, there is one invertebrate chordate, *Polyandrocarpa misakiensis* (budding ascidians), where both an RXR (termed *Pm*RXR) and an RAR (termed *Pm*RAR) have been cloned. In this invertebrate, it was shown that the *Pm*RXR and *Pm*RAR can indeed hetermodimerize to form a *Pm*RXR/*Pm*RAR complex and can also then function as a transcriptional activator in

response to RA (Kamimura et al., 2000). There is also evidence from a closely related species of mollusc, *Biomphalaria glabrata*, that the RXR can function as a heterodimer with a mammalian RARα, suggesting that it also has the potential to bind with a RAR (although no RAR has been cloned from *B. glabrata*) (Bouton et al., 2005). Considering that my newly cloned *Lym*RXR cDNA is almost identical (97% amino acid identity) to the *B. glabrata* RXR, this suggests that the *Lym*RXR may have similar capabilities of binding with an RAR. Future experiments, however, are needed to explore the possibility that *Lym*RXR and *Lym*RAR may act as heterodimeric partners in RA-mediated signaling. There is also currently no evidence from any species to implicate an RXR/RAR complex acting in a non-genomic manner, so it would be interesting to determine if this is the case during RA-mediated growth cone turning in *Lymnaea*.

In this study, it is interesting that some of the effects of all-*trans* and 9-*cis* RA appeared to be very similar, as was the case in the embryogenesis experiments. Both endogenously applied all-*trans* and 9-*cis* RA had very similar effects in producing eye defects, shell malformations, and/or halted development. There is also evidence from our lab that both all-*trans* and 9-*cis* RA have very similar effects on enhancing neurite outgrowth, mediating growth cone turning and enhancing electrical excitability of cultured neurons. However, there are other studies from our lab that indicate isomer-specific effects of RA on *Lymnaea* neurons. For example, it has been shown that all-*trans* RA can induce acute effects on firing properties of neurons, but that 9-*cis* RA has no significant effect (Vesprini and Spencer, 2009). These data suggest that all-*trans* and 9-*cis* RA might possibly be capable of acting independently of each other. In vertebrate systems, it is known that RARs bind both all-*trans* and 9-*cis* RA, whereas RXRs only

bind 9-*cis* RA (Heyman et al., 1992). However, in the locust (non-chordate), there is evidence that the RXR binds both all-*trans* and 9-*cis* RA with similar affinities (Nowickyj et al., 2008). Future experiments will be required to determine the binding affinities of both *Lym*RXR and *Lym*RAR for all-*trans* and 9-*cis* RA. Once this has been determined, we can then investigate whether the effects shown here, involving non-chordate development and regeneration, support a combinatorial role of these newly discovered retinoid receptors.

Perspectives

RA has long been known to play an important role in embryonic development, but its role in invertebrate development is far less clear. Furthermore, although RA and its various signaling components have been identified in adult species, and its role in adult regeneration has been implicated, the exact processes involved have not been determined. In this study, I undertook the task of identifying key genes involved in mediating the effects of RA on adult vertebrate regeneration, as well as invertebrate development and neurite outgrowth. My identification of these novel retinoid receptors and the evidence presented here for their functional roles in their respective systems, will significantly contribute to future research into retinoid-mediated effects on both development and regeneration.

6. References

Aggarwal S, Kim SW, Cheon K, Tabassam FH, Yoon JH, Koo JS (2006) Nonclassical action of retinoic acid on the activation of the cAMP response element-binding protein in normal human bronchial epithelial cells. Mol Biol Cell 17:566-575.

Albalat R, Canestro C (2009) Identification of Aldh1a, Cyp26 and RAR orthologs in protostomes pushes back the retinoic acid genetic machinery in evolutionary time to the bilaterian ancestor. Chem Biol Interact 178:188-196.

Allenby G, Janocha R, Kazmer S, Speck J, Grippo JF, Levin AA (1994) Binding of 9-cis-retinoic acid and all-trans-retinoic acid to retinoic acid receptors alpha, beta, and gamma. Retinoic acid receptor gamma binds all-trans-retinoic acid preferentially over 9-cis-retinoic acid. J Biol Chem 269:16689-16695.

Beck CW, Christen B, Barker D, Slack JM (2006) Temporal requirement for bone morphogenetic proteins in regeneration of the tail and limb of Xenopus tadpoles. Mech Dev 123:674-688.

Benraiss A, Arsanto JP, Coulon J, Thouveny Y (1999) Neurogenesis during caudal spinal cord regeneration in adult newts. Dev Genes Evol 209:363-369.

Bettinger BT, Gilbert DM, Amberg DC (2004) Actin up in the nucleus. Nat Rev Mol Cell Biol 5:410-415.

Biesalski HK, Doepner G, Tzimas G, Gamulin V, Schroder HC, Batel R, Nau H, Muller WE (1992) Modulation of myb gene expression in sponges by retinoic acid. Oncogene 7:1765-1774.

Blomhoff R, Blomhoff HK (2006) Overview of retinoid metabolism and function. J Neurobiol 66:606-630.

Bonnet E, Touyarot K, Alfos S, Pallet V, Higueret P, Abrous DN (2008) Retinoic acid restores adult hippocampal neurogenesis and reverses spatial memory deficit in vitamin A deprived rats. PLoS One 3:e3487.

Borel F, de Groot A, Juillan-Binard C, de Rosny E, Laudet V, Pebay-Peyroula E, Fontecilla-Camps JC, Ferrer JL (2009) Crystal structure of the ligand-binding domain of the retinoid X receptor from the ascidian Polyandrocarpa misakiensis. Proteins 74:538-542.

Bouton D, Escriva H, de Mendonca RL, Glineur C, Bertin B, Noel C, Robinson-Rechavi M, de Groot A, Cornette J, Laudet V, Pierce RJ (2005) A conserved retinoid X receptor (RXR) from the mollusk Biomphalaria glabrata transactivates transcription in the presence of retinoids. J Mol Endocrinol 34:567-582.

Brown MD, Cornejo BJ, Kuhn TB, Bamburg JR (2000) Cdc42 stimulates neurite outgrowth and formation of growth cone filopodia and lamellipodia. J Neurobiol 43:352-364.

Calderon F, Kim HY (2007) Role of RXR in neurite outgrowth induced by docosahexaenoic acid. Prostaglandins Leukot Essent Fatty Acids 77:227-232.

Campo-Paysaa F, Marletaz F, Laudet V, Schubert M (2008) Retinoic acid signaling in development: tissue-specific functions and evolutionary origins. Genesis 46:640-656.

Canestro C, Postlethwait JH, Gonzalez-Duarte R, Albalat R (2006) Is retinoic acid genetic machinery a chordate innovation? Evol Dev 8:394-406.

Carter CJ, Farrar N, Carlone RL, Spencer GE (2010) Developmental expression of a molluscan RXR and evidence for its novel, nongenomic role in growth cone guidance. Dev Biol 343:124-137.

Carter CJ, Spencer GE (2009) Cloning of a retinoic acid receptor (RAR) from the CNS of a non-chordate, invertebrate protostome and its role in embryonic development. Program# 225.11, 2009 Neuroscience Meeting Planner. Chicago, IL: Society for Neuroscience, 2009. Online. pp 152-157.

Chandrasekaran V, Zhai Y, Wagner M, Kaplan PL, Napoli JL, Higgins D (2000) Retinoic acid regulates the morphological development of sympathetic neurons. J Neurobiol 42:383-393.

Chernoff EA (1996) Spinal cord regeneration: a phenomenon unique to urodeles? Int J Dev Biol 40:823-831.

Chernoff EA, Stocum DL, Nye HL, Cameron JA (2003) Urodele spinal cord regeneration and related processes. Dev Dyn 226:295-307.

Chung AC, Durica DS, Clifton SW, Roe BA, Hopkins PM (1998) Cloning of crustacean ecdysteroid receptor and retinoid-X receptor gene homologs and elevation of retinod-X receptor mRNA by retinoic acid. Mol Cell Endocrinol 139:209-227.

Clark AM (2010) Inhibition of RAR-ß Signaling Delays Tail Regeneration in the Adult Newt, *Notopthalmus viridescens*. Master's Thesis, Brock University.

Collins MD, Mao GE (1999) Teratology of retinoids. Annu Rev Pharmacol Toxicol 39:399-430.

Corcoran J, Shroot B, Pizzey J, Maden M (2000) The role of retinoic acid receptors in neurite outgrowth from different populations of embryonic mouse dorsal root ganglia. J Cell Sci 113 (Pt 14):2567-2574.

Corcoran J, So PL, Barber RD, Vincent KJ, Mazarakis ND, Mitrophanous KA, Kingsman SM, Maden M (2002) Retinoic acid receptor beta2 and neurite outgrowth in the adult mouse spinal cord in vitro. J Cell Sci 115:3779-3786.

Creton R, Zwaan G, Dohmen R (1993) Specific developmental defects in molluscs after treatment with retinoic acid during gastrulation. Develop Growth&Differ 35:357-364.

Croll RP, Voronezhskaya EE (1996) Early elements in gastropod neurogenesis. Dev Biol 173:344-347.

de The H, Marchio A, Tiollais P, Dejean A (1989) Differential expression and ligand regulation of the retinoic acid receptor alpha and beta genes. EMBO J 8:429-433.

DeFranco DB (1997) Subnuclear trafficking of steroid receptors. Biochem Soc Trans 25:592-597.

del Rincon SV, Scadding SR (2002) Retinoid antagonists inhibit normal patterning during limb regeneration in the axolotl, Ambystoma mexicanum. J Exp Zool 292:435-443.

Dmetrichuk JM, Carlone RL, Jones TR, Vesprini ND, Spencer GE (2008) Detection of endogenous retinoids in the molluscan CNS and characterization of the trophic and tropic actions of 9-cis retinoic acid on isolated neurons. J Neurosci 28:13014-13024.

Dmetrichuk JM, Carlone RL, Spencer GE (2006) Retinoic acid induces neurite outgrowth and growth cone turning in invertebrate neurons. Dev Biol 294:39-49.

Dmetrichuk JM, Spencer GE, Carlone RL (2005) Retinoic acid-dependent attraction of adult spinal cord axons towards regenerating newt limb blastemas in vitro. Dev Biol 281:112-120.

Dos Remedios CG, Chhabra D, Kekic M, Dedova IV, Tsubakihara M, Berry DA, Nosworthy NJ (2003) Actin binding proteins: regulation of cytoskeletal microfilaments. Physiol Rev 83:433-473.

Duester G (2008) Retinoic acid synthesis and signaling during early organogenesis. Cell 134:921-931.

Durston AJ, Timmermans JP, Hage WJ, Hendriks HF, de Vries NJ, Heideveld M, Nieuwkoop PD (1989) Retinoic acid causes an anteroposterior transformation in the developing central nervous system. Nature 340:140-144.

Egea PF, Mitschler A, Rochel N, Ruff M, Chambon P, Moras D (2000) Crystal structure of the human RXRalpha ligand-binding domain bound to its natural ligand: 9-cis retinoic acid. EMBO J 19:2592-2601.

Endo T, Yoshino J, Kado K, Tochinai S (2007) Brain regeneration in anuran amphibians. Dev Growth Differ 49:121-129.

Escriva H, Bertrand S, Germain P, Robinson-Rechavi M, Umbhauer M, Cartry J, Duffraisse M, Holland L, Gronemeyer H, Laudet V (2006) Neofunctionalization in vertebrates: the example of retinoic acid receptors. PLoS Genet 2:e102.

Escriva H, Holland ND, Gronemeyer H, Laudet V, Holland LZ (2002) The retinoic acid signaling pathway regulates anterior/posterior patterning in the nerve cord and pharynx of amphioxus, a chordate lacking neural crest. Development 129:2905-2916.

Farboud B, Privalsky ML (2004) Retinoic acid receptor-alpha is stabilized in a repressive state by its C-terminal, isotype-specific F domain. Mol Endocrinol 18:2839-2853.

Farrar NR, Dmetrichuk JM, Carlone RL, Spencer GE (2009) A novel, nongenomic mechanism underlies retinoic acid-induced growth cone turning.

Farrar NR, Spencer GE (2008) Pursuing a 'turning point' in growth cone research. Dev Biol 318:102-111.

Feng ZP, Zhang Z, van Kesteren RE, Straub VA, van NP, Jin K, Nejatbakhsh N, Goldberg JI, Spencer GE, Yeoman MS, Wildering W, Coorssen JR, Croll RP, Buck LT, Syed NI, Smit AB (2009) Transcriptome analysis of the central nervous system of the mollusc Lymnaea stagnalis. BMC Genomics 10:451.

Franke WW (2004) Actin's many actions start at the genes. Nat Cell Biol 6:1013-1014.

Fujiwara S, Kawamura K (2003) Acquisition of retinoic acid signaling pathway and innovation of the chordate body plan. Zoolog Sci 20:809-818.

Gale E, Zile M, Maden M (1999) Hindbrain respecification in the retinoid-deficient quail. Mech Dev 89:43-54.

Giguere V, Ong ES, Evans RM, Tabin CJ (1989) Spatial and temporal expression of the retinoic acid receptor in the regenerating amphibian limb. Nature 337:566-569.

Gu PL, Gunawardene YI, Chow BC, He JG, Chan SM (2002) Characterization of a novel cellular retinoic acid/retinol binding protein from shrimp: expression of the recombinant protein for immunohistochemical detection and binding assay. Gene 288:77-84.

Gudas LJ (1994) Retinoids and vertebrate development. J Biol Chem 269:15399-15402.

Heyman RA, Mangelsdorf DJ, Dyck JA, Stein RB, Eichele G, Evans RM, Thaller C (1992) 9-cis retinoic acid is a high affinity ligand for the retinoid X receptor. Cell 68:397-406.

Hill J, Clarke JD, Vargesson N, Jowett T, Holder N (1995) Exogenous retinoic acid causes specific alterations in the development of the midbrain and hindbrain of the zebrafish embryo including positional respecification of the Mauthner neuron. Mech Dev 50:3-16.

Hopkins PM, Durica DS (1995) Effects of All-Trans-Retinoic Acid on Regenerating Limbs of the Fiddler-Crab, Uca Pugilator. Journal of Experimental Zoology 272:455-463.

Hopp TP, Woods KR (1981) Prediction of protein antigenic determinants from amino acid sequences. Proc Natl Acad Sci U S A 78:3824-3828.

Hubbard SJ, Thorton JM (1993) NACCESS. Department of Biochemistry and Molecular Biology, University College London.

Huber AB, Kolodkin AL, Ginty DD, Cloutier JF (2003) Signaling at the growth cone: ligand-receptor complexes and the control of axon growth and guidance. Annu Rev Neurosci 26:509-563.

Hunter K, Maden M, Summerbell D, Eriksson U, Holder N (1991) Retinoic acid stimulates neurite outgrowth in the amphibian spinal cord. Proc Natl Acad Sci U S A 88:3666-3670.

Imsiecke G, Borojevic R, Custodio M, Muller WEG (1994) Retinoic Acid Acts As A Morphogen in Fresh-Water Sponges. Invertebrate Reproduction & Development 26:89-98.

Iten LE, Bryant SV (1976) Stages of tail regeneration in the adult newt, Notophthalmus viridescens. J Exp Zool 196:283-292.

Kaffman A, O'Shea EK (1999) Regulation of nuclear localization: a key to a door. Annu Rev Cell Dev Biol 15:291-339.

Kamimura M, Fujiwara S, Kawamura K, Yubisui T (2000) Functional retinoid receptors in budding ascidians. Dev Growth Differ 42:1-8.

Kern J, Schrage K, Koopmans GC, Joosten EA, McCaffery P, Mey J (2007) Characterization of retinaldehyde dehydrogenase-2 induction in NG2-positive glia after spinal cord contusion injury. Int J Dev Neurosci 25:7-16.

Kersten S, Kelleher D, Chambon P, Gronemeyer H, Noy N (1995) Retinoid X receptor alpha forms tetramers in solution. Proc Natl Acad Sci U S A 92:8645-8649.

Knutson DC, Clagett-Dame M (2008) atRA Regulation of NEDD9, a gene involved in neurite outgrowth and cell adhesion. Arch Biochem Biophys 477:163-174.

Kostrouch Z, Kostrouchova M, Love W, Jannini E, Piatigorsky J, Rall JE (1998) Retinoic acid X receptor in the diploblast, Tripedalia cystophora. Proc Natl Acad Sci U S A 95:13442-13447.

Kozak M (1991) An analysis of vertebrate mRNA sequences: intimations of translational control. J Cell Biol 115:887-903.

Krezel W, Dupe V, Mark M, Dierich A, Kastner P, Chambon P (1996) RXR gamma null mice are apparently normal and compound RXR alpha +/-/RXR beta -/-/RXR gamma -/- mutant mice are viable. Proc Natl Acad Sci U S A 93:9010-9014.

Liao YP, Ho SY, Liou JC (2004) Non-genomic regulation of transmitter release by retinoic acid at developing motoneurons in Xenopus cell culture. J Cell Sci 117:2917-2924.

Lin XF, Zhao BX, Chen HZ, Ye XF, Yang CY, Zhou HY, Zhang MQ, Lin SC, Wu Q (2004) RXRalpha acts as a carrier for TR3 nuclear export in a 9-cis retinoic acid-dependent manner in gastric cancer cells. J Cell Sci 117:5609-5621.

Lohof AM, Quillan M, Dan Y, Poo MM (1992) Asymmetric modulation of cytosolic cAMP activity induces growth cone turning. J Neurosci 12:1253-1261.

Maden M (1983) The effect of vitamin A on limb regeneration in Rana temporaria. Dev Biol 98:409-416.

Maden M (1993) The homeotic transformation of tails into limbs in Rana temporaria by retinoids. Dev Biol 159:379-391.

Maden M (1996) Retinoids in patterning: chimeras win by a knockout. Curr Biol 6:790-793.

Maden M (1997) Retinoic acid and its receptors in limb regeneration. Semin Cell Dev Biol 8:445-453.

Maden M (1998) Retinoids as endogenous components of the regenerating limb and tail. Wound Repair Regen 6:358-365.

Maden M (2002) Retinoid signalling in the development of the central nervous system. Nat Rev Neurosci 3:843-853.

Maden M (2007) Retinoic acid in the development, regeneration and maintenance of the nervous system. Nat Rev Neurosci 8:755-765.

Maden M, Corcoran J (1996) Role of thyroid hormone and retinoid receptors in the homeotic transformation of tails into limbs in frogs. Dev Genet 19:85-93.

Maden M, Gale E, Kostetskii I, Zile M (1996) Vitamin A-deficient quail embryos have half a hindbrain and other neural defects. Curr Biol 6:417-426.

Maden M, Hind M (2003) Retinoic acid, a regeneration-inducing molecule. Dev Dyn 226:237-244.

Maden M, Keen G, Jones GE (1998) Retinoic acid as a chemotactic molecule in neuronal development. Int J Dev Neurosci 16:317-322.

Maghsoodi B, Poon MM, Nam CI, Aoto J, Ting P, Chen L (2008) Retinoic acid regulates RARalpha-mediated control of translation in dendritic RNA granules during homeostatic synaptic plasticity. Proc Natl Acad Sci U S A 105:16015-16020.

Mahapatra PK, Mohantyhejmadi P (1994) Vitamin-A-Mediated Homeotic Transformation of Tail to Limbs, Limb Suppression and Abnormal Tail Regeneration in the Indian Jumping-Frog Polypedates-Maculatus. Development Growth & Differentiation 36:307-317.

Mangelsdorf DJ, Borgmeyer U, Heyman RA, Zhou JY, Ong ES, Oro AE, Kakizuka A, Evans RM (1992) Characterization of three RXR genes that mediate the action of 9-cis retinoic acid. Genes Dev 6:329-344.

Mansfield SG, Cammer S, Alexander SC, Muehleisen DP, Gray RS, Tropsha A, Bollenbacher WE (1998) Molecular cloning and characterization of an invertebrate cellular retinoic acid binding protein. Proc Natl Acad Sci U S A 95:6825-6830.

Mark M, Ghyselinck NB, Chambon P (2009) Function of retinoic acid receptors during embryonic development. Nucl Recept Signal 7:e002.

McCaffery P, Drager UC (1994) High levels of a retinoic acid-generating dehydrogenase in the meso-telencephalic dopamine system. Proc Natl Acad Sci U S A 91:7772-7776.

McCaffery P, Wagner E, O'Neil J, Petkovich M, Drager UC (1999) Dorsal and ventral retinal territories defined by retinoic acid synthesis, break-down and nuclear receptor expression. Mech Dev 82:119-130.

McCaffery PJ, Adams J, Maden M, Rosa-Molinar E (2003) Too much of a good thing: retinoic acid as an endogenous regulator of neural differentiation and exogenous teratogen. Eur J Neurosci 18:457-472.

Meshcheryakov VN (1972) The common pond snail *Lymnaea stagnalis*. In: Animal species for the developmental studies (Dettlaff T.A., Vassetzky S.G., eds), pp 69-132. New York: Consultants Bureau.

Mey J, McCaffery P (2004) Retinoic acid signaling in the nervous system of adult vertebrates. Neuroscientist 10:409-421.

Mey J, Morassutti J, Brook G, Liu RH, Zhang YP, Koopmans G, McCaffery P (2005) Retinoic acid synthesis by a population of NG2-positive cells in the injured spinal cord. Eur J Neurosci 21:1555-1568.

Mohanty-Hejmadi P, Dutta SK, Mahapatra P (1992) Limbs generated at site of tail amputation in marbled balloon frog after vitamin A treatment. Nature 355:352-353.

Moraes LA, Swales KE, Wray JA, Damazo A, Gibbins JM, Warner TD, Bishop-Bailey D (2007) Nongenomic signaling of the retinoid X receptor through binding and inhibiting Gq in human platelets. Blood 109:3741-3744.

Muley PD, McNeill EM, Marzinke MA, Knobel KM, Barr MM, Clagett-Dame M (2008) The atRA-responsive gene neuron navigator 2 functions in neurite outgrowth and axonal elongation. Dev Neurobiol 68:1441-1453.

Nagatomo K, Fujiwara S (2003) Expression of Raldh2, Cyp26 and Hox-1 in normal and retinoic acid-treated Ciona intestinalis embryos. Gene Expr Patterns 3:273-277.

Nagpal S, Friant S, Nakshatri H, Chambon P (1993) RARs and RXRs: evidence for two autonomous transactivation functions (AF-1 and AF-2) and heterodimerization in vivo. EMBO J 12:2349-2360.

Nagpal S, Zelent A, Chambon P (1992) RAR-beta 4, a retinoic acid receptor isoform is generated from RAR-beta 2 by alternative splicing and usage of a CUG initiator codon. Proc Natl Acad Sci U S A 89:2718-2722.

Nagy T, Elekes K (2000) Embryogenesis of the central nervous system of the pond snail Lymnaea stagnalis L. An ultrastructural study. J Neurocytol 29:43-60.

Neufeld DA, Day FA, Settles HE (1996) Stabilizing role of the basement membrane and dermal fibers during newt limb regeneration. Anat Rec 245:122-127.

Niederreither K, Dolle P (2008) Retinoic acid in development: towards an integrated view. Nat Rev Genet 9:541-553.

Niederreither K, Subbarayan V, Dolle P, Chambon P (1999) Embryonic retinoic acid synthesis is essential for early mouse post-implantation development. Nat Genet 21:444-448.

Nordlander RH, Singer M (1978) The role of ependyma in regeneration of the spinal cord in the urodele amphibian tail. J Comp Neurol 180:349-374.

Nowickyj SM, Chithalen JV, Cameron D, Tyshenko MG, Petkovich M, Wyatt GR, Jones G, Walker VK (2008) Locust retinoid X receptors: 9-Cis-retinoic acid in embryos from a primitive insect. Proc Natl Acad Sci U S A 105:9540-9545.

O'Steen WK, Walker B (1962) Radioautographic studies or regeneration in the common newt. III. Regeneration and repair of the intestine. Anat Rec 142:179-187.

Ochoa WF, Torrecillas A, Fita I, Verdaguer N, Corbalan-Garcia S, Gomez-Fernandez JC (2003) Retinoic acid binds to the C2-domain of protein kinase C(alpha). Biochemistry 42:8774-8779.

Ohta K, Kawachi E, Inoue N, Fukasawa H, Hashimoto Y, Itai A, Kagechika H (2000) Retinoidal pyrimidinecarboxylic acids. Unexpected diaza-substituent effects in retinobenzoic acids. Chem Pharm Bull (Tokyo) 48:1504-1513.

Park UH, Kim EJ, Um SJ (2010) A novel cytoplasmic adaptor for retinoic acid receptor (RAR) and thyroid receptor functions as a Derepressor of RAR in the absence of retinoic acid. J Biol Chem 285:34269-34278.

Pecorino LT, Entwistle A, Brockes JP (1996) Activation of a single retinoic acid receptor isoform mediates proximodistal respecification. Curr Biol 6:563-569.

Peng X, Maruo T, Cao Y, Punj V, Mehta R, Das Gupta TK, Christov K (2004) A novel RARbeta isoform directed by a distinct promoter P3 and mediated by retinoic acid in breast cancer cells. Cancer Res 64:8911-8918.

Pietsch P (1987) The Effects of Retinoic Acid on Mitosis During Tail and Limb Regeneration in the Axolotl Larva, Ambystoma-Mexicanum. Rouxs Archives of Developmental Biology 196:169-175.

Pignatello MA, Kauffman FC, Levin AA (1999) Multiple factors contribute to the toxicity of the aromatic retinoid TTNPB (Ro 13-7410): interactions with the retinoic acid receptors. Toxicol Appl Pharmacol 159:109-116.

Pignatello MA, Kauffman FC, Levin AA (2002) Liarozole markedly increases all trans-retinoic acid toxicity in mouse limb bud cell cultures: a model to explain the potency of the aromatic retinoid (E)-4-[2-(5,6,7,8-tetrahydro-5,5,8,8-tetramethyl-2-naphthylenyl)-1-propeny l] benzoic acid. Toxicol Appl Pharmacol 178:186-194.

Poon MM, Chen L (2008) Retinoic acid-gated sequence-specific translational control by RARalpha. Proc Natl Acad Sci U S A 105:20303-20308.

Prince DJ, Carlone RL (2003) Retinoic acid involvement in the reciprocal neurotrophic interactions between newt spinal cord and limb blastemas in vitro. Brain Res Dev Brain Res 140:67-73.

Ragsdale CW, Jr., Gates PB, Hill DS, Brockes JP (1993) Delta retinoic acid receptor isoform delta 1 is distinguished by its exceptional N-terminal sequence and abundance in the limb regeneration blastema. Mech Dev 40:99-112.

Ragsdale CW, Jr., Petkovich M, Gates PB, Chambon P, Brockes JP (1989) Identification of a novel retinoic acid receptor in regenerative tissues of the newt. Nature 341:654-657.

Renaud JP, Rochel N, Ruff M, Vivat V, Chambon P, Gronemeyer H, Moras D (1995) Crystal structure of the RAR-gamma ligand-binding domain bound to all-trans retinoic acid. Nature 378:681-689.

Ridgway RL, Syed NI, Lukowiak K, Bulloch AG (1991) Nerve growth factor (NGF) induces sprouting of specific neurons of the snail, Lymnaea stagnalis. J Neurobiol 22:377-390.

Rochette-Egly C, Germain P (2009) Dynamic and combinatorial control of gene expression by nuclear retinoic acid receptors (RARs). Nucl Recept Signal 7:e005.

Romert A, Tuvendal P, Simon A, Dencker L, Eriksson U (1998) The identification of a 9-cis retinol dehydrogenase in the mouse embryo reveals a pathway for synthesis of 9-cis retinoic acid. Proc Natl Acad Sci U S A 95:4404-4409.

Sanchez A (2000) Regeneration in the metazoans: why does it happen? BioEssays 22:578-590.

Scadding SR (1986) Vitamin A inhibits amphibian tail regeneration. Can J Zool 65:457-459.

Schrage K, Koopmans G, Joosten EA, Mey J (2006) Macrophages and neurons are targets of retinoic acid signaling after spinal cord contusion injury. Eur J Neurosci 23:285-295.

Shearer MC, Niclou SP, Brown D, Asher RA, Holtmaat AJ, Levine JM, Verhaagen J, Fawcett JW (2003) The astrocyte/meningeal cell interface is a barrier to neurite outgrowth which can be overcome by manipulation of inhibitory molecules or axonal signalling pathways. Mol Cell Neurosci 24:913-925.

Siegenthaler JA, Ashique AM, Zarbalis K, Patterson KP, Hecht JH, Kane MA, Folias AE, Choe Y, May SR, Kume T, Napoli JL, Peterson AS, Pleasure SJ (2009) Retinoic Acid from the Meninges Regulates Cortical Neuron Generation. Cell 139:597-609.

Simoes-Costa MS, Azambuja AP, Xavier-Neto J (2008) The search for non-chordate retinoic acid signaling: lessons from chordates. J Exp Zoolog B Mol Dev Evol 310:54-72.

Singer M (1952) The influence of the nerve in regeneration of the amphibian extremity. Q Rev Biol 27:169-200.

Sive HL, Draper BW, Harland RM, Weintraub H (1990) Identification of a retinoic acid-sensitive period during primary axis formation in Xenopus laevis. Genes Dev 4:932-942.

Smith SJ (1988) Neuronal cytomechanics: the actin-based motility of growth cones. Science 242:708-715.

Solomin L, Johansson CB, Zetterstrom RH, Bissonnette RP, Heyman RA, Olson L, Lendahl U, Frisen J, Perlmann T (1998) Retinoid-X receptor signalling in the developing spinal cord. Nature 395:398-402.

Spencer GE, Syed NI, van Kesteren E, Lukowiak K, Geraerts WP, van Minnen J (2000) Synthesis and functional integration of a neurotransmitter receptor in isolated invertebrate axons. J Neurobiol 44:72-81.

Stratford T, Horton C, Maden M (1996) Retinoic acid is required for the initiation of outgrowth in the chick limb bud. Curr Biol 6:1124-1133.

Sturzenbaum SR, Kille P (2001) Control genes in quantitative molecular biological techniques: the variability of invariance. Comparative Biochemistry and Physiology B-Biochemistry & Molecular Biology 130:281-289.

Sumida K, Igarashi Y, Toritsuka N, Matsushita T, Abe-Tomizawa K, Aoki M, Urushidani T, Yamada H, Ohno Y (2011) Effects of DMSO on gene expression in human and rat hepatocytes. Hum Exp Toxicol.

Sun K, Montana V, Chellappa K, Brelivet Y, Moras D, Maeda Y, Parpura V, Paschal BM, Sladek FM (2007) Phosphorylation of a conserved serine in the deoxyribonucleic acid binding domain of nuclear receptors alters intracellular localization. Mol Endocrinol 21:1297-1311.

Theodosiou M, Laudet V, Schubert M (2010) From carrot to clinic: an overview of the retinoic acid signaling pathway. Cell Mol Life Sci 67:1423-1445.

Thompson HG, Maynard TM, Shatzmiller RA, Lamantia AS (2002) Retinoic acid signaling at sites of plasticity in the mature central nervous system. J Comp Neurol 452:228-241.

Tryggvason K, Romert A, Eriksson U (2001) Biosynthesis of 9-cis-retinoic acid in vivo. The roles of different retinol dehydrogenases and a structure-activity analysis of microsomal retinol dehydrogenases. J Biol Chem 276:19253-19258.

Umemiya H, Fukasawa H, Ebisawa M, Eyrolles L, Kawachi E, Eisenmann G, Gronemeyer H, Hashimoto Y, Shudo K, Kagechika H (1997) Regulation of retinoidal actions by diazepinylbenzoic acids. Retinoid synergists which activate the RXR-RAR heterodimers. J Med Chem 40:4222-4234.

Vesprini ND, Spencer GE (2009) Acute exposure to retinoic acid changes the firing properties of identified cultured neurons. Program# 623.12, 2009 Neuroscience Meeting Planner. Chicago, IL: Society for Neuroscience, 2009. Online.

Vesprini ND, Spencer GE (2010) Retinoic acid induced regeneration *in situ* following nerve crush injury. Program #68. 2010 Southern Ontario Neuroscience Association Meeting. Brock University, Ontario.

Viviano CM, Brockes JP (1996) Is retinoic acid an endogenous ligand during urodele limb regeneration? Int J Dev Biol 40:817-822.

Wagner E, Luo T, Drager UC (2002) Retinoic acid synthesis in the postnatal mouse brain marks distinct developmental stages and functional systems. Cereb Cortex 12:1244-1253.

Werner EA, Deluca HF (2002) Retinoic acid is detected at relatively high levels in the CNS of adult rats. Am J Physiol Endocrinol Metab 282:E672-E678.

Wiens M, Batel R, Korzhev M, Muller WE (2003) Retinoid X receptor and retinoic acid response in the marine sponge Suberites domuncula. J Exp Biol 206:3261-3271.

Wildering WC, Hermann PM, Bulloch AG (2001) Lymnaea epidermal growth factor promotes axonal regeneration in CNS organ culture. J Neurosci 21:9345-9354.

Williams DD (1959) Liver Regeneration in the Subtotal Hepatectomized Salamander, Triturus-Viridescens. Anatomical Record 133:351-352.

Wong LF, Yip PK, Battaglia A, Grist J, Corcoran J, Maden M, Azzouz M, Kingsman SM, Kingsman AJ, Mazarakis ND, McMahon SB (2006) Retinoic acid receptor beta2 promotes functional regeneration of sensory axons in the spinal cord. Nat Neurosci 9:243-250.

Wong RG, Hadley RD, Kater SB, Hauser GC (1981) Neurite outgrowth in molluscan organ and cell cultures: the role of conditioning factor(s). J Neurosci 1:1008-1021.

Wuarin L, Sidell N, de Vellis J (1990) Retinoids increase perinatal spinal cord neuronal survival and astroglial differentiation. Int J Dev Neurosci 8:317-326.

Yasmin R, Williams RM, Xu M, Noy N (2005) Nuclear import of the retinoid X receptor, the vitamin D receptor, and their mutual heterodimer. J Biol Chem 280:40152-40160.

Yip PK, Wong LF, Pattinson D, Battaglia A, Grist J, Bradbury EJ, Maden M, McMahon SB, Mazarakis ND (2006) Lentiviral vector expressing retinoic acid receptor beta2 promotes recovery of function after corticospinal tract injury in the adult rat spinal cord. Hum Mol Genet 15:3107-3118.

Zelent A, Mendelsohn C, Kastner P, Krust A, Garnier JM, Ruffenach F, Leroy P, Chambon P (1991) Differentially expressed isoforms of the mouse retinoic acid receptor beta generated by usage of two promoters and alternative splicing. EMBO J 10:71-81.

Zhang F, Ferretti P, Clarke JD (2003) Recruitment of postmitotic neurons into the regenerating spinal cord of urodeles. Dev Dyn 226:341-348.

Zhelyaznik N, Mey J (2006) Regulation of retinoic acid receptors alpha, beta and retinoid X receptor alpha after sciatic nerve injury. Neuroscience 141:1761-1774.

Zile MH (2001) Function of vitamin A in vertebrate embryonic development. J Nutr 131:705-708.

Zimmer A, Zimmer AM, Reynolds K (1994) Tissue specific expression of the retinoic acid receptor-beta 2: regulation by short open reading frames in the 5'-noncoding region. J Cell Biol 127:1111-1119.

Zipori D (2004) Mesenchymal stem cells: harnessing cell plasticity to tissue and organ repair. Blood Cells Mol Dis 33:211-215.

Zukor KA, Kent DT, Odelberg SJ (2011) Meningeal cells and glia establish a permissive environment for axon regeneration after spinal cord injury in newts. Neural Dev 6:1.

7. Appendix I

```
Human_RXRalpha          ATFATTRRAAASARRRRHRSRRLPAARARAGRAGGRRARRPLPAPPAGHELVADMDTKHF 60
Notophthalmus_RXR       ------------------------------------------------------------

Human_RXRalpha          LPLDFSTQVNSSLTSPTGRGSMAAPSLHPSLGPGIGSPGQLHSPISTLSSPINGMGPPFS 120
Notophthalmus_RXR       ------------------------------------------------------------

Human_RXRalpha          VISSPMGPHSMSVPTTPTLGFSTGSPQLSSPMNPVSSSEDIKPPLGLNGVLKVPAHPSGN 180
Notophthalmus_RXR       ------------------------------------------------------------

Human_RXRalpha          MASFTKHICAICGDRSSGKHYGVYSCEGCKGFFKRTVRKDLTYTCRDNKDCLIDKRQRNR 240
Notophthalmus_RXR       ----------------GKHYGVYSCEGCKGFFKRTIRKDLTYTCRDNKDCIVDKRQRNR 43
                                        ******************:**************::********

Human_RXRalpha          CQYCRYQKCLAMGMKREAVQEERQRGKDRNENEVESTSSANEDMPVERILEAELAVEPKT 300
Notophthalmus_RXR       CQYSRYQKCLATGMKREAVQEERQRGRER-DGDMEYSSGVNEEMPVDKILEAELAVEQKS 102
                        ***.******* ***************::* :.::* :*..**:***::********* *:

Human_RXRalpha          ETYVEANMGLNPSSPNDPVTNICQAADKQLFTLVEWAKRIPHFSELPLDDQVILLRAGWN 360
Notophthalmus_RXR       DQSVDG-SGIGGSSPNDPVTNICQAADKQLFTLVEWAKRIPHFSELPLDDQVILLRAGWN 161
                        :  *:.  * . ************************************************

Human_RXRalpha          ELLIASFSHRSIAVKDGILLATGLHVHRNSAHSAGVGAIFDRVLTELVSKMRDMQMDKTE 420
Notophthalmus_RXR       ELLIASFSHRSISVKDGILLATGLHVHRNSAHSAGVGAIFDRVLTELVSKMRDMRMDKTE 221
                        ************:*********************************************:*****

Human_RXRalpha          LGCLRAIVLFNPDSKGLSNPAEVEALREKVYASLEAYCKHKYPEQPGRFAKLLLRLPALR 480
Notophthalmus_RXR       LGCLRAIILFNPDAKGPSNPGEVELLREKVYASLESYCKHKYPEQ---------------- 266
                        *******:*****:** ***.*** **********:*********

Human_RXRalpha          SIGLKCLEHLFFFKLIGDTPIDTFLMEMLEAPHQMT 516
Notophthalmus_RXR       ------------------------------------
```

Figure 36. The partial *Notophthalums viridescens* RXR protein sequence. Multiple sequence alignment of the partial *N. viridescens* RXR that I have cloned (Notophthalus_RXR; accession no. ADI24671) with the full-length Human RXRalpha subtype (accession no. AAH63827). Within the partial Notophthalus_RXR sequence, there is 85% amino acid identity, and 93% amino acid similarity with the Human RXRalpha. This region contains most of the ligand binding pocket which corresponds with the E domain.

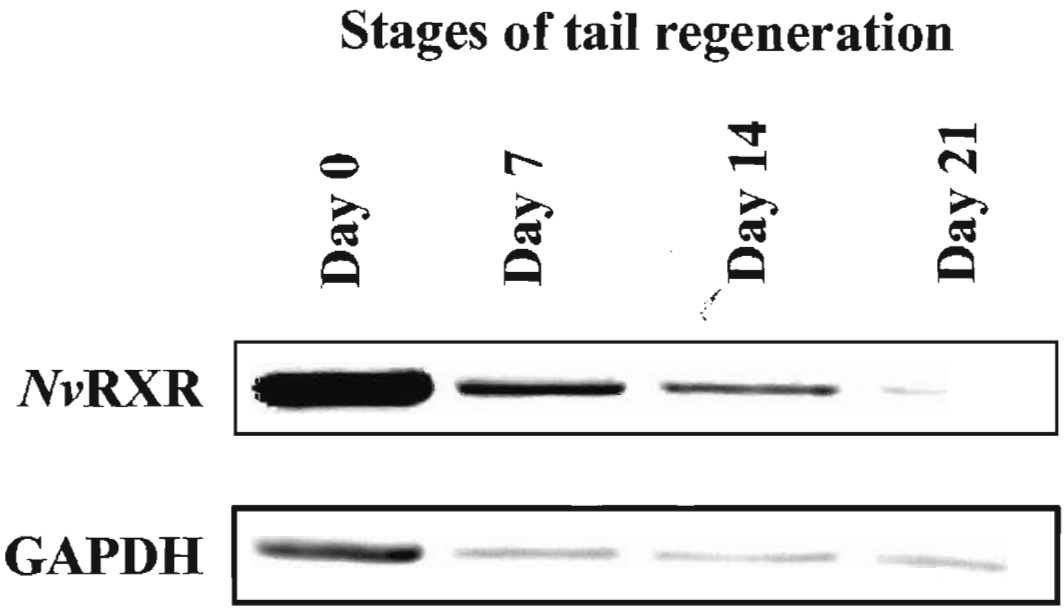

Figure 37. *Nv*RXR protein levels decrease in progressing stages of tail regeneration. Western blot analysis at 4 different stages of newt tail regeneration revealed a stepwise decrease in the levels of *Nv*RXR protein from day 0 through day 21. The newt GAPDH was used as a control.

8. Appendix II

Figure 38. The full-length *Lymnaea* RALDH protein sequence. Multiple sequence alignment of the *Lymnaea stagnali*s RALDH (accession no. ACL79834) with the Human RALDH (accession no. O94788). There is 64% amino acid identity, and 80% amino acid similarity between this non-chordate and chordate RALDH.